AD-773 292

PROBLEM OF THE APPLICATION OF TURBOFAN
ENGINES IN AIR TRANSPORT. METHODS OF
INCREASE IN EFFICIENCY OF TURBOFAN ENGINE
WITH HIGH BYPASS RATIOS

A. L. Klyachkina

Foreign Technology Division
Wright-Patterson Air Force Base, Ohio

28 November 1973

EDITED MACHINE TRANSLATION

FTD-MT-24-661-73   28 November 1973

PROBLEM OF THE APPLICATION OF TURBOFAN ENGINES
IN AIR TRANSPORT. METHODS OF INCREASE IN
EFFICIENCY OF TURBOFAN ENGINE WITH HIGH BYPASS
RATIOS

By: A. L. Klyachkina

English pages: 148

Source: Trudy Rizhskiy Institut Inzhenerov
         Gradzhanskoy Aviatsii Imeni Leninskogo
         Komsonola. Problemy Primeneniya DTRD
         v Vozdushnom Transporte, No. 174, 1971,
         pp. 1-153.

Country of origin: USSR

Requester: FTD/PDTA

This document is a SYSTRAN machine aided
translation, post-edited for technical accuracy
by: SSgt Michael L. Seidel

Approved for public release;
distribution unlimited.

PREPARED BY:

TRANSLATION DIVISION
FOREIGN TECHNOLOGY DIVISION
WP-AFB, OHIO.

DOCUMENT CONTROL DATA - R & D

(Security classification of title, body of abstract and indexing annotation must be entered when the overall report is classified)

1. ORIGINATING ACTIVITY (Corporate author)	2a. REPORT SECURITY CLASSIFICATION
Foreign Technology Division	Unclassified
Air Force Systems Command	2b. GROUP
U. S. Air Force	

3. REPORT TITLE

PROBLEM OF THE APPLICATION OF TURBOFAN ENGINES IN AIR TRANSPORT.
METHODS OF INCREASE IN EFFICIENCY OF TURBOFAN ENGINE WITH HIGH
BYPASS RATIOS

4. DESCRIPTIVE NOTES (Type of report and inclusive dates)

Translation

5. AUTHOR(S) (First name, middle initial, last name)

A. L. Klyachkina

6. REPORT DATE	7a. TOTAL NO. OF PAGES	7b. NO. OF REFS
1971	148	52

8a. CONTRACT OR GRANT NO.	9a. ORIGINATOR'S REPORT NUMBER(S)
b. PROJECT NO. JDM3	FTD-MT-24-661-73
c.	9b. OTHER REPORT NO(S) (Any other numbers that may be assigned this report)
d.	

10. DISTRIBUTION STATEMENT

Approved for public release;
distribution unlimited.

11. SUPPLEMENTARY NOTES	12. SPONSORING MILITARY ACTIVITY
	Foreign Technology Division
	Wright-Patterson AFB, Ohio

13. ABSTRACT

21

DD FORM 1473
1 NOV 65

All figures, graphs, tables, equations, etc.
merged into this translation were extracted
from the best quality copy available.

C

U. S. BOARD ON GEOGRAPHIC NAMES TRANSLITERATION SYSTEM

Block	Italic	Transliteration	Block	Italic	Transliteration
А а	*А а*	A, a	Р р	*Р р*	R, r
Б б	*Б б*	B, b	С с	*С с*	S, s
В в	*В в*	V, v	Т т	*Т т*	T, t
Г г	*Г г*	G, g	У у	*У у*	U, u
Д д	*Д д*	D, d	Ф ф	*Ф ф*	F, f
Е е	*Е е*	Ye, ye; E, e*	Х х	*Х х*	Kh, kh
Ж ж	*Ж ж*	Zh, zh	Ц ц	*Ц ц*	Ts, ts
З з	*З з*	Z, z	Ч ч	*Ч ч*	Ch, ch
И и	*И и*	I, i	Ш ш	*Ш ш*	Sh, sh
Й й	*Й й*	Y, y	Щ щ	*Щ щ*	Shch, shch
К к	*К к*	K, k	Ъ ъ	*Ъ ъ*	"
Л л	*Л л*	L, l	Ы ы	*Ы ы*	Y, y
М м	*М м*	M, m	Ь ь	*Ь ь*	'
Н н	*Н н*	N, n	Э э	*Э э*	E, e
О о	*О о*	O, o	Ю ю	*Ю ю*	Yu, yu
П п	*П п*	P, p	Я я	*Я я*	Ya, ya

* ye initially, after vowels, and after ъ, ь; e elsewhere.
When written as ё in Russian, transliterate as yё or ё.
The use of diacritical marks is preferred, but such marks
may be omitted when expediency dictates.

FOLLOWING ARE THE CORRESPONDING RUSSIAN AND ENGLISH

DESIGNATIONS OF THE TRIGONOMETRIC FUNCTIONS

Russian	English
sin	sin
cos	cos
tg	tan
ctg	cot
sec	sec
cosec	csc
sh	sinh
ch	cosh
th	tanh
cth	coth
sch	sech
csch	csch
arc sin	$\sin^{-1}$
arc cos	$\cos^{-1}$
arc tg	$\tan^{-1}$
arc ctg	$\cot^{-1}$
arc sec	$\sec^{-1}$
arc cosec	$\csc^{-1}$
arc sh	$\sinh^{-1}$
arc ch	$\cosh^{-1}$
arc th	$\tanh^{-1}$
arc cth	$\coth^{1}$
arc sch	$\sech^{-1}$
arc csch	$\csch^{-1}$

---

rot	curl
lg	log

DESIGNATION LIST

       DTRD =   ДТРД = turbofan engine
        TJE =   ТРД = turbojet engine
         VD =   ВД = high-pressure
        TVD =   ТВД = turboprop engine
        GTE =   ГТД = gas turbine engine
      DTRDF =   ДТРДФ = turbofan engine with afterburner
        KPD =   НПД = efficiency
      ETsVM =   ЭЦВМ = electronic digital computer
         LP =   НД = low-pressure
        RJE =   ПВРД = ramjet
    TJEW-AB =   ТРДФ = turbojet engine with afterburner
        AMC =   ФСН = afterburner mixing chamber

TABLE OF CONTENTS

PREFACE

The scientific-technical collection submitted to the readers' attention unites thematically a group of articles dedicated to the different aspects of an increase in efficiency of contemporary [DTRD = turbofan engine] (ДТРД) with a high bypass ratio.

They include theoretical studies of different methods of improvement of the thermodynamic cycle of DTRD and of the optimum selection of operating conditions parameters, as a result of which specific fuel consumption decreases. To these methods on one hand one ought to relate the use of high bypass ratios on the basis of the forced operating conditions according to parameters (temperature of the gas before the turbine, the compression ratio of the compressor) of the cycle of engine; on the other hand - the application of heat recovery in DTRD with high bypass ratio on the basis of a high-temperature cycle with a low compression ratio.

A comparative efficiency of these two alternative methods to a considerable degree will be determined by design perfection and specific weight, and operational reliability of the accomplished power plants.

A series of articles is dedicated to the methods of the experimental and theoretical investigation of DTRD with the booster-mixing chambers and to the creation, for this purpose, of original experimental installations.

Finally, a series of articles is dedicated to the extremely acute and actual problem of contemporary civil aviation - to the problem of a reduction DTRD noise at large bypass ratio values.

In these articles the basic physical characteristics of the noise of aviation [GTE = gas turbine engine] (ГТД) and the mechanism of noise formation at the basic sources (reactive jet, compressor, fan) are examined; the range of bypass ratios is determined, in which the noise of fan turns out to be predominant; the methods of calculation of the noise of reactive jets and compressor are examined.

Furthermore, in these articles are examined: the role and place of full-scale experiment in acoustic studies, possible schemes of the open stands created for this purpose, the enumeration of studies which can be executed on such stands.

The published articles are a summarization of several scientific investigations made in the Department for the Theory of Aircraft Engines [RKIIGA] (РКИИГА) during 1968-69.

The present scientific-technical collection is of interest to specialists who work in the area of aircraft engine construction, and also to the graduates and students of aviation [VTUZ's] (ВТУЗ).

From editor

AN ENERGY STUDY OF THE EFFICIENCY OF TURBOFAN JET ENGINES AT SUBSONIC SPEEDS OF FLIGHT

A. L. Klyachkin, A. Ya. Dantsyge

In this article the results of the calculated study of the effect of operating condition parameters and the bypass ratio on the efficiencies of useful action of prospective non-boosted DTRD at the subsonic speeds of flight are examined.

The physical interpretation of the obtained laws is given, and recommendations regarding the development of DTRD parameters which provide its best cost-effectiveness are also given.

It is known that the efficiency of a DTRD as any jet engine, it is estimated at three efficiencies: effective (η_e), thrust (η_R) and total (η_o), where

$$\eta_o = \eta_e \cdot \tau_{iR}. \tag{1}$$

At a fixed flying speed total efficiency [KPD] (НПД) uniquely determines the specific fuel consumption that follows from the relationship:

$$C_{y\lambda} = 8,43 \frac{V}{H_u \eta_o}. \tag{2}$$

The advantage of non-boosted DTRD over the turbojet engine according to cost-effectiveness is explained by the fact that the introduction of the secondary circuit during the optimum or close to optimum energy distribution between contour retards the

outflow of gas from the jet nozzles of the contours. Thus, the thrust engine efficiency substantially increases. However, in this case the added losses of energy are introduced during its transfer from the first contour to the second, as a result of which the effective efficiency is lowered.

Thus, total efficiency increases (and consequently, the cost-effectiveness of a DTRD is increased) when an increase in the thrust efficiency substantially predominates a reduction in the effective efficiency, or when as a result of the development of the DTRD parameters both efficiencies increase: effective and thrust.

The evaluation of the effect of the development of the operating condition and bypass ratio parameters on the efficiency of prospective DTRD is of considerable interest. This evaluation makes it possible to objectively establish the prospects for an improvement in the cost-effectiveness of DTRD in the coming years.

Effect of the Parameters of Operating
Conditions (π_{H}^{*} and T_{3}^{*}) and Bypass
Ratio (y) on the Efficiency of (η_{e},
η_{R} and η_{o}) DTRD

Figures 1-4 depict the results of the calculations according to the study of the effect of the parameters of operating conditions (π_{H}^{*}, T_{3}^{*}) and bypass ratio (y) on the specific parameters ($R_{\text{уд}}$ and $C_{\text{уд}}$), and also on efficiency (η_{e}, η_{R}, η_{o}) of turbofan engine for standard subsonic design conditions ($M_{0} = 0.8$ and $H = 11$ km).

In these calculations the parameters of the DTRD changed over a wide range of the values:

$$T_{3}^{*} = 1200-1800°K;$$
$$\pi_{\text{к}}^{*} = 20-70;$$
$$y = 0 \div 20.$$

Fig. 1. The effect $\pi_{\text{к}}^{*}$ and T_{3}^{*} on the specific parameters of the DTRD (y = 0.5). KEY: (1) DTRD; (2) kg/kg·h; (3) kg/kg·s.

Fig. 2. The effect $\pi_{\text{к}}^{*}$ and T_{3}^{*} on the specific parameters of the DTRD (y = 10). KEY: (1) DTRD; (2) kg/kg·h; (3) kg/kg·s.
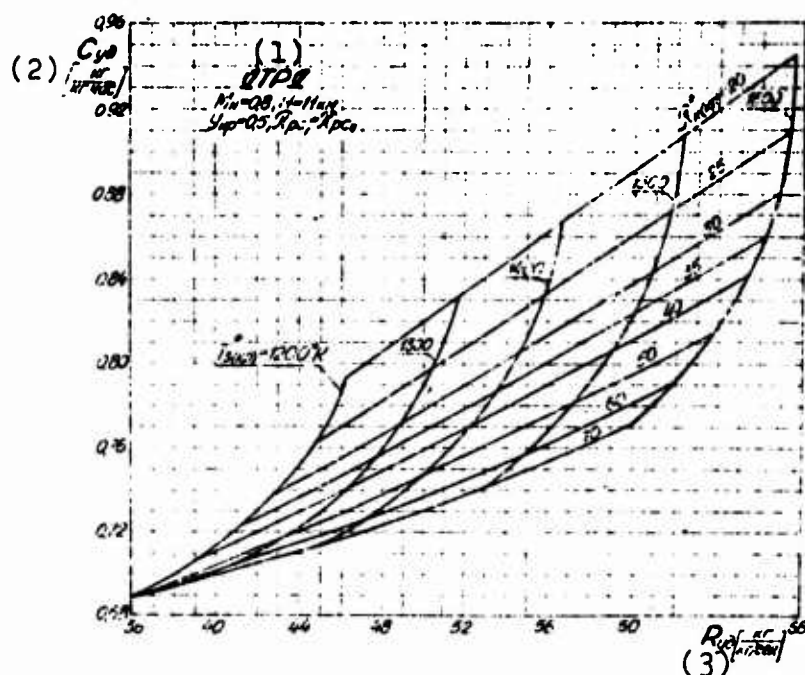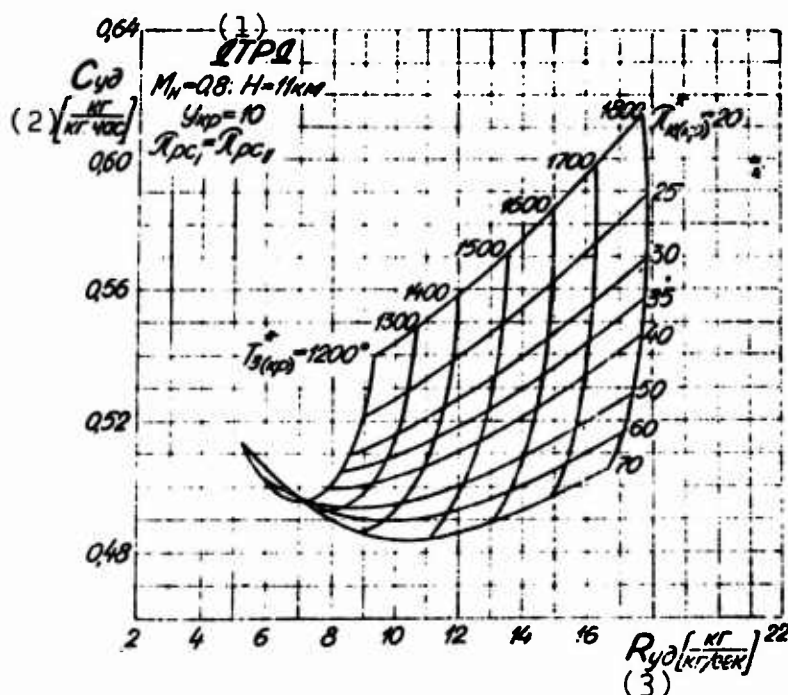
Fig. 3. The effect π_K^* and T_3^* on the
specific parameters of the DTRD (y = 20).
KEY: (1) DTRD; (2) kg/kg h; (3) kg/kg s.

Fig. 4. The effect of the parameters of the operating conditions
with y = 0.5 and y = 10 on the efficiency of the DTRD.

The following improved values of the particular efficiencies and loss factors of the main centers of prospective[1] triple shaft DTRD were accepted.

$$\eta_{\text{в}}^* = 0{,}89; \quad \eta_{\text{к(вд)}}^* = \eta_{\text{к(сд)}}^* = 0{,}87;$$
$$\eta_{\text{тк(вд)}}^* = \eta_{\text{тк(сд)}}^* = \eta_{\text{т(нд)}}^* = 0{,}92;$$
$$\sigma_{\text{вх}} = 1{,}0; \quad \sigma_{\text{кс}}^* = 0{,}97; \quad \varphi_{\text{рс}} = 0{,}99; \quad \xi_{\text{кс}} = 0{,}99.$$

In the calculation the air bleed from the high pressure compressor for the cooling of turbine blades [VD] (ВД) was also considered, which comprised, dependent on the level of the temperature of gases T_3^*, from 4 to 10%.

In Fig. 4 in coordinates η_e and η_R (with the applied hyperbolic grid of the isolines η_o = const) represented the total effect of $\pi_{\text{к}}^*$ and T_3^* at fixed values of y (y = 0.5 and 10) on the efficiency of DTRD. Such a coordinate system makes it possible to estimate in demonstrative form how development (change) of the parameters of engine simultaneously affects the three efficiencies.

We see that an increase of the bypass ratio from 0 [TJE] (ТРД)[2] to 10 and more in the entire range of parameters of operating conditions sharply increases the total efficiency because of the predominant increase in the thrust efficiency with an insubstantial reduction in the effective efficiency. A change of T_3^* and $\pi_{\text{к}}^*$ with y = const in dependence on the numerical value of the initial parameters of engine affects its efficiency differently.

---

[1]Taking into account the possibility of an improvement in the hydraulic and gas-dynamic perfection of the air-gas flow area of the engine.

[2]In Fig. 4 y = 0.5.

From Fig. 4 it is possible to make an important conclusion. It is advantageous·to produce increase $\pi_{\text{к}}^{*}$ only up to a value of η_{e} which differs little from the maximum ($\eta_{e\ \text{макс}}$). If with low bypass ratio the increase of $\pi_{\text{к}}^{*}$ over $\pi_{\text{к}}^{*}(\eta_{e=\text{макс}})$ still can somewhat increase η_{o}, then with large y a similar increase of $\pi_{\text{к}}^{*}$ leads to a drop of η_{o}. Thus, an approach to the selection of the computed value of $\pi_{\text{к}}^{*}$ at large values of y should be analogous to that made at high pressure turbines.

Another conclusion is that increase of T_{3}^{*}, as a rule, makes the cost-effectiveness of DTRD worse at all values of y in question, with the exception of very high values of $\pi_{\text{к}}^{*}$ (~70).
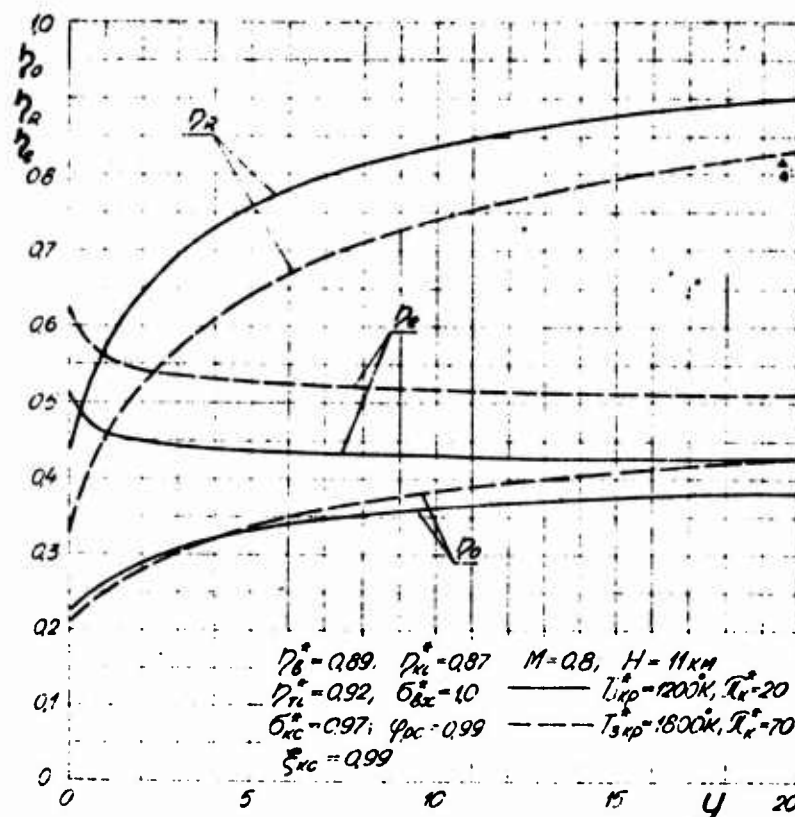
Fig. 5. The effect of bypass ratio on the efficiency of DTRD.

Figure 5 shows the effect of bypass ratio (for fixed values of T_3^* and π_H^*) on the efficiency of DTRD. We see that an increase of y from 0 to 20 sharply increases thrust efficiency from 0.34-0.44 to 0.83-0.90, i.e., more than 2 times. Effective efficiency in this case initially decreases somewhat from 0.51-0.62 to 0.43-0.52, i.e., to approximately 20%; it is characteristic that in the range of values y = 4-20 effective efficiencies virtually retain an invariable value.

The total efficiency of a DTRD with an increase of y continuously grows from 0.21-0.23 to 0.37-0.43, i.e., almost to 80-100%, whereupon it is especially intense using the high parameters of operating conditions (T_3^* = 1800°K and π_H^* = 70).

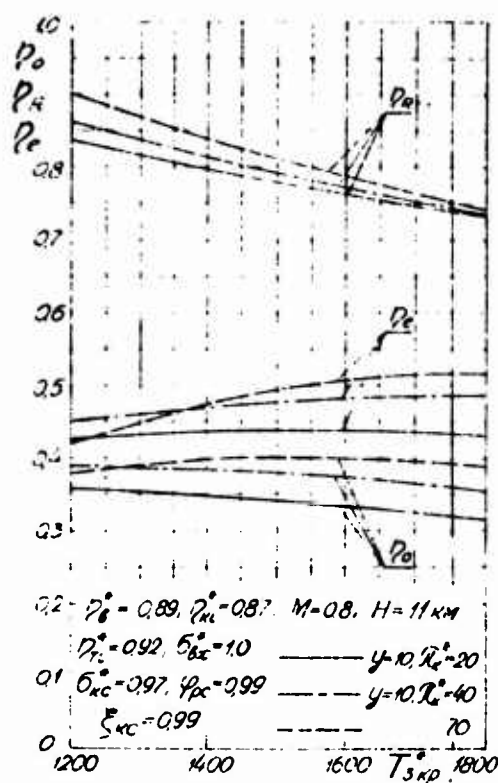Fig. 6.   Fig. 7.

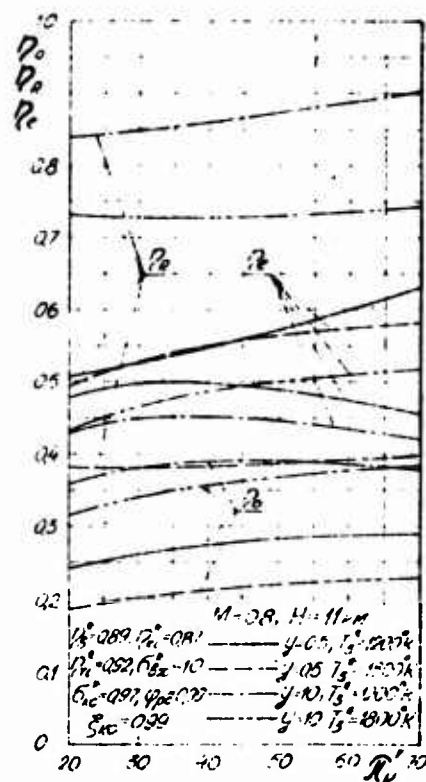Fig. 6. The temperature effect of the gas before the turbine on the efficiency of DTRD.

Fig. 7. The effect of the compression ratio of the compressor on the efficiency of DTRD.

7

Figure 6 shows the temperature effect of the gas before the turbine (for a series of fixed values y and π_{H}^{*}) on engine efficiency. We will see, that an increase T_{3}^{*} continuously lowers thrust efficiency (losses with outlet velocity grow). It is characteristic that a drop in the thrust efficiency, as a rule, compensates for an increase in the effective efficiency. In summation, with an increase of T_{3}^{*} the total efficiency falls with the exception of high values of y ($y = 10$) and π_{H}^{*} ($\pi_{H}^{*} = 70°$); however, even in this case the economic value of T_{3}^{*} (to which corresponds the maximum of total efficiency and minimum $C_{уд}$) does not exceed a value of 1400°K.

Finally, Fig. 7 depicts the effect of the compression ratio of compressor π_{H}^{*} (for a series of fixed values y and T_{3}^{*}) on the efficiency of DTRD. From this figure it follows that with an increase of π_{H}^{*}, dependent on the level of parameters y and T_{3}^{*}, effective efficiency can be changed differently: with low y and T_{3}^{*} it continuously grows; with large y and low T_{3}^{*} it continuously falls. Curves η_{e} can have a maximum on π_{H}^{*}.

The total efficiency of the engine with an increase of π_{H}^{*} increases at high values of T_{3}^{*} and has a maximum with $\pi_{H}^{*} \simeq 40$, when $T_{3}^{*} = 1200°K$.

Conclusions

During an observed high level of the efficiency of units of prospective DTRD, calculated for the large subsonic speeds of flight, to provide for the best cost-effectiveness of the engine:

1. It is advantageous to increase the bypass ratio of engine to values of $y = 10-15$, whereupon the larger, the higher the accepted level of T_{3}^{*} and π_{H}^{*}.

8

2. It is inadvisable to increase the temperature of the gas before the turbine in cruising flight over values of 1400°K. This is profitable, however, from the viewpoint of an increase in the specific thrust of a DTRD, i.e., for reduction in the overall dimensions and weight of engine.

3. It is advisable to continuously increase $\pi_\text{к}^*$ (up to $\pi_\text{к}^* = 70\text{-}100$) only at high values of gas temperature before the turbine (when $T_3^* > 1400\text{-}1500°K$). When $y = 10$ and $T_3^* = 1200°K$ the economic value of $\pi_\text{к}^*$ does not exceed a value of 35-40.

4. The realization of a DTRD with parameters of operating conditions in cruising flight ($M_0 = 0.8$; $H = 11$ km); $T_3^* = 1400°K$; $\pi_\text{к}^* = 40$ and $y = 10$ makes it possible to create a third generation DTRD with specific fuel consumption $C_\text{уд} \simeq 0.50\text{-}0.52$ kg/kg·h at values of efficiency $\eta_\text{о} = 0.38\text{-}0.40$; $\eta_R = 0.82\text{-}0.84$; $\eta_e \simeq 0.46\text{-}0.48$.

Bibliography

1. Клячкин А. Л. Теория воздушно-реактивных двигателей. «Машиностроение», М., 1969.
2. Проблемы применения двухконтурных ТРД в гражданской авиации Под ред. проф. А. Л. Клячкина. Труды РКИИГА. вып. 115, 1967.

APPROXIMATION OF THE BASIC THERMODYNAMIC FUNCTIONS USED FOR THE CALCULATION OF GAS TURBINE ENGINES

M. P. Budzinauskas, V. P. Labendik

In this article equations are presented which approximate the thermodynamic functions used for the calculation of gas turbine engines, and the procedure of their application is presented. Tables are presented which make it possible to estimate the accuracy of the approximation of the basic thermodynamic functions.

Principal Notations

T - temperature

ΔT - change in temperature

$\bar{T} = \dfrac{T_2}{T_1}$ - relative temperature

i - enthalpy

S - entropy

ΔS - change in entropy

π - compression ratio (expansion)

m_i - the relative consumption of fuel

$\xi_{\text{кс}}$ - combustion completeness coefficient

H_u - fuel heating value

α - the excess air ratio

C_p - the specific heat at constant pressure

R - universal gas constant

A - thermal equivalent of work

e - Naperian base

Indices

Superscript:

* - stagnation parameter

n - order of approximation

Subscript:

1 - the beginning of process (entry to compressor)

2 - the end of the process (compressor outlet)

3, 4

and 5 - the parameters at the entry to turbine, turbine exhaust and in the section of jet nozzle

д - dynamic

к - compressor

т - turbine

ф - afterburner

рс - jet nozzle

в - air

г - combustion products (gas)

ад - adiabatic

Contractions

[GTE] (ГТД) - gas turbine engine

[DTRD] (ДТРД) - turbofan engine

[ETsVM] (ЭЦВМ) computer - electronic digital computer

11 .

At present gas turbine engines hold the ruling position in aviation. In accordance with this the front of the scientific work in the region of study of these engines was considerably expanded. The complexity of GTE of latter generations makes their calculations more laborious. It is logical, that the acute necessity of the rapid and precise thermodynamic calculation of these engines arises. For the acceleration of calculations, computers are being ever more widely applied. The necessity of more precise methods of thermodynamic calculation is especially strongly perceived in the case of investigation high-temperature DTRD with high compression ratios and bypass configuration. This problem is no less acute during studies of engines for supersonic aircraft.

One ought to consider the method of calculation of gas turbine engines, based on the application of thermodynamic tables, most adequate for accuracy and simplicity. Such tables on the basis of the newest data on the specific heat of gases were compiled in 1956 by V. M. Dorofeyev. The tables give the thermodynamic functions for air and combustion products of standard kerosene.

The method of calculation of DTRD by application of tables of thermodynamic functions can be easily used also for machine calculation, however in this case it is necessary to encumber the memory unit of the computer by a large quantity of tabulated data. The subsequent selection of these data and their unavoidable interpolation substantially complicate the program and increase calculation time. It is completely understandable that such an approach is acceptable in the case of applying large computers of the "Minsk-22" type.

In the case of the application of small-scale computers of the type of "Promin'" etc., it is necessary either to simplify procedure with a loss of accuracy, or to search for adequate methods of approximation of thermodynamic functions by equations.

12

The proposed method for the calculation of GTE is based on approximation by polynomials of the basic thermodynamic functions. Such an approach maximally decreases the necessity to have large immediate access memory, since the relatively small quantity of the initial values and coefficients is easily introduced directly from a console.

During the calculation of the processes of compression and expansion for a GTE it is necessary and sufficient to have the following analytical expressions of thermodynamic functions for air ($\alpha = \infty$) and pure combustion products ($\alpha = 1$)

$$i = f(T); \quad T = \varphi(i) \text{ and } \Delta S = \psi(\Delta T; \bar{T}),$$

and for the calculation of combustion chambers (basic and booster) – cofunction $f(T^*)$.

The analytical expressions of thermodynamic functions $i = f(T)$ and $T = \varphi(i)$ were obtained by means of the approximation of the tabulated data polynomials of the form:

$$i = aT^4 + bT^3 + cT^2 + dT \tag{1}$$

and

$$T = \alpha i^4 + \beta i^3 + \gamma i^2 + \zeta i. \tag{2}$$

Approximation of thermodynamic functions by polynomials of the fourth degree makes it possible to attach equations to five points of the tabular values of these functions.

The coefficients of equations (1) and (2) were determined at reference points by the solution of systems of linear algebraic equations of the fourth order relative to these coefficients. The solution of the systems of equations was carried out on the "Promin'" computer. The values of the coefficients of equations (1) and (2) respectively for air and combustion products ($\alpha = 1$) are given in the following table:

13

Table 1.

Coeffi- cients	a	b	c	d
Air $\alpha = \infty$	$-0.10353 \cdot 10^{-10}$	$0.35002 \cdot 10^{-7}$	$-0.15931 \cdot 10^{-4}$	0.24089
Combustion products $\alpha = 1.0$	$-0.71294 \cdot 10^{-11}$	$0.21554 \cdot 10^{-7}$	$0.12027 \cdot 10^{-4}$	0.24163

Coeffi- cients	α	β	γ	ζ
Air $\alpha = \infty$	$0.90875 \cdot 10^{-8}$	$-0.7331 \cdot 10^{-5}$	$0.5910 \cdot 10^{-3}$	4.1765
Combustion products $\alpha = 1.0$	$0.25872 \cdot 10^{-8}$	$-0.12449 \cdot 10^{-5}$	$-0.1451 \cdot 10^{-2}$	4.1613

Equation of the adiabatic curve is

$$\pi = e^{\frac{\Delta S}{AR}} \tag{3}$$

in coordinates of π, and S gives the simple dependence of the compression ratio (expansion) on a change of entropy, and in the last analysis on the temperatures of the beginning and end of the processes of adiabatic compression or expansion.

Let us find dependence of ΔS on the temperatures of the beginning and end of the adiabatic processes

$$\Delta S = \int_{T_1}^{T_2} \frac{c_p}{T} dT. \tag{4}$$

14

In accordance with the form of the equation $i = f(T)$, the dependence of the true values of specific heats on the temperatures is written by the equation

$$c_p = AT^3 + BT^2 + cT + D \tag{5}$$

As a result of the integration of expression (4) taking into account equation (5) we obtain, that

$$\Delta S = \frac{A}{3}(T_2^3 - T_1^3) + \frac{B}{2}(T_2^2 - T_1^2) + c(T_2 - T_1) + D\ln\frac{T_2}{T_1}. \tag{6}$$

It is not difficult to demonstrate that the coefficients A, B, C and D unambiguously depend on the coefficients of a, b, c and d of equation (1).

Actually,

$$i = aT^4 + bT^3 + cT^2 + dT = \int\limits_0^T c_p \, dT.$$

After replacement of c_p in integrand by its value from equation (5) we obtain the equality,

$$aT^4 + bT^3 + cT^2 + dT = \frac{A}{4}T^4 + \frac{B}{3}T^3 + \frac{C}{2}T^2 + DT,$$

from which it follows that

$$A = 4a; \quad B = 3b; \quad C = 2c \text{ and } D = d.$$

Then expression (6) is finally written:

$$\Delta S = \frac{4}{3}a(T_2^3 - T_1^3) + \frac{3}{2}b(T_2^2 - T_1^2) + 2c(T_2 - T_1) + d\ln\frac{T_2}{T_1}. \tag{7}$$

i.e., they obtained thermodynamic function $\Delta S = \psi(\Delta T; T)$, which makes it possible to determine adiabatic compression or expansion ratio by equation (3) when the temperatures at the beginning and end of these processes are known.

Equations (3) and (7) can be utilized directly for determining the dynamic compression ratio $\pi_{\text{Д}}$ at the input device of the engine and the expansion ratio of gas in the turbine, π_T^*, since the initial and final temperatures for these processes are unambiguously

15

determined. It is somewhat more complex to determine the temperature at the end of the process of compression in compressor and the thermodynamic temperature in a jet nozzle, since in these cases, as a rule, they are known as π_{H}^{*} and π_{pc}. Let us show how to use equations (3) and (7) to determine the temperature at the end of the adiabatic process of compression ($T_{2\text{ад}}^{*}$) in the example of the calculation of a compressor. If π_{H}^{*} is given, then according to equation (3) we determine a change in entropy ΔS_{H}. Further for determining temperature $T_{2\text{ад}}^{*}$ with the assigned in advance accuracy equation (7) we solve by the method of successive approximations. In the first approximation of $T_{2\text{ад}}^{*\prime}$, we find according to the formula

$$T_{2\text{ад}}^{*\prime} = T_1^{*} + \frac{L_{\text{а1н}}^{*}}{102.5},$$

where

$$L_{\text{а1н}}^{*} = 102.5\, T_1^{*}\, (\pi_{\text{н}}^{*0.286} - 1).$$

That found in the first approximation of $T_{2\text{ад}}^{*\prime}$ we substitute in modified equation (7), which we will rewrite:

$$F = \frac{4}{3}\, a\, (T_{2\text{ад}}^{*3} - T_1^{*3}) + \frac{3}{2}\, b\, (T_{2\text{ад}}^{*2} - T_1^{*2}) + 2c\, (T_{2\text{ад}}^{*} - T_1^{*}), \qquad (8)$$

where

$$F = \Delta S - d \ln \frac{T_{2\text{ад}}^{*}}{T_1^{*}}. \qquad (9)$$

From expression (9) we find the new value of temperature $T_{2\text{ад}}^{*}$, i.e.,

$$T_{2\text{ад}}^{*} = T_1^{*}\, e^{\frac{\Delta S_{\text{н}} - F}{d}}.$$

The found value of $T_{2\text{ад}}^{*}$ we again substitute in (8). The process of approximation is continued, when the difference $T_{2\text{ад}}^{*n} - T_{2\text{ад}}^{*(n-1)}$ in absolute value does not become equal to or less than the preassigned value (for example $0.1°$).

The thermodynamic temperature T_5 in jet nozzle is analogously determined, if π_{pc} is known.

For determining the relative consumption of fuel m_τ both in basic and afterburners it is most convenient to use the formulas given in [1]:

a) basic combustion chamber

$$m_\tau = \frac{i_n^* - i_2^*}{\xi_{\kappa c} H_u - f(T_3^*) + i_3^*},$$ (10)

b) afterburner

$$m_{\tau \phi} = \frac{i_\phi^* - i_4^* + m_\tau [f(T_\phi^*) - f(T_4^*)]}{\xi_{\phi \kappa c} H_u - f(T_\phi^*) + i_3^*},$$ (11)

where the enthalpies i_2^*, i_3^*, i_4^* and i_ϕ^* are determined for the approximate temperatures on air.

The values of functions $f(T^*)$ in expressions (10) and (11) are given in the table located in [1]. The tabular values of functions of $f(T^*)$ are approximated with a sufficient degree of accuracy by the equation

$$f(T) = AT^3 + BT^2 + CT + D,$$ (12)

where A = -0.33025·10^{-7}
       B = 0.25084·10^{-3}
       C = 0.35186
       D = -17.533.

To evaluate the accuracy of the approximation of the basic thermodynamic functions by equations (1), (2), (7) and (12), in the following tables precise (tabular) and computed values of these functions are given.

17

Table 2.

T°K	i_s kcal/kgf $\quad i=\infty$	i_r kcal/kgf $\quad a=1,0$	Determined by formulas (11, 12)			
			$i=f(T)$		$T=\varphi(T)$	
			i_s	i_r	T_s	T_r
203,16	48,50		48,557		203,16	
403,16	96,53	100,57	96,518	100,60	402,87	402,81
603,16	145,76	153,88	145,81	153,91	602,73	602,89
803,16	197,12	210,14	197,01	210,03	803,80	803,98
1003,16	250,67	269,27	250,48	269,04	1004,1	1004,6
1203,16	306,04	330,85	306,05	330,79	1203,2	1203,6
1403,16	362,80	394,43	363,22	394,65	1400,3	1401,7
1603,16	420,64	459,58	421,08	460,01	1600,3	1600,6
1803,16	479,44	526,00	478,34	525,82	1810,5	1804,2

The comparison of precise values of the basic thermodynamic functions with the values of these functions, calculated from formulas (1), (2), (7) and (12), shows that in the temperature range in question (see Tables 2, 3 and 4) the deviation of the calculated values from their precise values does not exceed 0.5%. Keeping in mind, that tabular (precise) values of the basic thermodynamic functions in question are determined with an accuracy of 0.5% (see V. M. Dorofeyev's work "Thermodynamic Tables for the Calculation of Gas Turbine Engines"), then it is evident that the error obtained during the calculation of these functions according to formulas (1), (2), (7) and (12) does not exceed the limits of accuracy of the available tables of the basic thermodynamic functions.

Good convergence of results of the approximation of thermo-dynamic functions by the equations presented above makes it possible to apply formulas (1), (2), (7) and (12) with a sufficient degree of accuracy for the thermodynamic calculation of gas turbine engines.

Table 3. $\Delta S = \phi(\Delta T;\ T^2)$, where $\Delta T = T_2 - T_1$, and $T_{1в}^{*} = 203.16°K$; $T_{1г}^{*} = 403.16°K$.

$\Delta T°$			200	400	600	800	1000	1200	1400	1600	1800	2000
$\Delta S_в$ (1) ккал/кг·град	$\lambda=\infty$	Точные значения (2)	0,16447	0,26352	0,33699	0,39648	0,44679	0,49012	0,52895	0,56346	0,59470	0,62325
ΔS_r (1) ккал/кг·град	$\lambda=1,0$		0,10719	0,18764	0,25333	0,30928	0,35814	0,40155	0,44058	0,47603	0,50848	
$\Delta S_в$ (1) ккал/кг·град	$\lambda=\infty$	По формуле (7)	0,16420	0,26340	0,33650	0,39620	0,44660	0,49050	0,52890	0,56260	0,59150	0,61560
ΔS_r (1) ккал/кг·град	$\lambda=1,0$		0,10720	0,18750	0,25320	0,30900	0,35820	0,40160	0,44040	0,4745	0,5042	

(3)

KEY: (1) kcal/kg·deg; (2) Precise values; (3) According to formula (7).

Table 4.

$T^{*}°K$		400	600	800	1000	1200	1400	1600	1800	2000
$f(T^{*})$	Точные значения (1)	161,23	276,68	407,60	552,02	708,30	876,11	1052,64	1236,32	1425,45
$f(T^{*})$	Расч. по форму-ле (12) (2)	161,23	276,76	407,59	552,14	708,84	876,10	1052,4	1236,0	1425,4

KEY: (1) Precise values; (2) Calculation according to formula (12).

Bibliography

1. Марков Н. П., Бакулев В. И. Расчет высотно-скоростных характеристик турбореактивных двигателей. Оборонгиз. М., 1960.

2. Таблицы термодинамических свойств газов. Всесоюзный теплотехнический институт. Госэнергоиздат. М., 1956.

METHOD FOR THE CALCULATION OF DTRD
WITH HEAT RECOVERY

M. P. Budzinauskas

The work gives the procedure for approximate
computation of the parameters of efficiency of
DTRD with heat recovery in the first duct.

Principal Notations

T – temperature

p – pressure

i – enthalpy

Δi – change in enthalpy

q – heat

c – rate of flow of gas (air) stream

v – flight speed

y – bypass ratio

π – compression (expansion) ratio

G – flow rate per second

φ – velocity coefficient

$\xi_{\text{кс}}$ – coefficient of completeness of combustion

H_u – fuel heating value

c_p – specific heat at constant pressure

L_o – quantity of air theoretically necessary for complete
combustion of 1 kg of fuel

R - universal gas content

k - adiabatic index

Indices

Superscript:

* - stagnation parameter

Subscripts:

I - parameter in the first contour of engine

II - the parameter in the second contour of engine

2, 3, 4 - the parameters in characteristic cross sections of engine (see Fig. 1)

в - parameter for air

г - parameter for gases or pure combustion products

р - regeneration

т - fuel

рс - jet nozzle

Abbreviations

[DTRD] (ДТРД) - turbofan engine

[TVD] (ТВД) - turboprop engine

[KPD] (НРД) - efficiency

Introduction

The successful solution of the problem of creation of an aircraft of large passenger capacity and flying range within the framework of acceptable profitableness requires an essential reduction in the specific fuel consumption of the power plants.

The selection of engine type first of all affects the level of specific fuel consumption, however, for a passenger aircraft the possibilities of such a selection are limited. In practice, selection falls exclusively to DTRD.

A reduction in the specific fuel consumption of DTRD may be attained by an increase in the compression ratio of air in the first contour of an engine with a simultaneous increase in its bypass ratio and gas temperature in front of the turbine. The transfer to higher gas temperatures in front of the turbine makes it possible, to a great extent, to maintain sufficiently high values of the specific thrust of the engine.

The possibilities of reduced specific fuel consumption by increased efficiency of the basic engine components are very limited, and, at the present time, exhausted to a great extent.

Besides the mentioned factors which facilitate an increase in the cost-effectiveness of DTRD, the so-called regenerative method of reduction in the specific fuel consumption, which is widely applied for stationary gas-turbine power plants, is of great interest. Successful attempts at the application of a regenerative cycle for TVD are known, [1], [2] and [3].

The essence of regenerative cycle consists in the fact that the preheating of air entering the combustion chamber, the heat of the gases which escape from the first contour of the DTRD is partially utilized. Thus, the degree of the preheating of air in the combustion chamber, and, accordingly, also fuel consumption is reduced.

The schematic diagram of DTRD with heat recovery is depicted on Fig. 1. The reaction gases of the basic contour are guided to the heat exchanger arranged directly after the turbine where part of the heat is given up to the compressed air which enters the

combustion chamber from the compressor. Reaction gases, in their turn, passing through the heat exchanger, are cooled.
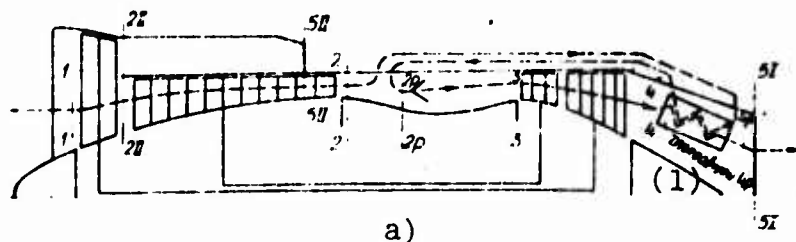

Fig. 1. Schematic diagram of a turbofan engine with heat recovery.
KEY: (1) Heat exchange.

Method of Calculation

The gas-dynamic and thermal design of DTRD, which work on a regenerative cycle, is performed into two stages. During the first stage the parameters of gas in the basic sections of the turbo-compressor part of the engine and the relative consumption of fuel ($m_\text{T} = G_\text{T}/G_\text{в1}$) are calculated according to the usual procedure with the use of the well-known equations and formulas of the theory of turbofan engines [4]. The findings are accepted as initial and utilized in the second stage for determining the basic parameters of DTRD with heat recovery.

The regenerative cycle is considered given, if, besides the basic initial parameters and the coefficients of the particular losses of the usual cycle of a DTRD the degree of regeneration of heat η_p is known and total pressure losses σ_p^* along air and gas circuits of the heat exchanger are known.

By the degree of regeneration of heat is meant the relationship of the actual preheating of air $T_{2p}^* - T_2^*$ in the regenerator to the theoretically possible preheating $T_4^* - T_2^*$, i.e.,

$$\eta_\text{p} = \frac{T_{2p}^* - T_2^*}{T_4^* - T_2^*}. \qquad (1)$$

23

The total pressure losses along the air and gas circuits of the regenerator are estimated by the total pressure recovery coefficient.

$$\sigma_p^* = \eta_{\text{в.тр}}^* \sigma_{\text{г.тр}}^*,\qquad (2)$$

where $\sigma_{\text{в.тр}}^* = p_{2p}^*/p_p^*$ - the total pressure recovery coefficient in the air circuit of the regenerator system; $\sigma_{\text{г.тр}}^* = p_{4p}^*/p_4^*$ - the total pressure recovery coefficient in the gas circuit of the regenerator.

On the basis of the findings of calculating the turbo-compressor portion of the initial DTRD, the further calculation of the parameters of efficiency of an engine with heat recovery is conducted from the determination of the relative fuel consumption $m_{\text{тр}}$ ($m_{\text{гр}} = G_{\text{тр}}/G_1$, where $G_{\text{тр}}$ is conducted the fuel consumption per second of a DTRD with heat recovery).

For determining the relative fuel consumption let us write the equation of energy for two cross sections (at compressor and the combustion chamber outlet) of the first contour of a DTRD.

$$(1 + m_{\text{тр}} - m_{\text{отл}})\, i_s^* = (1 - m_{\text{отл}})\, i_2^* + (1 - m_{\text{отл}})\, \Delta i_p^* + $$
$$+ (1 - m_{\text{отл}})\, q_p + m_{\text{тр}}\, i_{0,}$$

where

$$m_{\text{отл}} = \frac{G_{\text{отл}}}{G_1}.$$

The latter equation is solved in conjunction with the equation of heat balance in the combustion chamber of the engine

$$\xi_{\text{кс}}\, H_u\, m_{\text{тр}} = (1 - m_{\text{отл}})\, q_p.$$

Bearing in mind, that

$$i_3^* = \frac{(1 + L_0)\, m_{\text{тр}}}{1 + m_{\text{тр}} - m_{\text{отл}}}\, i_{3r}^* + \left[1 - \frac{(1 + L_0)\, m_{\text{тр}}}{1 + m_{\text{тр}} - m_{\text{отл}}} \right] i_{3_в}^*.$$

where i_{3r}^* and i_{3B}^* - correspondingly the total enthalpies of air and pure combustion products at the entry to turbine; after simple, but bulky transforms we will obtain

$$m_{rp} = (1 - m_{0x.1})\, m_r \left(1 - \frac{T_{2p}^* - T_2^*}{T_3^* - T_3^*}\right).$$

From expression (1) it follows that

$$T_{2p}^* - T_2^* = (T_4^* - T_2^*)\, \eta_p.$$

Then finally

$$m_{rp} = (1 - m_{0x.1})\left(1 - \frac{T_4^* - T_2^*}{T_3^* - T_2^*}\, \eta_p\right) m_r. \tag{3}$$

For determining the specific thrust of the first contour of a DTRD with heat recovery we find the exhaust gas velocity from the nozzle of this contour:

$$C_{51p} = \tau_{pc1}\sqrt{2g\frac{k_r}{k_r - 1}\, R_r\, T_{4p}^* \left(1 - \frac{1}{\pi_{pc1p}^{*\frac{k_r-1}{k_r}}}\right)}. \tag{4}$$

The temperature T_{4p}^* can be found from the equation of heat flow through the heat-transmitting surfaces of the regenerator.

$$C_{pr}\,(1 + m_{rp})\,(T_4^* - T_{4p}^*) = C_{pa}\,(1 - m_{0x.1})\,(T_{2p}^* - T_2^*).$$

Since

$$T_{2p}^* - T_2^* = \tau_{ip}\,(T_4^* - T_2^*),$$

then

$$T_{4p}^* = T_4^* - \eta_p'\,(T_4^* - T_2^*), \tag{5}$$

where

$$\eta_p' = \frac{C_{pa}}{C_{pr}}\left(\frac{1 - m_{0x.1}}{1 + m_r}\right)\tau_{ip}.$$

25

Finally, the degree of expansion of gases in the jet nozzle of the first of a DTRD with heat recovery we find according to the formula:

$$\tau_{pclp}{}^{\bullet} = \sigma_p{}^{\bullet} \cdot \pi_{pcl}{}^{\bullet}. \tag{6}$$

In formula (6) π_{pcl}^{*} is the degree of expansion of gases in the jet nozzle of the first contour of the initial DTRD.

The specific thrust of the first contour of a DTRD with heat recovery will be

$$R_{yalp} = \frac{C_{slp} - v}{g}.$$

Then the specific thrust of a DTRD with heat recovery is written:

$$R_{ya\,p} = \frac{R_{yalp} + y R_{yall}}{1 + y}. \tag{7}$$

Finally, the specific fuel consumption of a DTRD with heat recovery is determined from the formula:

$$C_{ya\,p}^{\bullet} = 3600 \frac{m_{1p}}{R_{ya\,p}}. \tag{8}$$

Thus, formulas (3-8) at given values of η_p and σ_p^{*} make it possible to accomplish the successive calculation of the basic parameters of the efficiency of a turbofan engine with heat recovery according to the available data of initial DTRD.

Bibliography

1. Jaffe M. L. Allison plans regenerative engine family — Aviation Week, vol. 80, № 9, 1964.

2 Савостин А. Ф. Тихонов Н. Д. О применении регенерации сила и повышенных температур газа в вертолетных газотурбинных двигателях. Сборник статей Вертолетные газотурбинные двигатели. Изд. Машиностроение», М., 1966.

3. Interavia Review, № 11, 1964 г.

4. Клячкин А. Л Теория двухконтурных ВРД ПКВИЛАВУ, Рига, 1959.

STUDY OF THE EFFICIENCY OF A DTRD WITH HEAT RECOVERY

M. P. Budzinauskas

In the article are given some results of the investigation of the basic technical and economical indices of DTRD with heat recovery and long-distance main-line aircraft equipped by engines of this type.

Principal Notations

T_3^* - gas temperature before the turbine

$\pi_\text{к}^*$ - the compression ratio of air in compressor

$\pi_\text{в}^*$ - the compression ratio of air in ventilator

y - a bypass ratio

$\eta_\text{к}^*$ - compressor efficiency

$\eta_\text{в}^*$ - the efficiency of ventilator

$\eta_\text{т}^*$ - the efficiency of turbine

η_p - regeneration effectiveness[1]

σ_p^* - total pressure recovery factor in air and gas circuits of the regenerative system

$\sigma_\text{вх}^*$ - total pressure recovery factor in input device

---

[1]See page 23 of this collection.

$\sigma^*_{\text{кс}}$ - total pressure recovery factor in combustion chamber

$\xi_{\text{кс}}$ - completeness of combustion coefficient

$\varphi_{\text{рс}}$ - the velocity coefficient of jet nozzle

$C_{\text{уд}}$ - specific fuel consumption

$R_{\text{уд}}$ - specific thrust of the engine

$\overline{G}_{\text{пер}} = G_{\text{пер}}/G_{\text{вI}}$ - relative weight of the regenerative system, where $G_{\text{пер}}$ - weight of regenerative system; $G_{\text{вI}}$ - the flow rate per second of the air through the first contour of the engine

H - flight altitude

M - Mach number of flight

Indices

Superscript:

* - stagnation parameter

Subscript:

I - parameter in the first contour of engine

II - parameter in the second contour of engine

эк - economic

Contractions

[DTRD] (ДТРД) - turbofan engine

[GTE] (ГТД) - gas turbine engine

Introduction

The creation of subsonic main-line aircraft with a flying range of up to 15,000 km is possible in the presence of highly economical engines. The specific fuel consumption of such engines at a cruise setting (H = 11 km and M = 0.8) should be found within the limits from 0.5 to 0.53. Such a high cost-effectiveness of a

DTRD can be achieved either by an increase in the compression ratio of air in the first contour of the engine with a high bypass ratio and gas high temperature before the turbine or by use of a DTRD with heat recovery.

In this article are given some results of the investigation both of DTRD with the heat recovery and the long-distance main-line aircraft equipped with these engines.

The regenerative system of a DTRD with heat recovery always includes a heat exchanger (see Fig. 1 in the foregoing article).[1] For a transport GTE heat exchangers both of the recuperative type and periodic action with a rotating matrix ("rotating") are used. The "rotating" heat exchangers differ by the great compactness of the heat-transmitting elements, however the large weight of auxiliary parts impedes a creation of sufficiently light (engines) for application in aviation constructions. Furthermore, the presence of seals in the heat exchangers of this type limits the possibilities of use of elevated temperatures and compression ratios of the cycle, and the unavoidable overflow of air into engine cavity after the turbine lowers the effect of heat recovery. Thus, during selection of the fundamental characteristics of the regenerator η_p and σ_p, the use of tubular construction of the recuperative heat exchanger was proposed with the cold air duct within the tubes. The studies of recent years of regenerators of this type [1], [2] and [3] show that they can be made sufficiently lightly and compactly. From work [3] it follows that it is virtually possible to obtain a degree of heat recovery of $\eta_p = 0.75$, in this case the coefficient of retention of total pressure σ_p^* of approximately 0.914 in the air and gas circuits is obtained. The values η_p and σ_p^* were stated as the basis of the calculation of a DTRD with heat recovery.

---

[1] See page 23 of this collection.

In this article the results of the investigation of DTRD with $T_3^* = 1600°K$ over a wide range of change in the remaining operating conditions parameters ($\pi_{\text{к}I}^* = 5\text{-}20$, $y = 2\text{-}10$) are represented, with flight conditions $H = 11$ km and $M = 0.8$. Thus were accepted the following values of the coefficients of partial losses:

$$\sigma_{\text{вх}}^* = 0{,}98; \quad \sigma_{\text{кс}}^* = 0{,}96; \quad \xi_{\text{тс}} = 0{,}99;$$

$$\eta_{\text{к}I}^* = 0{,}85; \quad \eta_{\text{к}\text{в}}^* = 0{,}89; \quad \eta_{\text{т}}^* = 0{,}91; \quad \xi_{\text{рсI}} = \xi_{\text{рсII}} = 0{,}99.$$

The determination of the parameter of DTRD efficiency of the regenerative cycle was carried out according to the methods given in the foregoing article.[1]

Results of the Study of DTRD with
Heat Recovery

Figures 1-4 depicts the calculated dependences of the specific fuel consumption of a DTRD on the compression ratio of air in the second contour $\pi_{\text{в}}^*$ and on the bypass ratio y at different values of $\pi_{\text{к}I}^*$. The presented graphic dependences make it possible to visually estimate the possibilities of a reduction in the fuel consumption during heat recovery and to optimize engines according to compression ratios in contours.

The comparison of those dependences given in Figs. 1-4 for the simple and regenerative cycles of a DTRD (using identical operating condition parameters) shows that, in the first place, the cost-effectiveness of the engine substantially improves from heat recovery; in the second place, in the case of applying heat recovery smaller values of economic compression ratios in the second contour are obtained.

---

[1] See page 23 of this collection.
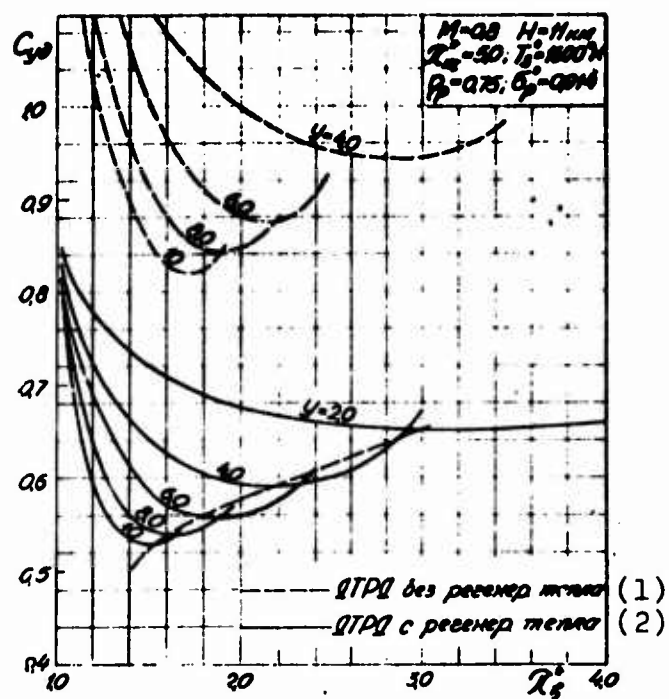
Fig. 1. Dependence of $C_{уд}$ on $\pi_в^*$ and y with $\pi_{нI}^* = 5.0$.

KEY: (1) DTRD without heat recovery; (2) DTRD with heat recovery.
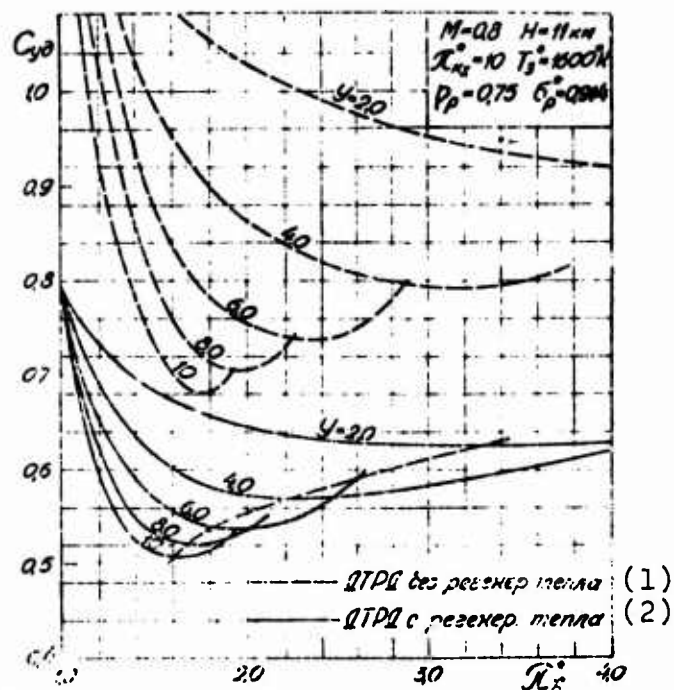

Fig. 2. Dependence of $C_{уд}$ on $\pi_в^*$ and y with $\pi_{нI}^* = 10$.

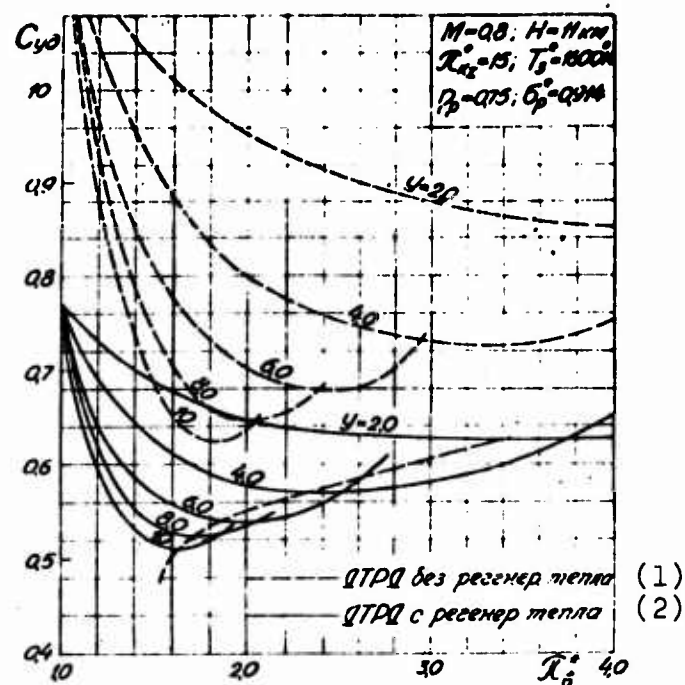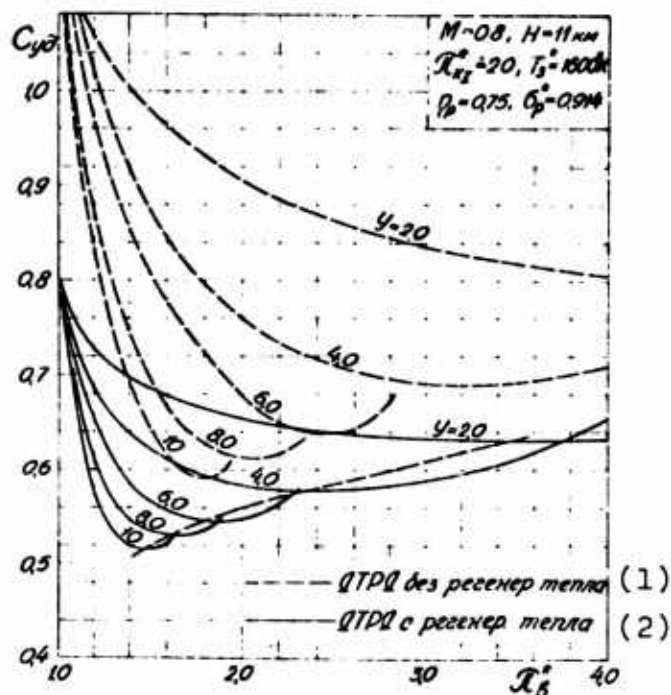KEY: (1) DTRD without heat recovery; (2) DTRD with heat recovery.

Fig. 3. Dependence of $C_{уд}$ on $\pi_{в}^{*}$ and y with $\pi_{кI}^{*} = 15$.

KEY: (1) DTRD without heat recovery;
(2) DTRD with heat recovery.

Fig. 4. Dependence $C_{уд}$ on $\pi_{в}$ and y with $\pi_{кI}^{*} = 20$.

KEY: (1) DTRD without heat recovery;
(2) DTRD with heat recovery.

For example from the graphs of Fig. 2 it is obvious, that with y = 2, the reduction of $C_{уд}$ because of heat recovery is 31.5%, and with y = 10, $C_{уд}$ drops to 25.7%.
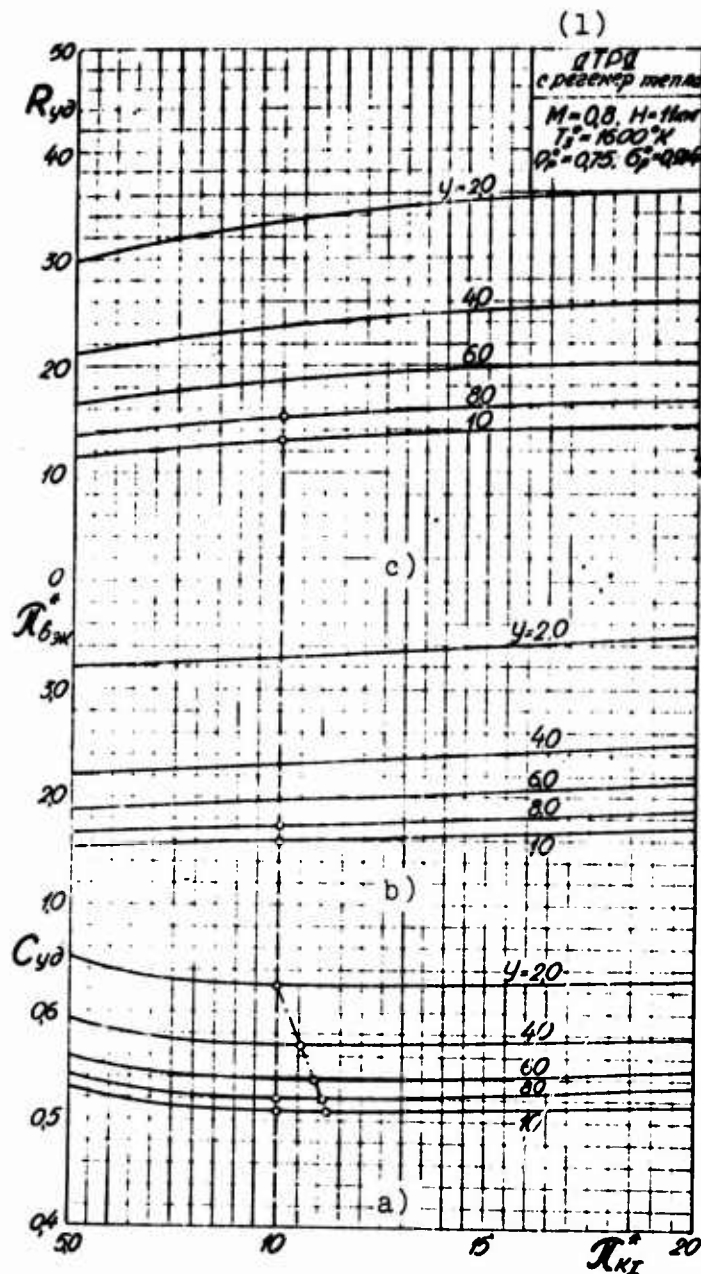
Fig. 5. Dependence of $C_{уд}$ $\pi_{в\ эк}$ and $R_{уд}$ on $\pi^*_{кI}$. (Results of the optimization of a DTRD with heat recovery for $C_{уд}$).

KEY: (1) DTRD with heat recovery.

The results of the optimization of the DTRD regenerative cycle according to specific fuel consumption depending on the compression ratio in the first contour and on the bypass ratio are given in Fig. 5a. These graphic dependences were constructed according to the data presented in Figs. 1-4 by selection of minimum values of $C_{y\text{д}}$ dependent on y and $\pi^*_{\text{к}I}$. The economic values of compression ratio in the second contour (Fig. 5c) correspond to these minimum values of $C_{y\text{д}}$. Furthermore, Fig. 5 depicts the corresponding values of $R_{y\text{д}}(c)$.

The analysis of the results of the optimization of engines for $C_{y\text{д}}$ shows that the economic values of $\pi^*_{\text{к}I}$ dependent on y are located in the interval of 10-13. The exclusively flat minimum of these dependences makes it possible to consider that for all values of y (from 2 to 10) $\pi^*_{\text{к}I\ \text{эк}} = 10$. To select lower values $\pi^*_{\text{к}I}$ is inexpedient, since this leads to a sharper reduction of $R_{y\text{д}}$ (see Fig. 5c).

The obtained minimum values of $C_{y\text{д}}$ for engines with heat recovery with $\pi^*_{\text{к}I} = 10$ (see Fig. 5a) in cruising flight and also possible to achieve for DTRD, that work on a simple cycle, by a very considerable increase in the compression ratio of the first contour compressor.

Figure 6 depicts a dependence of $C_{y\text{д}}$ and $R_{y\text{д}}$ on $\pi^*_{\text{к}I}$ for a simple DTRD. The comparison of the graphs presented in Fig. 5a and b shows that, for example, with y = 10, the level of $C_{y\text{д}}$ of a simple DTRD becomes the same as of the engine which works on regenerative cycle, only when the compression ratio $\pi^*_{\text{к}I} = 58$, but with y = 8, the identical specific fuel consumptions will be when $\pi^*_{\text{к}I} = 65$. The fact that the compared engines have virtually identical specific thrusts (see Figs. 5c and 6) is remarkable.
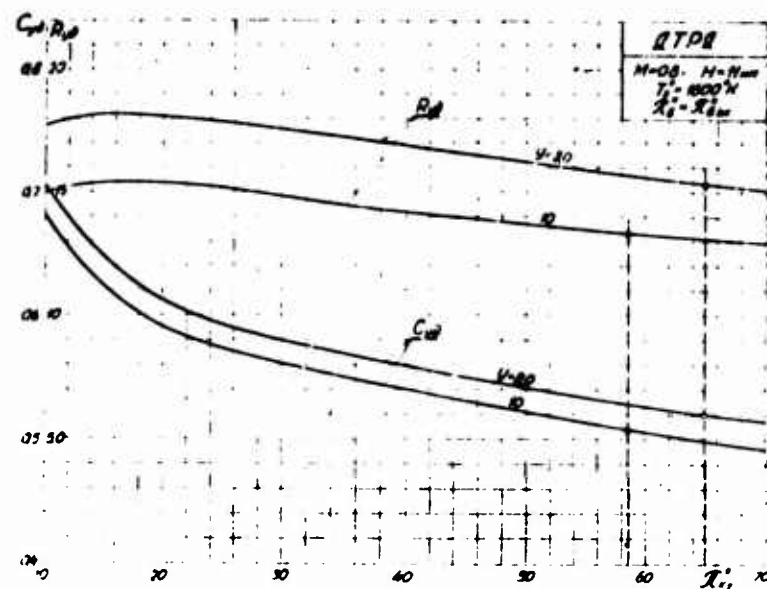
Fig. 6. Dependence of $C_{уд}$ and $R_{уд}$ on $\pi^*_{кI}$ for a simple DTRD.

The reduction of $C_{уд}$ both by heat recovery and by an increase in the compression ratio $\pi^*_{кI}$ unavoidably leads to an increase in the specific weight of the engine. In the first case the specific weight of the engine increases due to the weight of regeneration system, and in the second - due to a gain in weight of the turbo-supercharger and engine block.

The approximate estimate of the specific weight of the compared engines (having identical $C_{уд}$), shows that a simple DTRD, with $\pi^*_{кI} = 58$ and $y = 10$, has a specific weight up to 16% greater than a DTRD with heat recovery ($\pi^*_{кI} = 10$; $y = 10$ and $\overline{G}_{рег} = G_{рег}/G_I = 26$).

Results of the Study of DTRD Equipped
Aircraft with Heat Recovery

The study of the efficiency of long-distance aircraft equipped with DTRD with heat recovery is of great interest. These studies were carried out on the assumption that the operating conditions parameters of the engines were selected from the condition of ensuring minimum fuel consumption in cruising flight. DTRD with heat

35

recovery, that have T_3^* = 1600°K, $\pi_{\text{к}I}^*$ = 10, $\pi_{\text{в}}^*$ = 1.59 and y = 10 (see Fig. 2) correspond to the condition of a minimum $C_{\text{уд}}$.

The studies of the parameters of aircraft efficiency were carried out according to the methods given in work [4].

Since, at present, reliable data on the structural efficiency factor of heat exchangers with the increased degree of heat regeneration are lacking, during the calculations the relative weight of regenerator $(\overline{G}_{\text{per}})$ was varied within the limits from 4.0 to 26.

As one would expect with an increase of the relative weight of the regenerator the basic parameters of the efficiency of the aircraft studied deteriorate somewhat. For example, with increase $\overline{C}_{\text{per}}$ from 4.0 to 26, the takeoff weight and the prime cost of transport with a given flying distance respectively increase by 0.5 and 4.0 percent.

In the following table are presented the results of the study of the basic parameters of the efficiency of aircraft equipped both simple DTRD and those with heat recovery. In this case the relative weight of the regenerator was taken as $\overline{G}_{\text{per}}$ = 26.

From the comparison of the data presented in the table, it is apparent that according to the basic indices ($G_{\text{вз}л}$ and a), aircraft which have DTRD with heat recovery are indisputably more profitable, than aircraft equipped with simple DTRD. For example, because of the application of heat recovery, $G_{\text{вз}л}$ for aircraft Nos. 1, 2, 3 and 4 descends to 2.1, 10, 3.7 and 10.7 percent. In this case the prime cost of transport correspondingly drops to 1.44; 9.75; 3.34 and 10.4 percent. A more noticeable reduction both of takeoff weight and prime cost of transport is observed for long-distance aircraft No. 2 and No. 4.

36

Table.

(1) Самолет (2) Показатели	№ 1		№ 2		№ 3		№ 4	
	ДТРД (3) без регенер.	ДТРД (4) с регенер.	ДТРД без регенер.	ДТРД с регенер.	ДТРД без регенер.	ДТРД с регенер.	ДТРД без регенер.	ДТРД с регенер.
(5) Дальность L (км)	8000	8000	15000	8000	8000	8000	15000	15000
(6) Число пассажиров (n)	250	250	125	125	50	500	250	250
(7) Взлетный вес самолета $G_{взл}$	143	140	180	162	241	232	272	243
(8) Коммерческая нагрузка $G_{к.т}/\xi_к$	25 0,175	25 0,178	12,5 0,069	12,5 0,077	50 0,207	50 0,216	25 0,092	25 0,103
(9) Силовая установка $G_{су.т}/\xi_{су}$	10,1 0,07	9,8 0,071	14,0 0,077	11,2 0,069	19,1 0,079	16,7 0,072	20,9 0,077	16,5 0,08
(10) Себестоимость перевозок a коп/т км	6,95	6,85	14,85	13,40	5,38	5,20	9,38	8,40

KEY: (1) Aircraft; (2) Indices; (3) Turbofan without regen; (4) Turbofan with regen; (5) Distance L (km); (6) Number of passengers (n); (7) Aircraft takeoff weight $G_{взл}$; (8) Freight load $G_{к.т}/\xi_к$; (9) Power plant $G_{су.т}/\xi_{су}$; (10) Prime cost of transport A, коp/t km.

In conclusion it should be noted that at present on the way to practical implementation of DTRD, that work with a regeneration cycle, the main obstructions are the unsatisfactory performing characteristics, reliability, and structural efficiency factor of existing small-scale heat exchangers.

Conclusions

1. The studies carried out show the possibility in principle and the advisability of the creation of DTRD with heat recovery. When $T_3^* = 1600°K$; $\pi_{кI}^* = 10$, $\eta_p = 0.75$, and $\sigma_p^* = 0.914$, such engines will have $C_{уд} \cong 0.5$ kg/kg·hr.

2.   In comparison with simple DTRD, the minimum specific fuel consumption for DTRD with heat recovery is reached with substantially lower compression ratios of air in the first contour ($\pi^*_{\kappa I} \approx 10$).   For an optimum DTRD with heat recovery for C_{y_A} lower compression ratios are also required in the second contour (see Figs. 1, 2, 3 and 4).

3.   The application of DTRD with a regenerative cycle, makes it possible to raise the efficiency of long-distance main-line aircraft even with the low structural efficiency factor of the regeneration system.   The prime cost of transport in the case of applying engines with heat recovery, depending on the calculated flying range, drops from 1.44 to 10.4 percent (see table).

Bibliography

1. Гельфенбейн Л. Г. Регенераторы газотурбинных установок Машгиз, М., 1963.
2. F l i g h t, XI, № 2905, 1964.
3. I n t e r a v i a R e v i e w, № 11, 1964
4. Труды РКИИГА имени Ленинского комсомола, вып. 164, 1971 г «Влияние параметров ДТРД на технико-экономические характеристик дальних магистральных самолетов».

EFFECT OF THE SMALL DEVIATIONS OF OPERATING CONDITIONS AND LIGHT CONDITIONS PARAMETERS ON THE SPECIFIC PARAMETERS OF DTRD

V. P. Labendik

In the article the application of a method of low deviations is examined for the analysis of the efficiency and cost-effectiveness of a twin-shaft DTRD.

Working formulas for the calculation of coefficients of the influence of operating conditions and flight conditions parameters on specific engine characteristics are given. As an example the values of coefficients of influence are given with concrete data in connection with twin-shaft DTRD and the results of the calculation are analyzed.

Introduction

When selecting the basic operating conditions parameters of the projected engines it requires finding their optimum relationship for the assigned flight mode, and for this it is necessary to know how and to what degree the given parameters in the range in question affect the efficiency and the cost-effectiveness of the engine; a change in which of them causes the greatest effect. In other tasks it is required to obtain specific engine characteristics with the same initial parameters, but for several distinct flight conditions;

39

at other values of the loss factor, efficiency and so on. In this case it is necessary to calculate a series of variants which differ by a small change in the initial values.

These results can be obtained, and without resorting to repeated, sufficiently bulky calculations of the engine by the usual methods. As a simpler and more demonstrative method of solution it is convenient to use the method of small deviations.

When using this method it is necessary to conduct the gas-dynamic calculation and to determine the operating conditions parameters only for the initial system in question. The use of relationships of the low deviations method actually means the linearization of the initial equations of the process which considerably simplifies the analysis of the dependences between the increments of the connected parameters.

The system of fundamental equations in small deviations is obtained by differentiation of the usual equations of [GTE] (ГТД) operating conditions. The solution of the quite complex system of the latter is reduced to the solution of a system of linear equations, which substantially reduces the volume of calculation work. Independent from the complexity of the problem, the number of variables, and the nature of the connections between them, a solution can be obtained in the form of an explicit analytical dependence, which allows study in general form.

The limiting value of parameters changes, with which the use of a method of small deviations is possible, is determined by the value of permissible error of the final result. The relative changes of specific thrust and specific fuel consumption, connected with the deviation of any parameter by 10-15%, are almost exactly defined as the product of a relative change of the given parameter by the numerical value of the coefficient of influence [1]. The total values $\delta R_{уд}$ and $\delta C_{уд}$ during a change in several parameters are defined as the algebraic sums of the corresponding partial increases.

The calculation of the numerical coefficients of influence in general solutions turns out to be sufficiently simple. In all cases the range of applicability of the method of small deviations is expanded with an increase in the initial values of π_H^*, π_T^*, T_3^*, etc.

§ 1. Equations of Operating Conditions
of the Basic Elements of DTRD in Small
Deviations

Let us compose the fundamental equations of the process in the elements of a twin-shaft DTRD with separate exhaust from jet nozzles with complete gas expansion, and with air bleed due to compressor on the cooling of high-pressure turbine.

Let us assume

$$\pi_{\text{кII}}^* = \pi_{\text{кнд}}^*.$$

We will designate coefficients of influence for the entire engine in terms of K, for the low-pressure [LP] (НД) stage and the ventilator - A, and for the [VD] (ВД) stage - B with corresponding indexes.

The specific thrust of a DTRD is equal to

$$R_{y\text{д}} = \frac{R_{y\text{дI}} + y R_{y\text{дII}}}{1 + y}.$$

Logarithmizing and differentiating this expression, we obtain the connection between the relative increases:

$$\frac{d R_{y\text{д}}}{R_{y\text{д}}} = \frac{d R_{y\text{дI}}}{R_{y\text{дI}} + y R_{y\text{дII}}} + y \frac{d R_{y\text{дII}}}{R_{y\text{дI}} + y R_{y\text{дII}}} +$$
$$+ \left(\frac{R_{y\text{дII}}}{R_{y\text{дI}} + y R_{y\text{дII}}} - \frac{1}{1+y} \right) d y. \tag{1}$$

Let us introduce designations $\Delta R_{уд}/R_{уд} \approx dR_{уд}/R_{уд} = \delta R_{уд}$, etc. Then equation (1) is written in the following form:

$$\delta R_{уд} = K_1 \delta R_{удI} + (1 - K_1)\delta R_{удII} + (1 - K_1 - K_2)\delta y, \tag{1a}$$

where

$$K_1 = \frac{R_{удI}}{R_{удI} + y R_{удII}};$$

$$K_2 = \frac{y}{1+y}.$$

Specific thrust of contour I is:

$$R_{удI} = \frac{C_{5I} - V}{g} = \frac{1}{g}(\tau_{pc} \sqrt{2310 T_4^* \tau_{pcI}^*} - V).$$

Correspondingly, after logarithmic operation and differentiation, this expression in small deviations will take the form:

$$\delta R_{удI} = \frac{1}{2}K_3(2\delta\tau_{pcI} + \delta T_4^* + K_4\delta\pi_{pcI}) - (K_3 - 1)\delta V. \tag{2}$$

where

$$K_3 = \frac{c_{5I}}{g R_{удI}} = 1 + \frac{V}{g R_{удI}};$$

$$K_4 = \frac{0.25}{\pi_{pcI}^{0.25} - 1};$$

$$\delta\pi_{pcI} = \delta\pi_д + \delta\pi_{кI}^* + \delta\tau_{кc}^* - \delta\pi_т^*; \tag{3}$$

$$\delta\pi_д = 3.5 K_v \delta M + \delta\sigma_{вх}^*. \tag{4}$$

$$K_v = \frac{0.4 M^2}{1 + 0.2 M^2}.$$

The temperature of gas after the turbines is

$$T_4^* = T_{4нд}^* - \frac{L_{тнд}}{118} = T_{4нд}^*(1 - \varepsilon_{тнд}^* \tau_{iтнд}^*).$$

By similtude we obtain the expression:

$$\delta T_4^* = \delta T_{4нд}^* - A_0(A_5\delta\pi_{тнд}^* + \delta\tau_{iтнд}^*), \tag{5}$$

42

where

$$A_5 = \frac{\partial L_{\text{тнд}}^*}{\delta \pi_{\text{тнд}}^*} = \frac{0{,}25}{\pi_{\text{тнд}}^{*0{,}25} - 1};$$

$$A_6 = \frac{\Delta T_{\text{тнд}}^*}{T_4^*} = \frac{1}{\dfrac{1}{\varepsilon_{\text{тнд}}^* \eta_{\text{тнд}}^*} - 1}.$$

Taking into account air bleed for the cooling of a VD turbine, gas temperature after it will be:

$$T_{4\text{вд}}^* = T_{4\text{вд}}^{*\prime}\left(1 - \frac{m_{\text{ох}}}{1 + m_{\text{т}}}\right) + T_{21}^* \frac{m_{\text{ох}}}{1 + m_{\text{т}}}.$$

For $T_{4\text{вд}}^*$, let us write the equation in small deviations

$$\delta T_{4\text{вд}}^* = K_7 \delta T_{4\text{вд}}^{*\prime} + (1 - K_7)\delta T_{21}^* + K_7' \delta m_{\text{т}}, \tag{6}$$

where

$$K_7 = \frac{T_{4\text{вд}}^{*\prime}}{T_{4\text{вд}}^*}\left(1 - \frac{m_{\text{ох}}}{1 + m_{\text{т}}}\right);$$

$$K_7' = \frac{T_{4\text{вд}}^{*\prime} - T_{21}^*}{T_{4\text{вд}}^*} \cdot \frac{m_{\text{ох}} m_{\text{т}}}{(1 + m_{\text{т}})^2} \approx 0;$$

$$T_{4\text{вд}}^{*\prime} = T_3^* - \frac{L_{\text{твд}}}{118};$$

$$\delta T_{4\text{вд}}^{*\prime} = \delta T_3^* - B_6(B_5 \delta \pi_{\text{твд}}^* + \delta \eta_{\text{твд}}^*). \tag{7}$$

Coefficients B_5 and B_6 are analogous to A_5 and A_6

$$m_{\text{т}} = \frac{C_{\text{pm}}(T_3^* - T_2^*)(1 - m_{\text{ох}})}{\xi_{\text{кс}} H_u};$$

$$\delta m_{\text{т}} = K_5 \delta T_3^* - (K_6 - 1)\delta T_{21}^*. \tag{8}$$

where

$$K_5 = \frac{T_3^*}{T_3^* - T_{21}^*}.$$

The temperature of air after compressor contour I is

$$T_{21}^* = T_1^* + \frac{L_{\text{к1}}}{102{,}5} = T_1^*\left(1 + \frac{\varepsilon_{\text{к1}}^*}{\eta_{\text{к1}}^*}\right).$$

43

In small deviations this expression will be written:

$$\delta T_{2I}{}^* = \delta T_1{}^* + K_{10}(K_9 \delta \pi_{\kappa I}{}^* - \delta \eta_{\kappa I}{}^*), \tag{9}$$

where

$$K_9 = \frac{\delta L_{\kappa I}}{\delta \pi_{\kappa I}{}^*} = \frac{0,286 \pi_{\kappa I}{}^{*0,286}}{\pi_{\kappa I}{}^{*0,286} - 1};$$

$$K_{10} = \frac{\Delta T_{\kappa I}{}^*}{T_{2I}{}^*} = \frac{1}{1 + \dfrac{\eta_{\kappa I}{}^*}{\varepsilon_{\kappa I}{}^*}}.$$

$$\delta T_1{}^* = \delta T_{\text{H}} + K_v \delta M = K_{\text{H}} \delta H + K_v \delta M, \tag{10}$$

where

$$K_{\text{H}} = 1 - \frac{288}{T_{\text{H}}} = -\frac{6,5}{T_{\text{H}}} \quad \text{when } H \leq 11 \text{ km};$$

$$K_{\text{H}} = 0 \quad \text{when } H > 11 \text{ km}.$$

Specific thrust of contour II is

$$R_{y\text{A}} = \frac{1}{g}\left(\tau_{\text{pcII}} \mid \sqrt{2010\, T_{2II}{}^* \varepsilon_{\text{pcII}}} - V\right).$$

The expression for $R_{y\text{AII}}$ in the low deviations takes the form:

$$\delta R_{y\text{AII}} = \frac{1}{2} A_3 (2\delta \tau_{\text{pcII}} + \delta T_{2II}{}^* + A_4 \delta \pi_{\text{pcII}}) \quad (A_3 - 1)\delta V. \tag{11}$$

Coefficients A_3 and A_4 are analogous to K_3 and K_4:

$$\delta \pi_{\text{pcII}} = 3,5 K_v \delta M + \delta \tau_{\text{вх}}{}^* + \delta \pi_{\text{в..}}{}^*; \tag{12}$$

$$\delta T_{2II}{}^* = \delta T_1{}^* + A_{10}{}' (A_9 \delta \pi_{\kappa II}{}^* - \delta \tau_{\text{к} II}{}^*); \tag{13}$$

$$\delta V = \delta M + \frac{1}{2} \delta T_{\text{H}}. \tag{14}$$

The specific fuel consumption of a DTRD

$$C_{y\text{A}} = 3600 \frac{m_\text{т}}{R_{y\text{AI}} + y R_{y\text{AII}}}.$$

$$\delta C_{y\text{A}} = \delta m_\text{т} - \delta R_{y\text{A}} - K_2 \delta y. \tag{15}$$

44

§ 2. The Derivation of the Generalized Coefficients of Influence of the Parameters on the Design Conditions for $R_{уд}$ and $C_{уд}$ of a DTRD

Let us find dependences $\delta R_{удI}$, $\delta R_{удII}$, $\delta R_{уд}$ and $\delta C_{уд}$ on $\delta \pi_{к}^{*}$; δy, δT_{3}^{*}, δM, δH on $\delta \eta^{*}$, $\delta \sigma^{*}$ and $\delta \varphi_{рс}$.

We begin the solution of the system of equations with compilation of the equations of the balances of power on the shafts.

For the low-pressure stage

$$L_{тнд}(1 + m_{т}) = L_{кнд} + y L_{вп},$$

$$\delta L_{тнд} = K_{11} \delta L_{кнд} + (1 - K_{11}) \delta L_{вп} + (1 - K_{11}) \delta y, \tag{16}$$

where

$$K_{11} = \frac{L_{кнд}}{L_{тнд}(1 + m_{т})}.$$

For the high pressure stage the equation of the power balance takes the form:

$$L_{квд} = L_{твд}(1 + m_{т} - m_{ох}),$$

$$\delta L_{квд} = \delta L_{твд} + \frac{\dot{m}_{т}}{1 + m_{т} - m_{ох}} \delta m_{т}. \tag{17}$$

The coefficient during $\delta m_{т}$ is sufficiently low, therefore we disregard the second term.

After substituting in (16) the expressions for $\delta L_{тнд}$, $\delta L_{кнд}$ and $\delta L_{кII}$ and in (17) for $\delta L_{квд}$ and $\delta L_{твд}$, it is possible to determine the required changes in values $\pi_{твд}^{*}$ and $\pi_{тнд}^{*}$ from these equations, dependent on the change in the remaining parameters of the engines.

The further obtained expressions, $\delta\pi^*_{\text{твд}}$ and $\delta\pi^*_{\text{тнд}}$, are substituted in (3), (5) and (7) with the replacement $\delta\pi^*_{\text{кнд}} = \delta\pi^*_{\text{кII}}$ and $\delta\pi^*_{\text{квд}} = \delta\pi^*_{\text{кI}} - \delta\pi^*_{\text{кнд}}$.

After substitution of (10) in (9), (9) in (8); (7), (8), and (9) in (6); (6) in (5); (3), (4), and (5) in (2) and some transforms, let us find the dependence $\delta R_{\text{удI}}$ on a change in the initial parameters:

$$\delta R_{yдI} = K_3 \delta z_{pcI} - \frac{1}{2} K_3 (1 - K_{11}) K_{12} \delta y -$$

$$- \frac{1}{2} K_3 \left\{ A_9 K_{12} + (A_9 A_{10} - B_{10}) \left[\frac{K_4}{B_5} + B_6 K_7 (1 + K_{12}) \right] \right\} \delta \tau_{\text{кII}}^* +$$

$$+ \frac{1}{2} K_3 (1 - K_{11}) K_{12} \delta \tau_{\text{кII}}^* + \frac{1}{2} K_3 \left\{ K_4 \left(1 - \frac{B_9}{B_5} \right) + \right.$$

$$+ (1 + K_{12}) \left[K_9 K_{10} (1 - K_7) - B_6 K_7 B_9 \right] \right\} \delta \tau_{\text{кI}}^* -$$

$$- \frac{1}{2} K_3 \left[A_{10} (1 - K_1) (1 + K_{12}) - K_{11} K_{12} - \frac{K_4 A_{10}}{B_2} \right] \delta \tau_{\text{кнд}}^* -$$

$$- \frac{1}{2} K_3 \left\{ [B_{10} (1 - K_7) - B_6 K_7] (1 + K_{12}) - \frac{K_4}{B_3} \right\} \delta \tau_{\text{кнд}}^* +$$

$$+ \frac{1}{2} K_3 \frac{K_4}{B_5} \delta \tau_{\text{гнд}}^* + \frac{1}{2} K_3 \frac{K_4}{A_6} \delta \tau_{\text{гнд}}^* + \frac{1}{2} K_3 K_4 \delta \sigma_{\text{вх}}^* + \frac{1}{2} K_3 K_4 \delta \sigma_{\text{кс}}^* +$$

$$+ \frac{1}{2} K_3 \left[(1 + K_{12}) K_{13} + \frac{K_4}{B_6} \right] \delta T_{\text{в}}^* + \left\{ (1 - K_8) - \right.$$

$$- \frac{1}{2} K_3 K_5 \left[(1 + K_{12}) K_{13} + K_4 \left(\frac{1}{B_6} - 3.5 \right) - 1 \right] \right\} \delta M +$$

$$+ \frac{1}{2} \left\{ 1 - K_3 \left[(1 + K_{12}) K_{13} + \frac{K_4}{B_5} \right] \right\} K_8 \delta H.$$

where

$$K_{12} = A_9 + \frac{K_4}{A_6};$$

$$K_{13} = K_7 (1 + B_9).$$

Substituting (12) and (13) in (11), we obtain the expression for the change in $R_{\text{удII}}$:

46

$$\delta R_{y,\text{дII}} = \frac{1}{2} A_n (A_4 + A_0 A_{1u}) \delta \tau_{\text{вII}}^{\circ} - \frac{1}{2} A_a A_{10}' \delta \tau_{\text{кII}}^{\circ} +$$

$$+ \frac{1}{2} A_3 A_4 \delta \tau_{\text{вх}}^{*} + A_n \delta \varphi_{\text{рсII}} + \frac{1}{2} K_n \delta H +$$

$$+ \left[1 - A_n + \frac{1}{2} K_0 K_v (1 + 3,5 A_4) \right] \delta M.$$

For the relative fuel consumption per second

$$\delta m_t = K_u \delta T_u^{*} + (1 - K_u) [K_u \delta H + K_v \delta M +$$

$$+ K_9 K_{10} \delta \pi_{\text{кI}}^{*} - A_{10} \delta \tau_{\text{кмд}}^{*} - B_{10} \delta \tau_{\text{квд}}^{*}].$$

With the aid of the obtained dependences it is possible to find the relative changes in $\delta R_{y\text{д}}$ and $\delta C_{y\text{д}}$ in terms of the change of the independent parameters of the process in both contours and of the flight conditions, after substituting the relationships found above for $\delta R_{y\text{дI}}$, $\delta R_{y\text{дII}}$ and $\delta m_{\text{т}}$ into equations (1a) and (15).

For the determination of the numerical values of the coefficient of influence of the parameters, it is first necessary to determine the values of the initial influence coefficients by the values of $\pi_{\text{к}}^{*}$, $\pi_{\text{т}}^{*}$, $\pi_{\text{рс}}$, T_2^{*}, T_3^{*}, T_4^{*}, $R_{y\text{д}}$, etc. It is further advantageous to calculate the values of the combined coefficients. Using the general expressions of coefficients of influence and the found values K_1, K_2, K_3, etc., the numerical values of coefficients of influence are found. It is more convenient to calculate these coefficients first for $\delta R_{y\text{дI}}$, $\delta R_{y\text{дII}}$ and $\delta m_{\text{т}}$, and then to substitute them into the expressions $\delta R_{y\text{д}}$ and $\delta C_{y\text{д}}$. The relative changes in the specific engine characteristics can be determined after multiplying the calculated coefficients of influence of the changed parameters times the relative changes in these parameters.

47

§ 3. The Analysis of the Numerical Values of the Coefficients of Influence of Selected Parameters on the Specific Characteristics of DTRD

Let us compile a numerical table of the coefficients of influence for DTRD with initial values of the parameters:

$$y = 8; \quad T_{a}^{*} = 1400°K; \quad \pi_{\kappa1}^{*} = 35;$$
$$\pi_{\kappa11}^{*} = \pi_{\kappa в д}^{*} = 1{,}5; \quad \gamma_{i к н д}^{*} = \gamma_{i к н д}^{*} = 0{,}86;$$
$$\eta_{\kappa11}^{*} = 0{,}87; \quad \eta_{i т в д}^{*} = \eta_{i т н д}^{*} = 0{,}92;$$
$$\sigma_{\kappa c}^{u} = 0{,}96; \quad \xi_{\kappa c} = 0{,}99; \quad \sigma_{в x}^{*} = 1{,}0;$$
$$\varphi_{pc1} = \varphi_{pc11} = 0{,}99; \quad m_{o x} = 0{,}08.$$

Rated flight conditions:

$$M = 0{,}8; \quad H = 11 \text{ km}.$$

Gas-dynamic and thermal design are determined by the following values of the parameters of the process:

$$T_{в11}^{*} = 278{,}5°K; \quad \pi_{pc1} = 2{,}285;$$
$$T_{в1}^{*} = 751{,}9°K; \quad L_{гнд} = 32400 \text{ kgm/kg};$$

$$L_{\kappa11} = 3540 \text{ kgm/km}; \quad T_{4вд}^{*} = 945{,}2°K;$$
$$T_{4}^{*} = 671{,}0°K; \quad \pi_{твд}^{*} = 5{,}27;$$
$$\pi_{гнд} = 4{,}53; \quad \pi_{pc1} = 2{,}15;$$
$$m_{т} = 0{,}0174; \quad R_{y.д} = 28{,}2 \text{ kg·s/kg};$$
$$R_{y.п11} = 10{,}45 \text{ kg·s/kg}; \quad R_{yд} = 12{,}41 \text{ kg·s/kg};$$
$$C_{yд} = 0{,}562 \text{ kg/kg·h}.$$

Further according to formulas we find the numerical values of the initial coefficients:

$$K_v = 0{,}227; \quad K_{_H} = -0{,}33; \quad K_1 = 0{,}252;$$
$$K_2 = 0{,}888; \quad K_3 = 1{,}858; \quad K_4 = 1{,}19;$$
$$K_5 = 0{,}207; \quad K_7 = 0{,}935; \quad K_8 = 2{,}16;$$
$$K_9 = 0{,}448; \quad K_{10} = 0{,}676; \quad K_{11} = 0{,}1105;$$
$$K_{12} = 2{,}588; \quad K_{13} = 1{,}345;$$
$$A_3 = 3{,}31; \quad A_4 = 1{,}088; \quad A_5 = 0{,}546;$$
$$A_6 = 0{,}405; \quad A_9 = 2{,}61; \quad A_{10} = 0{,}125;$$
$$B_5 = 0{,}472; \quad B_6 = 0{,}438; \quad B_9 = 0{,}482;$$
$$B_{10} = 0{,}629; \quad K_9 K_{10} = 0{,}303;$$
$$A_9 A_{10} = 0{,}326; \quad B_9 B_{10} = 0{,}303;$$
$$A_5 A_6 = 0{,}221; \quad B_5 B_6 = 0{,}207.$$

Substituting these values in the general expressions of the coefficients of influence, let us compile a numerical table of coefficients.

From the obtained table it is possible to directly define a series of the features of DTRD with the given values of the initial parameters.

So, according to the value of the coefficients of influence the advisability of increase T_3^* for increase in $R_{уд}$ is apparent, but with some increase in $C_{уд}$. An increase of $\pi_{\kappa I}^*$ and y somewhat decreases $C_{уд}$ and $R_{уд}$. The changes in $\sigma_{вх}^*$ and φ_{pcII} exert a strong influence on $R_{уд}$ and $C_{уд}$.

With the aid of the table it is possible to estimate the values of specific parameters of an engine with other initial data. Let us suppose it is necessary to calculate $R_{уд}$ and $C_{уд}$ of an DTRD with the parameters: $T_3^* = 1500°K$; $\pi_{\kappa I}^* = 40$; y = 9 during flight at H = 10 km with $M_{_H} = 0.9$.

The values of given magnitudes differ from the corresponding initial values by less than 15%. After multiplying relative changes in these parameters to the coefficients for them, and after totaling the results, it is possible to determine that $R_{уд}$ decreases by 9.56%, and $C_{уд}$ increases by 1.62%, which will comprise correspondingly: $R_{уд}$ = 11.23 kg s/kg and $C_{уд}$ = 0.571 kg/kg h.

Table. Numerical values of the coefficients of influence of the selected parameters during design on $R_{уд}$ and $C_{уд}$ of DTRD.

	$\partial R_{у.1}$	$\partial R_{у.11}$	$\delta R_{у.2}$	δm_τ	$\delta C_{у.2}$
$\delta \pi_{к1}^*$	−0,612	0	−0,154	−0,352	−0,198
$\delta \pi_{к11}^*$	−5,16	2,34	0,45	0	−0,45
δy	−2,14	0	−0,539	0	−0,349
δT_3^*	6,86	0	1,74	2,16	0,42
$\delta \eta_{к11}^*$	2,14	−0,207	0,384	0	−0,384
$\delta \eta_{кн.2}^*$	0,703	0	0,177	0,125	−0,052
$\delta \eta_{мв.2}^*$	3,58	0	0,978	0,73	−0,248
$\delta \tau_{ств.2}^*$	2,025	0	0,51	0	−0,51
$\delta \tau_{ств.2}^*$	2,343	0	0,592	0	−0,592
$\delta \sigma_{вх}^*$	1,106	1,8	1,623	0	−1,623
$\delta \sigma_{кс}^*$	1,106	0	0,278	0	−0,278
$\delta \varphi_{рс1}$	1,858	0	0,468	0	−0,468
$\delta \varphi_{рс11}$	0	3,31	2,47	0	−2,47
δM	−1,326	−0,505	−0,713	−0,264	0,449
δH	2,1	−0,165	0,406	0,383	−0,023

The method of the low deviations makes it possible, with considerably less expenditures of time, to compare a multitude of diverse variants and in the narrow area of the combinations of parameters to find their optimum relationship to provide for the required specific fuel consumption and an acceptable value of specific thrust.

Bibliography

1. Черкез А. Я. Инженерные расчеты газотурбинных двигателей методом малых отклонений. Машиностроение, М., 1965.

2. Клячкин А. Л. Теория воздушно-реактивных двигателей. Машиностроение, М., 1969.

METHOD OF CALCULATION OF THE MIXING OF GAS FLOWS IN THE DIFFUSERS OF THE AFTERBURNER MIXING CHAMBERS (AMC) OF DTRD

Ye. V. Barabanov

Accepted Designations

u - longitudinal component of flow rate;

v - transverse component of flow rate;

w - the average (by area) flow rate in a given cross section;

$\overline{c} = c_{pn1}/c_{pa1}$ - specific heat ratio of passive gas to active;

$\overline{f}_{\text{д}} = F_3/F_1$ - expansion ratio of diffuser;

$R_{\text{э}} = \sqrt{F}/\pi$ - equivalent radius of annular diffuser;

$\Theta_{\text{пр}}$ - given angle of flare of annular diffuser;

$\beta = tg\,(\Theta_{\text{пр}}/2)$ - expansion coefficient of rectilinear diffuser.

Indices

A_1 - parameters of active flow at inlet to the diffuser of an afterburner mixing chamber [AMC] (ФСН);

Π_1 - parameters of passive flow at inlet to diffuser;

I - total (averaged) parameters of the inlet to diffuser;

3 - parameters of mixed flow at output from diffuser;

a - parameters on the x axis.

51

The present work examines the overall task of calculating the mixing of gases, differing in chemical composition, (c_p and χ) in the annular channel of a variable cross section, which has a direct relationship to the design and study of the mixing chambers of [DTRDF] (ДТРДФ), and also the different compound propulsion systems ([TJE] (ТПД), [TJEW AB] (ТРДФ) + [RJE] (ПВРД), DTRDF + RJE, etc.) in the diffuser of their area behind the turbine.

Unfortunately, the predominant majority of known methods of calculation [6] is related to cylindrical mixing chambers and cannot be completely used by us in the present work. Thus this article is dedicated to the construction of the analytical method of calculation of the mixing of heterogeneous flows in the diffuser with the purpose of calculation of $\int p \, dF$, which, unlike cylindrical channels, in a diffuser is not equal to zero and introduces a substantial change in the entire procedure of calculation.

§ 1. Basic Assumptions

1. At the inlet to the diffuser of AMC the parameters of each of the flows are distributed on their cross sections evenly.

2. On the circuit of the diffuser of AMC the nonuniformity of the dimensionless speed is described by Schlichting's law [3]:

$$\bar{\delta u} = \frac{u - w}{u_a - w} = \frac{\bar{\tau}(\bar{\xi}) - A(1)}{1 - A(1)}. \tag{1}$$

where

$$\bar{\tau}(\bar{\xi}) = (1 - \bar{\xi}^{3/2})^2; \quad A(1) = 2 \int_0^1 \bar{\tau}(\bar{\xi}) \bar{\xi} \, d\bar{\xi}; \quad \bar{\xi} = \frac{y}{R_s}. \tag{2}$$

3. Static pressure in every cross section is assumed constant.

52

4. We consider the mixed gases incompressible. The latter
two assumptions are introduced on the ground, that in the diffuser
of AMC essentially the subsonic flows are examined, since to
provide for a stable combustion of mixture in afterburner it is
necessary to have $\lambda_{4\phi} \leq 0.2-0.3$, and $M_4 = 0.55-0.7$ [4].

5. The hydraulic losses of gas friction against the walls of
the diffuser we disregard in view of its low extent, which is
dictated by the very idea of AMC as a means of economy of the
overall sizes of the output part of a DTRDF.

6. The processes of flow and mixing of streams in the diffuser
of a AMC are stationary.

§ 2. The Fundamental Equations of Mixing

As it follows from assumptions 3 and 4 adopted above, at the
inlet to the diffuser of AMC $p_{A1} = p_{\eta 1}$, or:

$$\pi(\lambda_{A1}, \chi_{A1}) = \frac{\pi(\lambda_{n1}, \chi_{n1})}{\pi_\bullet}. \tag{3}$$

Under such a condition of inflow the fundamental equations of the
mixing of heterogeneous flows in the diffuser of AMC are:

1. The equation of continuity

$$G_\pi = G_{A1}(1+y). \tag{4}$$

2. The equation of energy

$$G_\pi c_{p\pi} T_\pi^\bullet = G_{A1} c_{pA1} T_{A1}^* + G_{n1} c_{p\eta} T_{\eta1}^*,$$

whence is determined

$$\vartheta_\pi^* = \frac{c_{p\pi} T_\pi^*}{c_{pA1} T_{A1}^*} = \frac{1 + y \bar{c} \vartheta^*}{1 + y} \tag{5}$$

and stagnation temperature

$$T_\pi^* = T_{A1}^* \frac{1 + y \bar{c} \vartheta^*}{1 + y \bar{c}}. \tag{6}$$

53

3. The equation of momentum

$$\left(\frac{G}{g}w + pF\right)_{\!0} = \left(\frac{G}{g}w + pF\right)_{\!A1} + \left(\frac{G}{g}w + pF\right)_{\!n1} + \int_{F_1}^{F_2} p\,dF,$$

which after using a Kiselev [1] formula of impulse, and also formulas (4) and (5), is converted to the form:

$$z(\lambda_3)\,B_3\,\sqrt{\overline{(1+y)(1+y\,\overline{c}\,\overline{\vartheta^*})}} = B_{A1}\,z(\lambda_{A1}) +$$
$$+ B_{n1}\,z(\lambda_{n1})\,y\,\sqrt{\overline{c}\,\overline{\vartheta^*}} + C\int_{F_1}^{F_2} p\,dF, \tag{7}$$

where

$$B = \sqrt{1 - \frac{1}{\lambda^2}},$$

$$C = \frac{1}{G_{A1}}\sqrt{\frac{2g\,\overline{A}}{i_{A1}^*}}\left(A = \frac{1}{427}\right).$$

The last member of (7), which differs it from similar momentum equations for cylindrical chambers, we convert to the more convenient form:

$$C\int_{F_1}^{F_2} p\,dF = \frac{p_1 F_1}{G_{A1}}\sqrt{\frac{2g\,A}{c_p\,T_{A1}^*}}\int_1^{\overline{f}}\frac{p}{p_1}\,d\overline{f} =$$
$$= \frac{\varkappa+1}{m_{\kappa p}\varkappa\,y(\lambda_{A1})}\sqrt{\frac{2(\lambda_r-1)}{\lambda_r}}\int_1^{\overline{f}}\frac{p}{p_1}\,d\overline{f}. \tag{8}$$

Considering that the constant before the sign of the integral of (8) is a function of the parameters of the 1st contour of a DTRD (i.e., combustion products), and by substituting (8) in (7), we will obtain in final form the equation of momentum for the diffuser of AMC:

$$z(\lambda_3)\,B_3\,\sqrt{\overline{(1+y)(1+y\,\overline{c}\,\overline{\vartheta^*})}} = B_{A1}\,z(\lambda_{A1}) +$$
$$B_{n1}\,z(\lambda_{n1})\,y\sqrt{\overline{c}\,\overline{\vartheta^*}} + \frac{1{,}045(1+\varkappa)}{y(\lambda_{A1})\,\varkappa}\int_1^{\overline{f}}\frac{p}{p_1}\,d\overline{f}. \tag{9}$$

It is completely obvious that the system given above of equations of mixing can have a determinate unique solution only in the search of the integral of static pressure in the last equation.

3. The Calculation of the Integral of Static Pressure

For the calculation of the integral of static pressure in general form (for isolated special cases successful solutions [5, 11] are known) it is necessary to know the analytical dependence of static pressure distribution along the diffuser of AMC. For the quasi-stationary turbulent flow of a Newtonian fluid such a dependence can be derived on the basis of the Navier-Stokes differential equations of motion and continuity which for the case interesting to us are converted, as is known from [8], to the form:

$$-\frac{dp}{dx} - \frac{1}{y}\frac{\partial}{\partial y}(y\tau_\tau) = \rho u \frac{\partial u}{\partial x} + \rho v \frac{\partial u}{\partial y}; \tag{10}$$

$$y\frac{\partial u}{\partial x} + \frac{\partial}{\partial y}(y v) = 0, \tag{11}$$

where tension of eddy viscosity, according to Prandtl [2]:

$$\tau_\tau = \rho l^2 \frac{\partial u}{\partial y}\left|\frac{\partial u}{\partial y}\right|. \tag{12}$$

The joint transforms of equations (10) and (11) reduce to the form:

$$-\frac{y^2}{2}\frac{dp}{dx} - \tau_\tau y = \frac{d}{dx}\int_0^y \rho u^2 y\, dy - y\frac{d}{dx}\int_0^y \rho u y\, dy. \tag{13}$$

Utilizing in (13) an equation of the constancy of consumption

$$\frac{d}{dx}\int_0^{R_s} \rho u y\, dy = 0$$

and having satisfied the boundary condition on wall $y = R_3$, $\tau_T = 0$, we obtain the fundamental integrodifferential equation for static pressure distribution:

$$\frac{dp}{dx} = -\frac{2\pi}{F} \frac{d}{dx} \int_0^{R_s} \gamma u^2 y \, dy. \tag{14}$$

which can be solved only in conjunction with equation (13).

For convenience and the universality of the solution, we will introduce the dimensionless coordinates and coefficients:

$$\bar{x} = x \left| \sqrt{\frac{\bar{\pi}}{F_1}} \right.; \quad \bar{\zeta} = y \left| \sqrt{\frac{\bar{\pi}}{F}} \right.;$$

where

$$\lambda^\circ = \frac{u\, a_{\kappa p\, u}}{(w/a_{\kappa p})_{cp}} = \frac{\lambda_u}{\lambda_{cp}\, |\, \vartheta_u{}^* E_u}; \quad \bar{\lambda} = \frac{(u\, a_{\kappa p})_s}{(w/a_{\kappa p})_{cp}} = \frac{\lambda_s}{\lambda_{cp}\, |\, \vartheta_s{}^* E_s}, \tag{15}$$

$$\vartheta_s = \frac{i_s{}^*}{i_s{}^*}; \quad E_s = \frac{\chi_s - 1}{\chi_s + 1} \frac{\chi_s + 1}{\chi_s - 1}; \quad \vartheta_u{}^* = \frac{i_s{}^*}{i_u{}^*}; \quad E_u = \frac{\chi_s - 1}{\chi_s + 1} \frac{\chi_u + 1}{\chi_u - 1}.$$

We solve equation (13) relative to the complex coefficient of diversity $\bar{\lambda}$, after making the replacement of variables in correspondence with (15) in it for this, utilizing Schlichting's law (1) and a procedure of transforms from work [10], whereupon we obtain:

$$\sqrt{\bar{f}}(1 + a\bar{\lambda}) \frac{d\bar{\lambda}}{dx} = -k(\bar{\lambda} - 1)^2 + 2\lambda(c + \bar{\lambda} d) \frac{d\sqrt{\bar{f}}}{dx} + 2e \frac{d\sqrt{\bar{f}}}{dx} \tag{16}$$

where

$$a = \frac{M(\bar{\zeta})}{L(\bar{\zeta})}; \quad k = b\varkappa^2(\bar{\zeta}); \quad b = \frac{N(\bar{\zeta})}{L(\bar{\zeta})}; \quad \varkappa(\xi) = \frac{l}{R_s};$$

$$c = \frac{I(\bar{\zeta})}{L(\bar{\zeta})}; \quad d = \frac{J(\bar{\zeta})}{L(\bar{\zeta})}; \quad e = \frac{H(\bar{\zeta})}{L(\bar{\zeta})};$$

l - mixing length where, in turn:

$$L(\xi) = p(\xi)[1 + \varphi(\xi)] + 2A(1)p(\xi) - 2[B(1)\xi^2 - 2B(\xi)];$$

$$M(\xi) = 2[B(\xi) - \xi^2 B(1)] - p(\xi)[3A(1) + \varphi(\xi)];$$

$$N(\xi) = 18\xi^2 \varphi(\xi);$$

$$I(\xi) = 2p(\xi)[1 + A(1)] + 2[\xi^2 B(1) - B(\xi)];$$

$$J(\xi) = B(\xi) \quad \xi^2 B(1) - 2A(1)p(\xi);$$

$$H(\xi) = B(\xi) - \xi^2 B(1) - 2p(\xi). \quad \text{in which,}$$

$$p(\xi) = A(\xi) - \xi^2 A(1); \quad A(\xi) = 2\int_0^\xi \varphi(\xi)\xi\,d\xi; \tag{17}$$

$$A(1) = 2\int_0^1 \varphi(\xi)\xi\,d\xi = 0.2571; \quad B(\xi) = 2\int_0^\xi \varphi^2(\xi)\xi\,d\xi;$$

$$B(1) = 2\int_0^1 \varphi^2(\xi)\xi\,d\xi = 0.1334.$$

and $\varphi(\xi)$ is in accordance with (2).

In the case interesting to us of the mixing of flows in a diffuser with rectilinear generatrices $\sqrt{f} = 1 + \beta\overline{x}$, the obtained Abel equation (16) of the 2nd order [9] is expressed in quadratures and is reduced to the following differential equation with separable variables.

$$\frac{(1 + a\overline{\lambda})d\overline{\lambda}}{(2\beta d - k)\overline{\lambda}^3 + 2(\beta c + k)\overline{\lambda} + (2\beta e - k)} = \frac{d\overline{x}}{1 + \beta\overline{x}}. \tag{18}$$

The relative coefficients entering this equation were calculated by computer as the mathematical expectations of the random variable ξ by Simpson's method and the following mean-integral values obtained:

$$a_{cp} = 0.93; \quad c_{cp} = 2.714; \quad d_{cp} = 0.573; \quad e_{cp} = -3.287; \quad b_{cp} = 39.6.$$

With consideration of empirical data $\kappa(\xi)$ of different authors [7, 8]

$$k_{cp} = b_{cp} \varkappa^2(\xi) = 0.618.$$

Equation (18) was solved by the method of the undetermined coefficients of the initial conditions $\bar{x} = 0$, $\bar{\lambda} = \bar{\lambda}_I$:

$$\left|\frac{\bar{\lambda} - \gamma_1}{\bar{\lambda}_1 - \gamma_1}\right|^n \left|\frac{\bar{\lambda} - \gamma_2}{\bar{\lambda}_1 - \gamma_2}\right|^m = 1 + \beta\bar{x}, \qquad (19)$$

where

$$n = \frac{\beta(1 + a\gamma_1)}{(2\beta d - k)(\gamma_1 - \gamma_2)}; \quad m = \frac{\beta(1 + a\gamma_2)}{(2\beta d - k)(\gamma_2 - \gamma_1)},$$

while γ_1, γ_2 are the roots of the trinomial of the denominator in equation (18).

After the transforms of equation (19), we obtain the final solution in the form:

$$\bar{f} = \left(\frac{\bar{\lambda} - 1}{\bar{\lambda}_1 - 1}\right)^{\frac{1}{2}} \left(\frac{\gamma - \bar{\lambda}_1}{\gamma - \bar{\lambda}}\right)^q, \qquad (20)$$

where

$$q = \frac{1 + a\gamma}{2(1 + a)}; \quad \gamma = \frac{2\beta(c + d) + k}{k - 2\beta d}.$$

From this equation it follows that $\bar{\lambda}$ depends on the geometry of the diffuser of AMC (β, $\bar{f}$) and the gas-dynamic coefficient of diversity at the inlet to it

$$\bar{\lambda}_1 = \frac{\lambda_{A1}}{\lambda_{cpl} \sqrt{\vartheta_s^\circ E_{A1}}},$$

since, according to assumption 1 (see § 1)

$$\lambda_s = \lambda_{A1}; \quad \vartheta_s^* = \vartheta_s^\circ; \quad E_s = E_{A1}.$$

Now already according to equation (14) we can find the distribution law of static pressure, for which we will carry out both of its parts to a constant value of ram pressure $\rho w_{cpI}^2/2$ in the reference section and, remembering that $w_{cp}/w_{cpI} = F_1/F = 1/\bar{f}$, after the transforms with consideration of (1), (15) and (17), we obtain

58

$$\frac{d\left(\frac{p}{p\,w_1^2/2}\right)}{dx} = \frac{d\bar{p}}{dx} = -\frac{s}{f}\frac{d}{dx}\left[\frac{h\,\bar{\lambda}^2 - 2h\,\bar{\lambda} + t}{f}\right]. \tag{21}$$

where in accordance with (17): $h = B(1) - A^2(1) = 0.0674$;
$t = 1 + B(1) - 2A(1) = 0.6192$; $s = 2/[1 - A(1)]^2 = 3.62$.

We integrate equation (21), having preliminary replaced its right side with the differential of the polynomial to the same degree, but with different coefficients, and $\bar{f}$ - by formula (20), whereupon, after conducting the transforms, we obtain the resultant expression for static pressure distribution:

$$\bar{p} - \bar{p}_1 = \Delta\bar{p} = (\Phi\,\bar{\lambda}_1^2 - \psi\,\bar{\lambda}_1 + \omega) -$$
$$- \left(\frac{\bar{\lambda}_1 - 1}{\bar{\lambda} - 1}\right)\left(\frac{\gamma - \bar{\lambda}}{\gamma - \bar{\lambda}_1}\right)^{2q}(\Phi\,\bar{\lambda}^2 - \psi\,\bar{\lambda} + \omega), \tag{22}$$

where

$$\Phi = \frac{0.244}{\chi}[\beta(a - 2d) + k]; \quad \psi = 0.488\left(1 + \frac{\beta}{\chi}\right);$$

$$\omega = 1.81\left[0.6192 - 0.0674\frac{2\beta e - k}{\chi}\right]; \quad \chi = 2\beta(a - d) + k.$$

As we see, formula (22) is given as a function of $\bar{\lambda}$ and static pressure distribution along the diffuser of AMC can be constructed only during the joint solution of equations (22) and (20). Since the latter is a complex dependence of $\bar{\lambda}$ on β, $\bar{f}$, $\bar{\lambda}_1$, which cannot be expressed in an explicit form, then, for the imparting of an engineering nature to the solution of the system of these equations by the computer of "MIR-1," equation (20) for the entire reasonable range of parameters of the diffusers of AMC DTRDF was computed: $\Theta_{\text{пр}}/2 = 3\text{-}16°$ with pitch of $1°$ and $\bar{\lambda} = 1\text{-}\bar{\lambda}_{\text{Max}} = \gamma$ with pitch $\Delta\bar{\lambda} = 0.05$. As a result of these calculations a universal nomogram Fig. 1, was constructed for any value of $\bar{\lambda}_I$, with which it is possible to find both $N_I = (\bar{\lambda}_1 - 1)^{1/2}/(\gamma - \bar{\lambda}_I)^q$ and $\bar{\lambda}$ in any (dependent on $\bar{f}$) cross section of the diffuser (see Fig. 1) for a given $\Theta_{\text{пр}}^{\perp}$, which significantly simplifies practical calculations. After thus finding the value of $\bar{\lambda}$ according to formula (22) from Fig. 1, it is now unambiguously possible to determine $\Delta\bar{p}$ in this cross section.
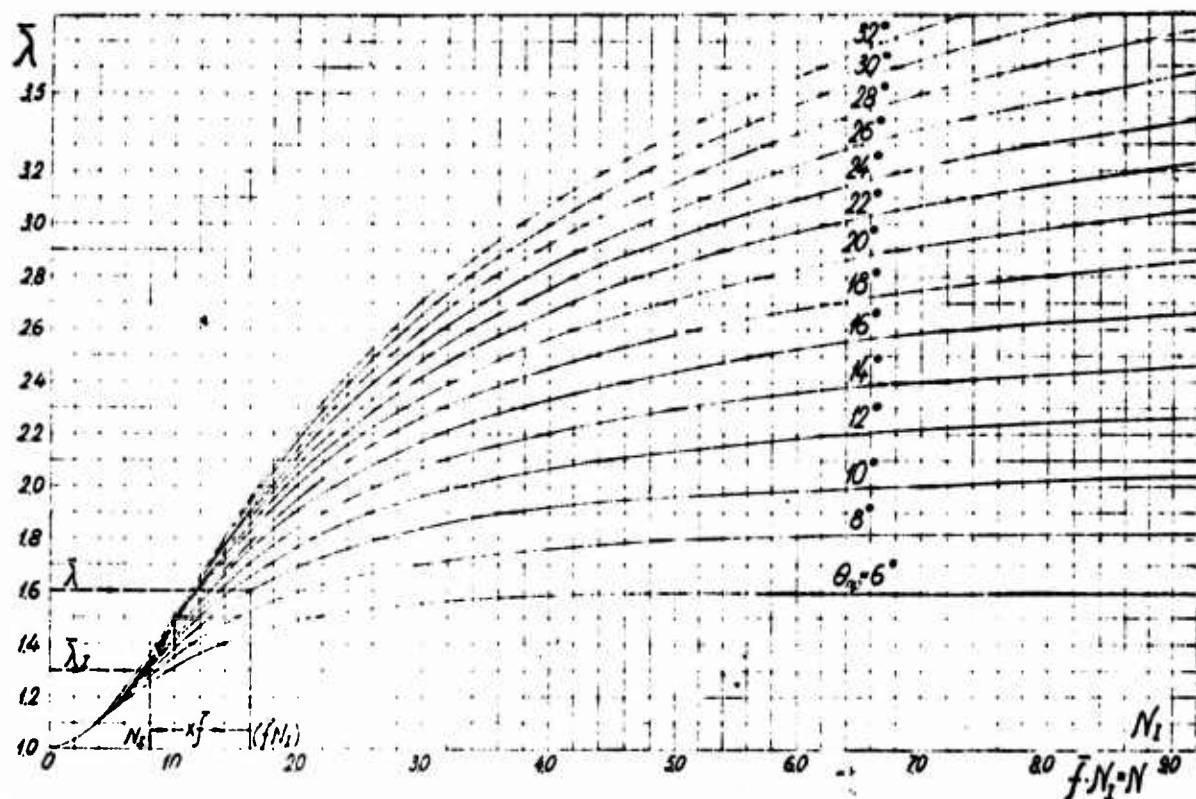
Fig. 1.

However with the purpose of achievement of greater accuracy and, simultaneously, of engineering calculations we have conducted the joint solution of equations (20) and (22) for the system

$$\left.\begin{array}{l} \Delta\overline{p} = \\ \overline{f} = \end{array}\right\} \varphi(\overline{\lambda}) \text{ with } \Delta\overline{\lambda} = 0.05 \text{ over a wide range of the gas-dynamic and}$$

geometric parameters of the subsonic diffusers of AMC on the "MIR-1" computer: $\overline{\lambda}_I = 1.0$-$1.8$ and $\Theta_{np} = 10$-$30°$. According to the results of this calculation the graph, Fig. 2, of $\Delta\overline{p} = \varphi(\overline{f})$ was constructed, which is also universal, since in the indicated range of $\Theta_{np}°$ it is applicable for diffusers of different length. The presence of the graph Fig. 2 makes it possible in engineering calculations, generally, to not use formulas (20) and (22), but to directly take the necessary value of $\Delta\overline{p}$ from the graph.
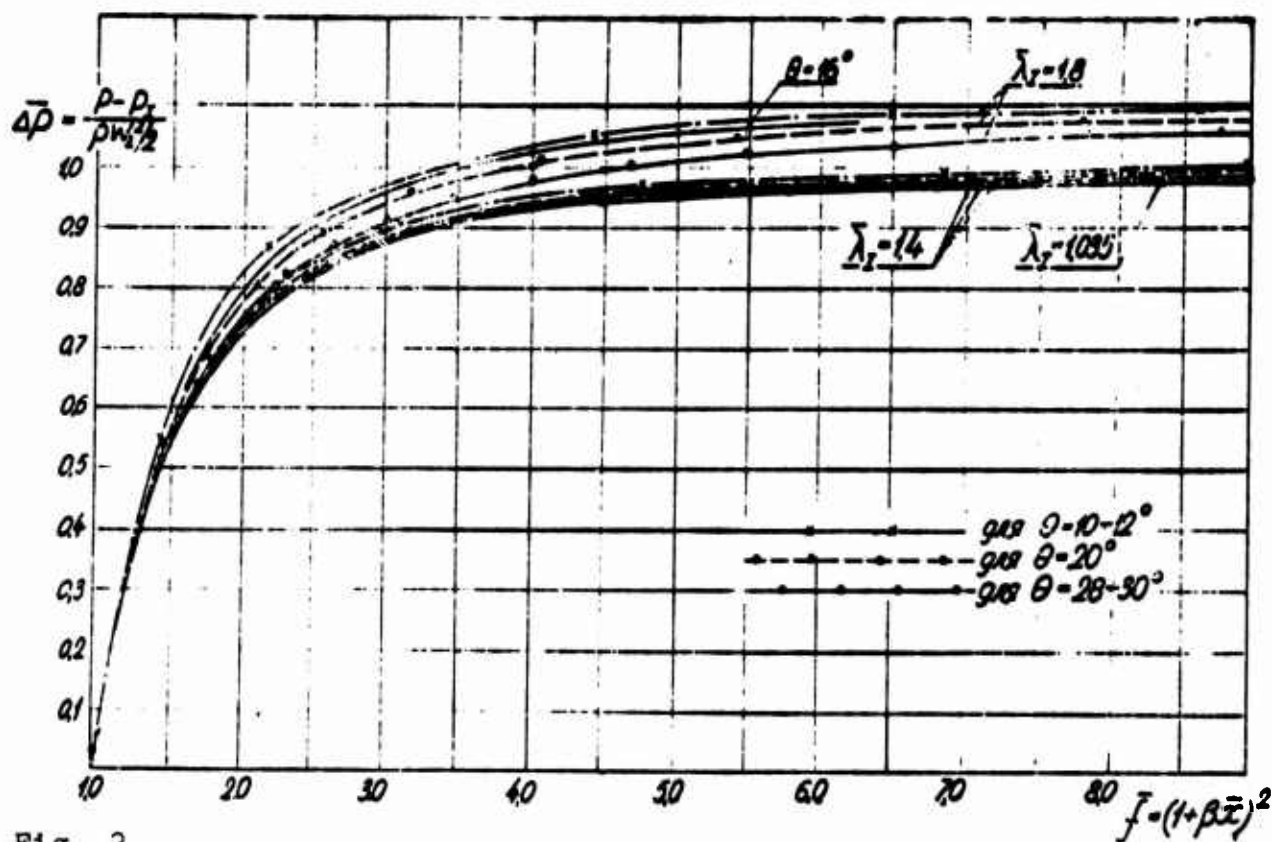
Fig. 2.

Knowing the dependence of static pressure distribution on $\bar{f}$, we can now solve the basic task of calculation of the integral of static pressure. As it appears from equation (9), this integral ought to be solved in the form $\displaystyle\int_1^{f_{\text{A}}} \frac{p}{p_1}\,d\bar{f}$. In accordance with (21) and (22) let us introduce into the integrand the relative function $\bar{p} = p/pw_1^2/2$:

$$\int_1^{f_{\text{A}}} \frac{p}{p_1}\,d\bar{f} = \int_1^{f_{\text{A}}} \mu\,\bar{p}\,d\bar{f}.$$

where

$$\mu = \frac{\rho\,w_1^2}{2p_1} = \frac{\chi_{\text{в}}}{2}\,M_{\text{1ср}}^2 = \frac{\chi_{\text{в}}}{\chi_{\text{в}}+1}\cdot\frac{\lambda_{\text{1ср}}^2}{\left(1-\dfrac{\chi_{\text{в}}-1}{\chi_{\text{в}}+1}\lambda_{\text{1ср}}^2\right)}.$$

Let us make "integration by parts" of the obtained integral, after replacing for this the differential $d\bar{p}$ with its expression (21):

61

$$\int_{\bar{t}_1}^{\bar{t}_3} \mu\bar{p}\,d\bar{f} = \mu\bar{p}\,\bar{f} - \mu\int \bar{f}\,d\bar{p} = \mu\,\bar{p}(\bar{\lambda})\,\bar{f}(\bar{\lambda})\Big|_{\bar{t}_1}^{\bar{t}_3} +$$

$$+ \mu\int_{t_1}^{\bar{t}_3} s\,d\left(\frac{h\bar{\lambda}^2 - 2h\bar{\lambda} + t}{\bar{f}}\right) = \mu[\bar{p}_3\bar{f}_3 - \bar{p}_1\bar{f}_1] +$$

$$+ s\,\mu\left[\frac{h\bar{\lambda}_3^2 - 2h\bar{\lambda}_3 + t}{\bar{f}_3} - (h\bar{\lambda}_1^2 - 2h\bar{\lambda}_1 + t)\right].$$

Considering that $\mu = 1/\bar{p}_I$, $\bar{f}_I = 1$, and in accordance with (22), $p_3 = \bar{p}_I + \Delta\bar{p}$, the final solution of the integral of static pressure for the diffusers of AMC with rectilinear generatrices obtained in the following final form:

$$I = (\bar{f}_3 - 1) + \mu\Delta\bar{p}\,\bar{f}_3 + 3.62\,\mu\left[\frac{h\bar{\lambda}_3^2 - 2h\bar{\lambda} + t}{\bar{f}_3} - (h\bar{\lambda}_1^2 - 2h\bar{\lambda} + t)\right]. \tag{23}$$

where $\bar{f}_\text{д}$ - the usually assigned magnitude of the expansion ratio of a diffuser; $\Delta\bar{p}$ - the increase of static pressure at the assigned diffuser length, computed according to formula (22) or determined from Fig. 2; $\bar{\lambda}_3$ - determined from Fig. 1 from assigned magnitudes of Θ_0, $\bar{f}_\text{д}$ and from the computed value

where
$$\bar{\lambda}_1 = \frac{\lambda_{\Lambda I}}{\lambda_{cpi}\sqrt{\bar{\dot{w}}_3^{*}\bar{E}_{\Lambda I}}},$$

$$E_{\Lambda I} = \frac{\lambda_{\Lambda I} + 1}{\lambda_{\Lambda I} - 1}\frac{\lambda_3 - 1}{\lambda_3 + 1}.$$

According to formula (23) we conducted the calculations of $\int_1^{\bar{f}} \mu\bar{p}\,d\bar{f}$ for that diffuser length of the space behind the turbine which is most acceptable for aircraft engine construction, $\bar{l} = 2.5$ calibers [4], in the following range of parameters: $\Theta_{\text{пр}} = 12\text{-}28°$; $\bar{\lambda}_1 = 1\text{-}1.8$; and $M_{I\text{cp}} = 0.2\text{-}1.0$. The results of the calculations are given in Fig. 3, from which it is clearly evident that to the

62

greatest degree the numerical value of integral depends on the
divergence angle of the diffuser θ° and to the least degree on the
criteria of the initial divergence, $\overline{\lambda}_1$, as this effect becomes
the lesser, the lesser the value of M_{Icp}.
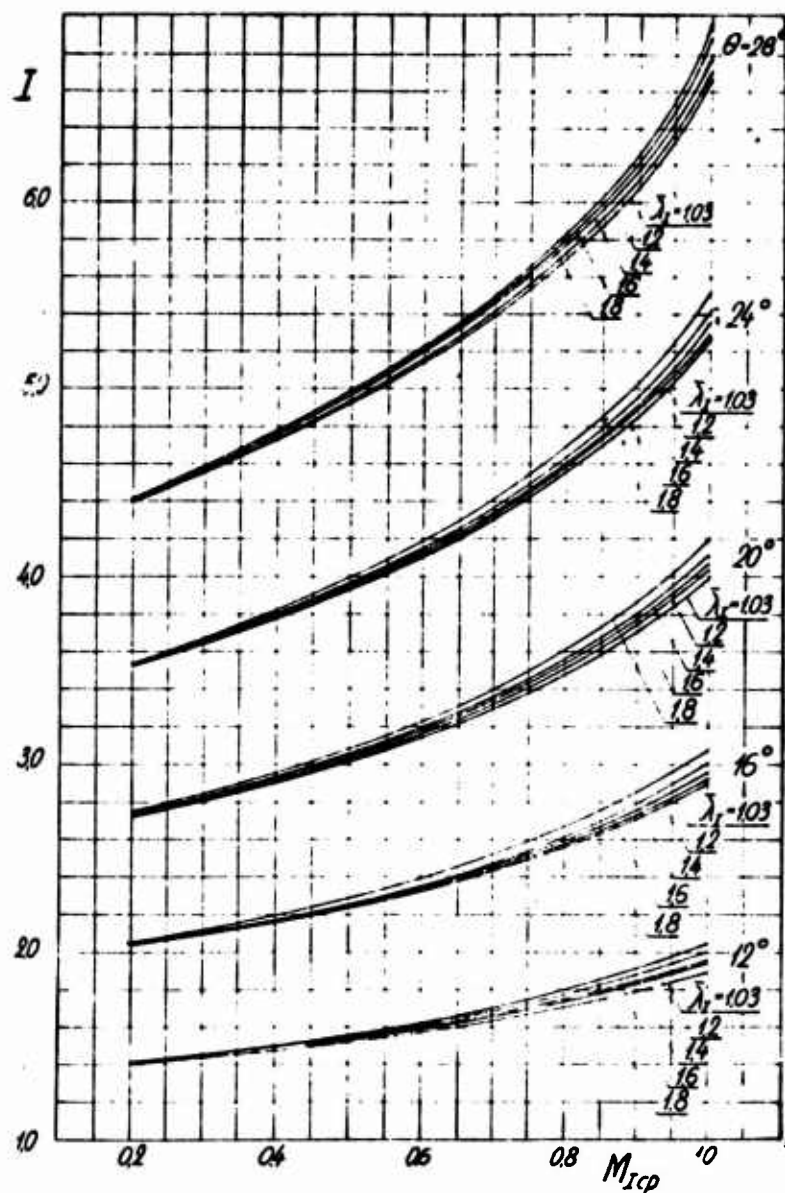
Fig. 3.

§ 4. Determination of $\pi_\text{э}$, in the Diffuser of AMC

The basic purpose of the calculation of any mixing chamber is the determination of its criterial parameter - the pressure ratio $\pi_\text{э} = p_3^*/p_{\text{п}1}^*$, it always is possible to find the total pressure of mixture at the chamber outlet, which is especially important in our case of calculating the diffuser or AMC. Thus for its determination we utilize in relationship (4) the known consumption equation:

$$p_3^* D_\text{э} q(\lambda_\text{э}, \chi_\text{э}) F_\text{э} = p_{\text{Л}1}^* D_{\text{Л}1} q(\lambda_{\text{Л}1}, \chi_{\text{Л}1}) F_{\text{Л}1} \sqrt{\bar{\theta}_\text{э}^*}(1+y).$$

Utilizing in this the equality of expression (5) and $F_3 = \overline{f}_\text{д}(F_{\text{Л}1} + F_{\text{п}1})$, after the transforms we obtain:

$$\pi_\text{э} = \frac{p_\text{э}^*}{p_{\text{п}1}^*} = \frac{D_{\text{Л}1} q(\lambda_{\text{Л}1}, \chi_{\text{Л}1}) z}{D_\text{э} q(\lambda_\text{э}, \chi_\text{э}) \overline{f}_\text{д}(1+z)} \pi_\text{о} \sqrt{(1+y)(1+y\overline{c}\,\overline{\vartheta}^*)}. \tag{24}$$

where

$$y = \frac{G_{\text{п}1}}{G_{\text{Л}1}} = \frac{D_{\text{п}1} q(\lambda_{\text{п}1}, \chi_{\text{п}1})}{D_{\text{Л}1} z \pi_\text{о} \sqrt{\overline{c}\,\overline{\vartheta}^*} q(\lambda_{\text{Л}1}, \chi_{\text{Л}1})}. \tag{25}$$

$$z = \frac{F_{\text{Л}1}}{F_{\text{п}1}}; \quad D = \chi\left(\frac{2}{\chi+1}\right)^{\frac{\chi}{\chi-1}}\sqrt{\frac{\chi+1}{\chi-1}}. \tag{26}$$

Since we are investigating the mixing of heterogeneous flows, the gas-dynamic functions in the given formulas are each found for their own index x. The adiabatic index of the gas mixtures is determined from the known formula:

$$\chi_\text{э} = \chi_{\text{Л}1}\frac{1+y\overline{c}}{1+y\overline{c}\,\chi_{\text{Л}1}/\chi_{\text{п}1}}. \tag{27}$$

The integral of static pressure affects the value $\pi_\text{э}$ in terms of a function of $q(\lambda_3, \chi_3)$ in (24), determined in accordance with equation (9).

In the method given above the calculation of $\pi_\text{э}$ was conducted depending on the available pressure differential $\pi_0 = p^*_{A1}/p^*_{\Pi 1}$ for a series of diffusers of AMC in the range $\Theta = 12\text{--}28°$; and also for the cylindrical mixing chamber ($\Theta = 0°$), for which equations (9) and (24) were simplified due to the introduction of conditions of cylindricity: $\int\limits_{1}^{f} \bar{p}\ d\bar{f} = 0$ and $\bar{f}_\text{д} = 1$.

The calculation was performed at constant values of $\clubsuit^* = 0.45$ and $M_{1\text{cp}} = 0.6$, those most characteristic and optim.m for space behind the turbine of a [TJE] (ТРД) and DTRD [4, 5]. As can be seen from graph 4, constructed according to the results of the aforementioned calculation, the values $\pi_\text{э}$ in the range actually used in DTRD, $\pi_0 = 1.0\text{--}1.3$ for a cylindrical mixing chamber do not considerably exceed that for the diffusers of AMC: for example in a diffuser with $\Theta° = 12°$, $\pi_\text{э}$ is only 0.5-1.3% less than in the cylindrical chamber. However, as the same calculations showed, in the cylindrical chamber λ_3 at the indicated values of π_0 and $\pi_\text{э}$ it remains at a level ≈ 0.6; while in diffuser with $\Theta = 12°$ at the same values of π_0 and $\pi_\text{э}$, $\lambda_3 = 0.24$, i.e., it completely corresponds to the conditions of an afterburner [4]. It we consider moreover the savings of weight and overall sizes of such a DTRDF, then the advantages of organization of mixing in the diffuser of AMC are indisputable as compared with mixing in the cylindrical chamber of DTRDF.

Conclusions

1. The experimentally checked and sufficiently substantiated initial assumptions form the basis of the proposed method of calculation of mixing in the diffusers of afterburner mixing chambers.
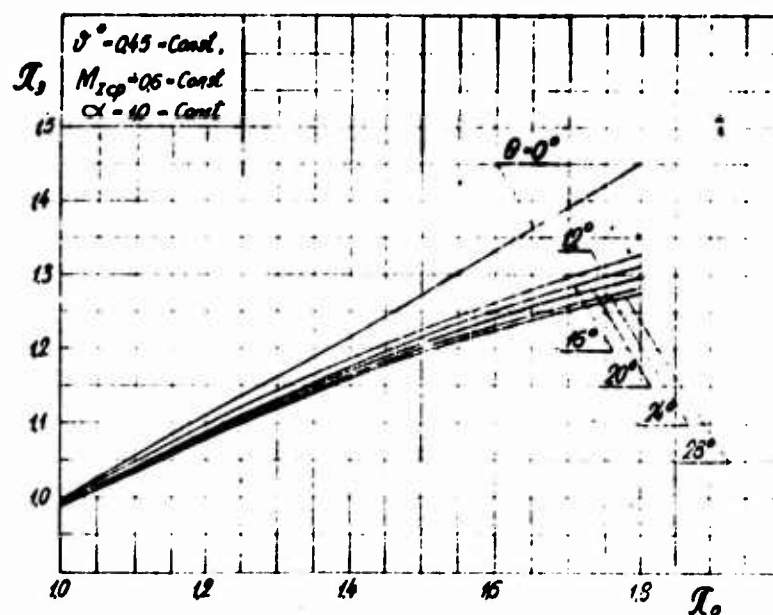
Fig. 4.

2. On the basis of continuity and the joint solution of the differential Navier-Stokes equations, the analytical calculation of the integral of static pressure for diffusers of AMC with rectilinear generatrices is given in the final form, which afforded the possibility to transform the equation of momentum in connection with the diagram in question.

3. On the basis of the proposed dependences universal nomograms for the single-valued determining of the criterion of diversity of $\overline{\lambda}$, $\Delta\overline{p}$, and $\int \overline{p} \, d\overline{f}$ are calculated as a function of the initial gas-dynamic and geometric parameters of the diffuser of AMC.

4. The calculations, carried out according to this method, showed the great advisability of organization of the mixing of flows of both contours of DTRDF directly in the diffuser of the AMC, rather than in the preliminary cylindrical mixing chamber.

66 .

Bibliography

1. Киселев Б. М. Расчет одномерных газовых течений. «Прикладная математика и механика», т. XI, вып. 1, 1947.

2. Прандтль Л. Гидроаэромеханика. И.-Л., 1949.

3. Шлихтинг Г. Теория пограничного слоя. И.-Л., «Машиностроение», М., 1969.

4. Стечкин Б. С., Казанджан П. К. и др. Теория реактивных двигателей (рабочий процесс и характеристики). Оборонгиз, 1958.

5. Клячкин А. Л. Теория двухконтурных ВРД (монография), РКВИАВУ, 1959.

6. Барабанов Е. В. Современные методы расчета газовых эжекторов. Сборник НТТ по прикладной газотермодинамике, ч. II. Труды РКИИГА, Рига, 1968.

7. Абрамович Г. Н. Теория турбулентных струй. Физматгиз, 1960.

8. Гиневский А. С. Теория турбулентных струй и следов. «Машиностроение», М., 1969.

9. Камке Э. Справочник по обыкновенным дифференциальным уравнениям. Физматгиз, 1961.

10. Яковлевский О. В. Смешение струй в канале с переменным поперечным сечением. Известия АН СССР, ОТН. «Механика и машиностроение», № 1, 1962.

11. Ененков В. Г. Графо-аналитический метод расчета эжекторов. Сборник НТТ по прикладной газотермодинамике, ч. I, вып. 116. Труды РКИИГА, Рига, 1967.

THE EXPERIMENTAL STUDY OF THE MIXING OF GAS FLOWS IN THE DIFFUSER OF THE AFTERBURNER MIXING CHAMBER OF A DTRDF

Ye. V. Barabanov

The present article is dedicated to the experimental research of the mixing of concentric heterogeneous gas flows in the annular diffuser of the afterburner mixing chamber of the DTRDF of a supersonic aircraft.

Investigation is conducted over a wide range of a change of the gas-dynamic and geometric parameters of diffuser mixing chambers. The optimum parameters of such chambers are revealed and the evaluation of their effect on relative specific impulse is produced, as is the efficiency of the mixing process on the most "integral" criterion.

The concrete quantitative and qualitative derivations and the recommendations regarding the design of optimum diffusers of afterburner mixing chambers are given, as is the selection of the most logical parameters of mixing in them.

Accepted Designations

p^*, *, T^* – pressure and temperature of stagnation

p – static pressure in the contour of device

G – flow rate per second of air (gas), kg/s

F – cross-sectional area

$n_{д} = F_{д}/F_1$ – expansion ratio of the diffuser

$\alpha_{пр}$ – given angle of flare of the diffuser

$\vartheta^* = T^*_{п1}/T^*_{А1}$ – available drop in total temperatures

$\pi_0 = P^*_{А1}/P^*_{п1}$ – available drop in total pressures

$y = G_{п1}/G_{А1}$ – bypass ratio

$\pi_{э} = p^*_9/p^*_{п1}$ – the pressure ratio

$\lambda = w/a_{кр}$ – velocity coefficient

$J_{уд\ i}$ – specific impulse in the appropriate cross section

$\overline{J}_{уд} = J_{уд9}/J_{уд1}$ – relative specific impulse at outlet from the diffuser

$\sigma^* = p^*_9/p^*_{ср1}$ – total pressure recovery coefficient

$\tau^*_{p9} = p^*_{Max}/p^*_{cp9};$

$\tau^*_{т9} = T^*_{Max}/T^*_{cp9}$ – variation factor of pressure and temperature in the exhaust section of the mixed flow

$\overline{\tau}^* = \tau^*_e/\tau^*_1$ – relative variation factor of flow

$кг/см^2$ – kg/cm^2

$сек$ – s

Indices

A_1 – parameters of primary (active) flow at inlet to diffuser

$П_1$ – parameters of secondary (passive) flow at inlet to diffuser

I – the total parameters of inlet to the model

$1, 2, 3, \ldots 9$ – cross sections along the length of the diffuser

9 – parameters of mixed flow of outlet from diffuser

69

Contractions

[DTRDF] (ДТРДФ) - turbofan engine with afterburner
[AMC] (ФСН) - afterburner mixing chamber

Introduction

In connection with wide application of forced DTRD on super-
sonic aircraft, the selection of the most logical layout of a DTRDF
with mixing chambers becomes urgent. The advisability of the
setting of such a task is determined by the trend toward reduction
in weight and overall sizes of the entire power plant of a super-
sonic aircraft, without worsening considerably its gas dynamics.

The existing requirements in gas dynamics [1-3] to provide
satisfactory mixing recommend construction of cylindrical mixing
chambers with a length of 6-7 calibers, and afterburners with a
length of 2-3 calibers. Thus, for a satisfactory afterburning of
the mixed flows in DTRDF with a mixing chamber a very bulky and
heavy system behind the turbine will be required.

At the same time the numerous experimental works on mixing
in the cylindrical chambers, which were carried out earlier [4-6],
did not confirm the assumptions of researchers for the expected
thrust increment of DTRD as a result of the increase of completeness
of mixing. As a result, there arose the need for study of the
mixing of gas flows directly in the diffuser of an AMC of a DTRDF
with the goal of development of the optimum mode and geometry
of such a diffuser located in the space behind the turbine.

The study of the mixing of heterogeneous flows in the diffuser
of an AMC was conducted for the solution of this problem on a
special experimental device [7] which simulates the operation of
the exhaust systems of DTRDF (Fig. 1). In every testing were taken
the diffuser performances of determined geometry assigned by the
setting of female cone 07 necessary for this (Fig. 2) with

70

determined λ_1 and by fixed settings of the corresponding exit nozzle 05. In all, each of the three investigated diffusers (with $\alpha_{np} = 12°$, 16° and 20°) was tested in the range of the velocities corresponding $\lambda_1 = 0.2-0.9$.
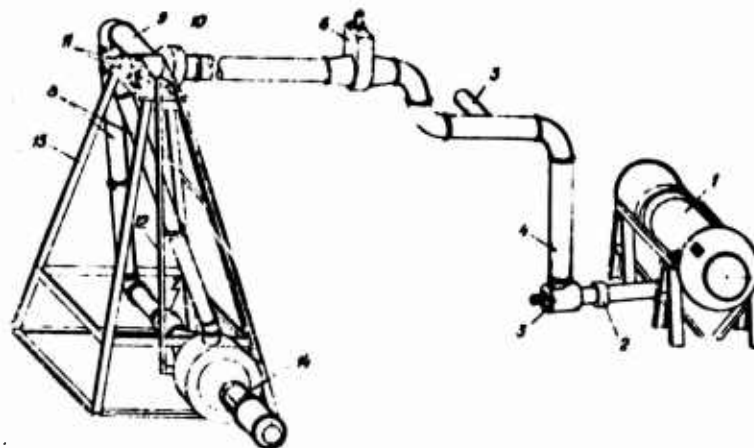
Fig. 1. The diagram of experimental devices for the study of the mixing of gas flows.
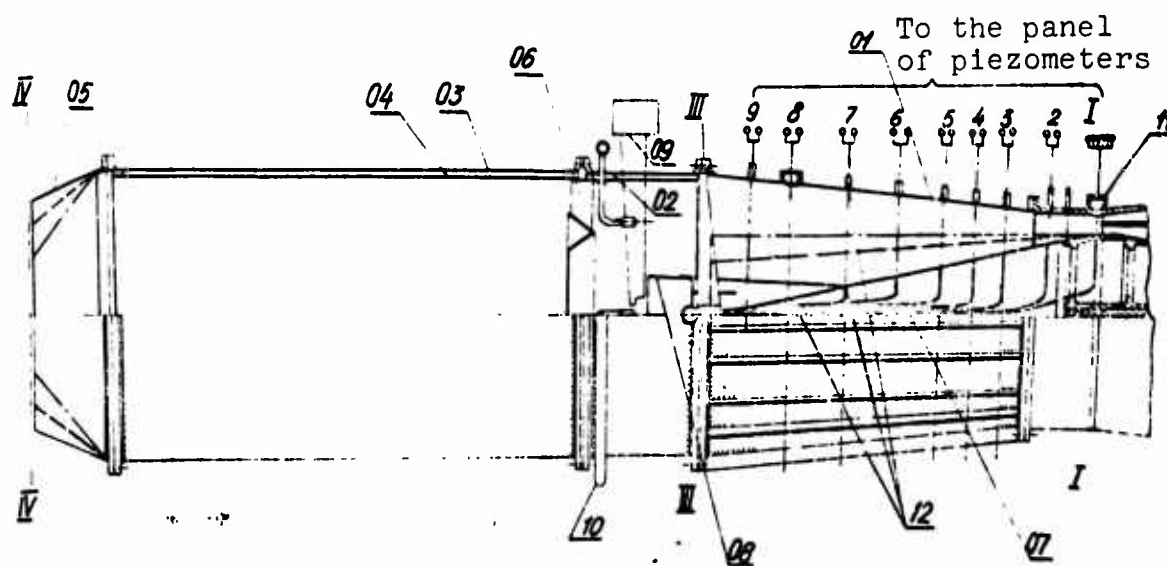
Fig. 2. Experimental afterburner mixing chamber.

71

The parameters of spatial flow during treatment which were measured in the process of the experiment at several points of every cross section were averaged both along the radius and along the circumference of an annular axisymmetric diffuser. For our mixer circuit of flows with different p^* and T^*, in accordance with [8] the principle of the simultaneous averaging of the parameters according to impulse and according to consumption was selected.

§ 1. The Fields of Flow Parameters
at the Outlet from a Diffuser

Figures 3 and 4 depict the fields of the total pressures and temperatures along an outlet radius of a diffuser measured in the experiment and averaged in the zones of the circumference of the corresponding radii. The rearrangement of flow pattern and the transformation of the fields $T_9^* = f(R_9)$ during a change of π_0 and the transformation of fields $p_9^* = f(R_9)$ during a change in the drop in temperatures is distinctly visible. Moreover as is evident from Fig. 3, a change of π_0 affects, to considerably greater degree than a change of $\$^*$, the structure of the field $T_9^* = f(R_9)$.

However, in spite of the great uniformity of the field $T_9^* = f(R_9)$ with a low π_0, these projections differ by the greater nondiffusion of the flow core.

As the consequence of greater uniformity of T_9^* on the cross section with $\pi_0 = 1.0-1.25$ and $\$^* = 0.64$, the warming up of mixed flow on the periphery of the diffuser proves to be substantially higher than at their greater values of $\pi_0 = 1.53$.

Together with this it follows to show that, concerning the increase in the available drop in the temperatures, the mixing in the diffuser of flows with small π_0 loses its advantage in the warming up of the peripheral zones, which is distinctly evident in Fig. 3, when $\$^* \cong 0.4$, where T_9^* on the periphery both for the flows with $\pi_0 = 1.25$ and with $\pi_0 = 1.52$, is identical and equal to $410°C$, which is $285°$ (or 230%) greater than T_{n1}^*.

72
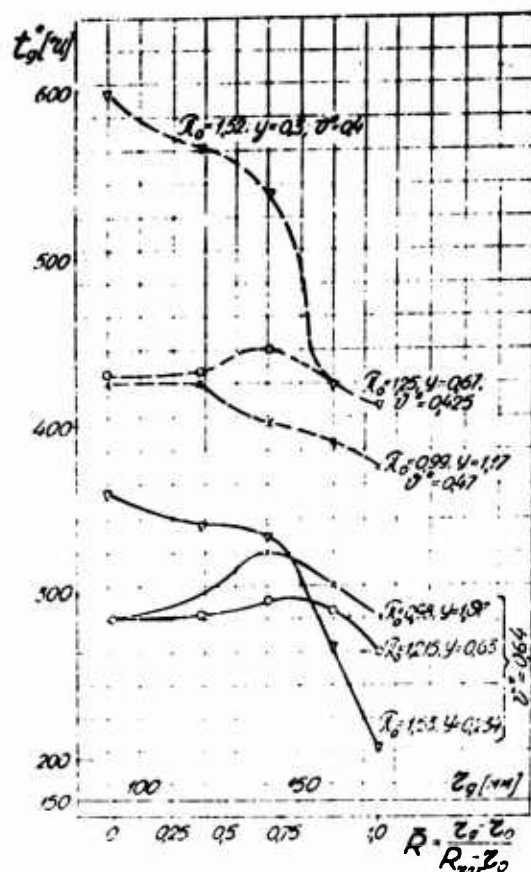
Fig. 3.　　　　　　　　　Fig. 4.

Fig. 3.　Temperature field at the outlet of mixed flow from the diffuser of an AMC with $\alpha_{np} = 16°$, $n = 3.2$ at $\lambda_{A1} = 0.7$-0.8.
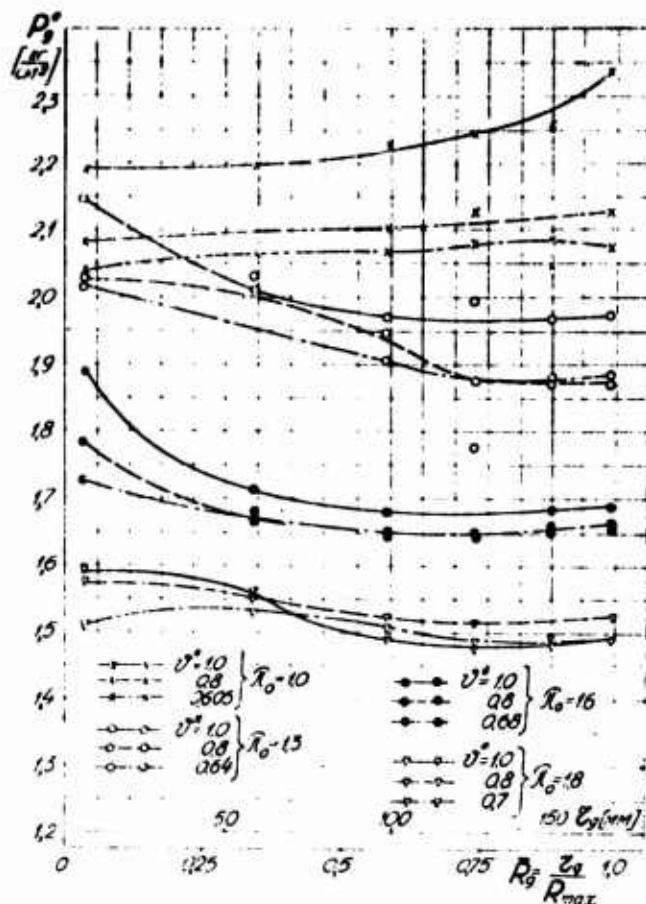
Fig. 4.　Field p^* of a mixed flow at the outlet from the diffuser of an AMC with $\alpha_{np} = 20°$, $n = 4.0$ with $\lambda_{A1} = 0.7$-0.8.

However fields $T_9^* = f(R)$ at low values of π_o also in the given case turn out to be more uniform than when $\pi_o = 1.52$, but this is achieved only due to the drop of T_9^* in the flow core. This explained, apparently, by the fact that during larger values π_o the active (central) flow possesses considerably greater mass than the passive (values of "y" are written on every curve in Fig. 3), and the low-pressure peripheral flow cannot show an essential effect on its nucleus, as it is three times lesser in mass. In spite of large nonuniformity when $\vartheta^* = 0.4$, the average T_9^* as a whole on cross section when $\pi_o = 1.52$ is greater than when $\pi_o \leq 1.25$,

73

and comprises 780°K (instead of 700°K when π_0 = 1.25), which cannot be said about the flows which are mixed when $\$^*$ = 0.64. In the latter case, the mean temperature at all values of π_0 (1.0; 1.215 and 1.53) is approximately identical and $\approx$560-570°K, but the field T_9^* is considerably more uniform with small π_0. Hence the conclusion about the advisability of an increase of π_0 (for the purpose of obtaining larger average value of T_9^*) with an increase in the drop in temperatures (by decreased $\$^*$) asserts itself and, contrarily, about the advisability of a decrease of π_0 with a decrease in the difference between the temperatures of the initial flows (Fig. 3).

In the process of the experiment numerous starts under identical conditions of the initial flows at the inlet to diffusers of different geometry (see page 70) were conducted. In this case it was noted that using identical available gas-dynamic parameters with a decrease in the slope of the diffuser (i.e., with a decrease in the values of n and α_{np}) increases the warming up of its peripheral areas, i.e., increases the uniformity of the field T_9^*, which indicates the preferability of smaller values of n (in the range n = 4-3).

In Fig. 4 attention is drawn to the transformation of fields p^* both during the change in the values of π_0 and during a change in the values of $\$^*$. Moreover it is noticeable that with an increase in the preheating of the active flow, fields p_9^* acquire a more uniform nature even at invariable value π_0, which speaks about the intensification of the process of mixing in diffuser with a preheating increase.

Furthermore, a determinate characteristic law governing a change in the structure of fields p_9^* with an increase of the available pressure differential was established.

74

With the retention of the constant value of the available drop in the temperatures, it was noted that with an increase of π_0 the nonuniformity of the field p_9^* sharply grows initially. For example, when $\theta^* = 0.8 = $ const, with an increase of π_0 from 1.0 to a value of 1.3 the nonuniformity of the field p_9^* grows from 2.4 to 7.7%, but with further increase of π_0, the nonuniformity remains approximately at the same level.

The indicated transformation of fields p_9^* was repeated with the blasting of diffusers differing from aforementioned in their geometry.

Thus, the geometry of diffuser did not exert a substantial influence on the transformation of fields p_9^* during a change in the available gas-dynamic parameters.

§ 2. A Change in the Pressure of Mixed
Flows Along the Diffuser

Graphs 5-8 present the results of the measurements of static pressure at the internal and external cowlings (07 and 01 in Fig. 2) along the investigated diffusers. The flow of the mixed flows passed with numbers Re = $(10-6.5) \cdot 10^5$, i.e., in self-similarity according to the coefficient of friction of the area.

For each of the indicated charts it is distinctly evident that an increase in the static pressure (but this means also a decrease in the velocity of the mixed flows) occurs most intensely in the initial part of the diffuser - at a length less than the half of the entire length of the investigated diffuser. Subsequently an increase in the static pressure is sharply retarded in all investigated systems and with any diffuser geometry. At comparatively low speeds of the order of $\lambda_1 = 0.3-0.5$ (Fig. 6) at the inlet to the same diffuser, the static pressure grows only up to a determinate cross section, which corresponds to expansion ratio =1.7-2.0, and then remains constant. But on one of the systems

($\pi_0 = 1.22$; $\varphi^* = 0.49$) at the end of the diffuser even a definite drop in the static pressure was fixed along the external cowling.
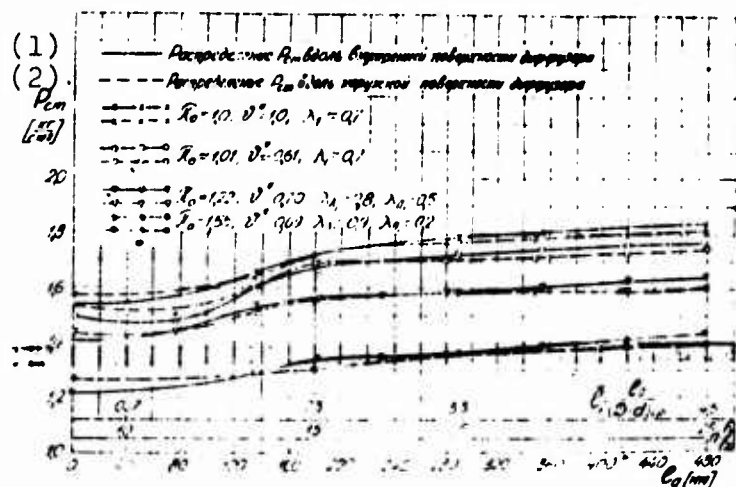
Fig. 5. The projection of static pressure distribution along a diffuser of an AMC with $\alpha_{пр} = 12°$ and n = 2.5.
KEY: (1) Distribution of $P_{см}$ along the internal surface of the diffuser; (2) Distribution of $P_{см}$ along the external surface of the diffuser.
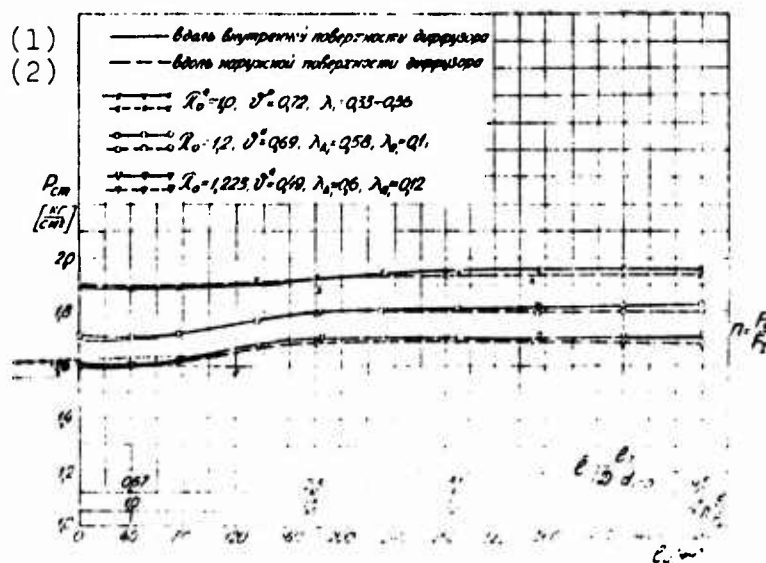
Fig. 6. The projection of distribution of $p_{ст}$ along diffuser of an AMC with $\alpha_{пр} = 12°$, n = 2.5.
KEY: (1) Along the internal surface of the diffuser; (2) Along external surface of the diffuser.

76
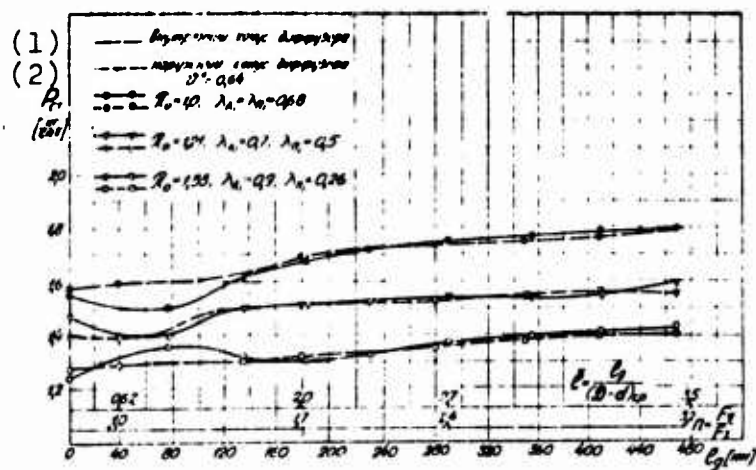
Fig. 7. The projection of distribution of p_{CT} along the diffuser of an AMC with α_{np} = 16° and n = 3.2.
KEY: (1) Internal diffuser cone;
(2) External diffuser cone.
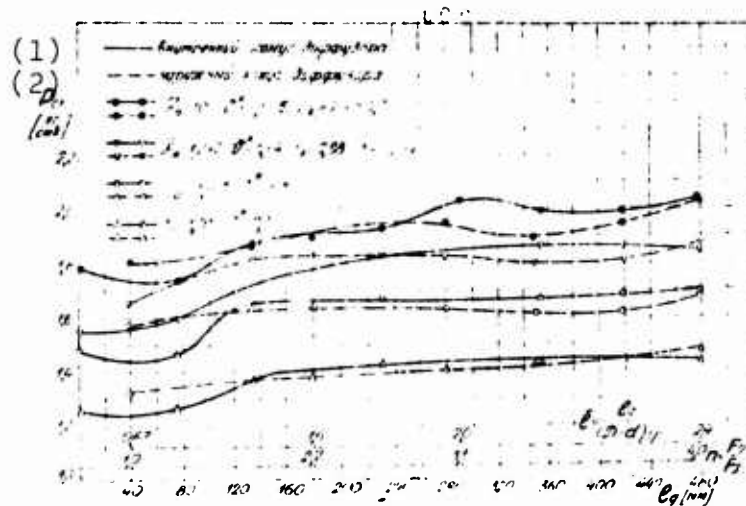
Fig. 8. The projection of distribution of p_{CT} along the diffuser of an AMC with α_{np} = 20°, n = 4.0.
KEY: (1) Internal diffuser cone;
(2) External diffuser cone.

This is explained by the fact that beginning with a certain, sufficiently low value of velocity, the increase in the static pressure, which appears as a result of deceleration, is compensated for by the increasing losses of pressure, but with the further drops in velocity proves to be even less than those losses in the recently noted case.

It was also established, that for every divergence angle of a diffuser there is its limiting value of the expansion ratio which corresponds to a maximum increase in static pressure. This limiting value of the expansion ratio depends also on the value of λ_1.

It is remarkable, that the limiting value of the expansion ratio depends on the parameters of mixing and in the entire range of the investigated parameters ($\pi_0 = 1.0-1.55$; $\$^* = 0.65-0.49$; $\lambda_{A1}/\lambda_{\pi1} = 1.0-5.8$) it remained constant.

Since an increase in the static pressure occurs most intensely in the initial part of the diffuser, then, in order to decrease its overall sizes during the design one ought to select an expansion ratio considerably less, namely: for diffusers with $\alpha_{\pi p} = 12°$ - the value n = 1.5; for diffusers with $\alpha_{\pi p} = 16°$ - the value n = 2.0; for diffusers with $\alpha_{\pi p} = 20°$ - the value n = 2.2, with which the pressure increment $\approx 90-95\%$ of the maximum. Such values of expansion ratios correspond to $\overline{l} = 2.3-1.6$ calibers (see Figs. 5-8).

Moreover the increase of static pressure at the beginning of the diffuser occurs faster, the greater λ_1, however, the limiting mode with greater λ_1 begins later.

Of special interest is the flow of the mixed flows in diffusers with a steeper opening (Figs. 7 and 8).

78

If the flow in a diffuser with $\alpha_{np} = 12°$ (Figs. 5 and 6) in the entire range of the investigated values of λ_1 and of the parameters of mixing (π_o, ϕ^*, $\lambda_{A1}/\lambda_{n1}$) was distinguished by the nonseparable nature on the entire length of the diffuser (with different expansion ratios); then this cannot be said about the flow of the mixing flows in diffusers of the same length, but with $\alpha_{np} = 16°$ and 20° (Figs. 7 and 8). On the basis of the analysis of the available experimental data the conclusion was made that with the purpose of the prevention of separate systems it is not recommended:

a) to use diffusers with $\alpha_{np} \geq 20°$ for the mixing in them of heterogeneous flows with $\lambda_1 \geq 0.7$;

b) to apply in diffusers with $\alpha_{np} = 16°$ available pressure differentials of ≥ 1.5 and $\lambda_{A1} > 0.8$ (see Fig. 7).

§ 3. Characteristics of the Diffuser
According to Pressure Differential
of the Mixed Flows

The most essential diffuser characteristic is the determination of the path losses which were estimated on the experiments carried out on the value of the coefficient of the rise of total pressure pressure - $\sigma_{\text{Д}}^*$. They also grew on all operating modes of the experimental device and with any geometry of the investigated diffuser with an increase π_o of loss. Moreover within the limits up to the value $\pi_o = 1.2$, losses remained constant, a result, mainly, of friction and diffuser flow expansion.

With an increase of π_o more than the value 1.2, the increase in losses (decrease of σ_9^*) became more essential due to the greater influence of the specific losses of mixing, which, at $\alpha_{np} = 12°$, were 2% when $\pi_o = 1.5$ (in comparison with the process when $\pi_o = 1.0-1.2$) and 3.5% when $\pi_o = 1.75$. The described phenomenon was explained by the fact that with an increase of π_o an increase in the difference of the initial flow rates (see Figs. 9 and 10) was observed. The essential difference in λ_1 mixed flows with

79

large π_0 produced a considerable stagnation of an active flow and, as a result, the added losses are analogous to the losses of collision of "inelastic spheres." These losses increased with an increase of the expansion ratio and α_{np} of the diffuser. In the experiment the degree of irregularity of the parameters on a pressure differential was determined also. As can be seen from Figs. 9 and 10, the coefficient of pressure irregularity grows more or less considerably to the value $\pi_0 = 1.4$, and with a further increase of π_0 to 1.8 it remains almost constant. This derivation is in complete agreement with the analysis of the fields p_9^* (see § 1 this chapter). During the tests of diffuers of different geometry, the maximum value of τ_{p9}^* did not exceed values of 1.06-1.075 (nonuniformity = 6-7.5%) when $\pi_0 = 1.5-1.8$.
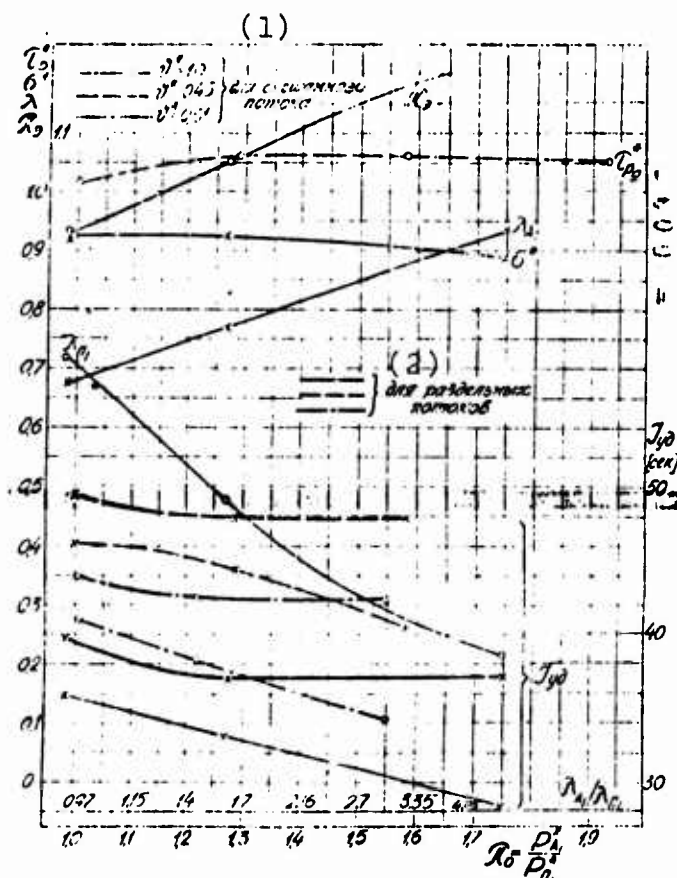
Fig. 9. Characteristic of a diffuser of an AMC with $\alpha_{np} = 12°$, $n = 2.5$ on π_0.
KEY: (1) For mixed flow; (2) For separate flow.

80
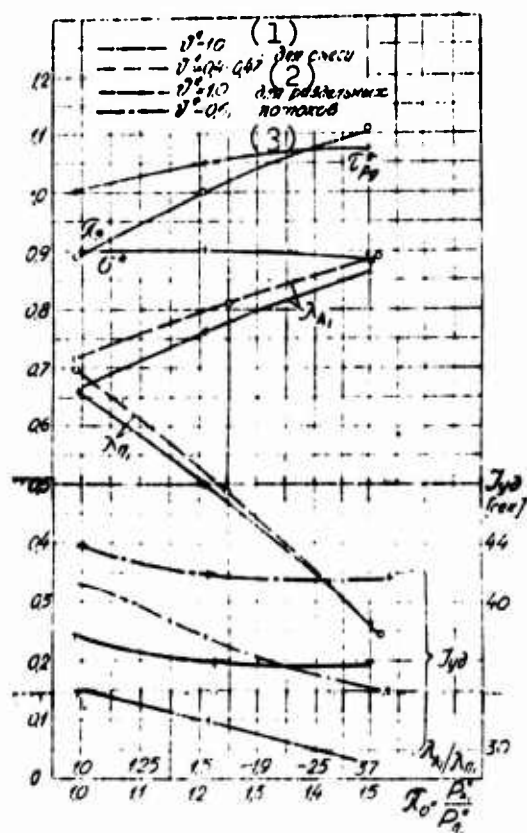
Fig. 10. Characteristic of the diffuser of an AMC with $\alpha_{np} = 16°$, $n = 3.2$ on π_0.
KEY: (1) For a mixture; (2) For separate flows.

The greatest interest in characteristics on a pressure differential is the comparison of specific impulses at the inlet and outlet from the diffusers in question. As can be seen from charts 9 and 10, if the value of output impulse falls sufficiently sharply with an increase of π_0, then the value of input impulse remains almost constant on π_0, which is completely understandable, since the value of $J_{y\text{д}1}$ was affected neither by loss nor the dissipation of energy as a result of the exchange of the impulses of the mixed flows.

The loss of the output impulse (in comparison with input), at any degree of preheating of the active flow (it is equal as without the same) with an increase of π_0, increased in diffusers of different geometry (Figs. 9 and 10), reaching, when $\pi_0 = 1.5-1.6$ and $\lambda_{A1} = 0.85-0.9$, the significant magnitude of 13-18%. Such a combination of the limiting values of π_0 and λ_1 in the given experiment clearly spoke of the inexpediency of their application.

81

And, the lesser the given available pressure drop in the experiment the lesser was the loss of impulse. However this decrease was not continuous for π_0, rather it had a certain optimum with π_0 which differed from one, namely when $\pi_0 = 1.1$.

Hence the conclusion is asserted that the most advisable of all considerations (losses, the momentum conservation, uniformity of the parameters, etc.) is a diffuser with the mixing of flows during low $\pi_0 \approx 1.1$. Moreover the advantage of the application of this π_{opt} is greater, the lesser $\$^{*}$.

§ 4. Characteristics of a Diffuser
of an AMC According to Drop in
Temperatures

With an increase of the temperatures drop of the initial flows the losses of pressure, the value of $\pi_{_9}$, τ_{p9}^{*}, and $\overline{\tau}_{p}^{*}$ remained virtually constant.

As can be seen from Figs. 11 and 12 and the range of temperature drops $\$^{*} = 0.6-0.4$ is most definite from the viewpoint of change in the basic gas-dynamic parameters of mixture.

The consequence of this, obviously, is also the increase in specific impulse of 25-40% with an increase of temperature drop in the aforementioned limits. Furthermore, with an increase of temperature drop the loss of outlet pulse noticeably decreases in comparison with the inlet. As can be seen from Fig. 11, this difference in the values of impulses for $\pi_0 \approx 1.0$ is decreased from the value of 9.5% when $\$^{*} = 1.0$ to 2.7% when $\$^{*} = 0.47$. This comparison was conducted for the case of high-speed mixing which occurred when $\lambda_{A1} \approx \lambda_{n1} \approx 0.7$ in a diffuser with geometric parameters $\alpha_{np} = 16°$, $n = 3.2$. The picture of a change in the relationship of inlet and outlet impulses in a temperature drop becomes even more favorable at lesser (than normally used) initial velocities of the mixed flows. So, with $\lambda_{A1} \approx \lambda_{n1} \approx 0.35$ and $\pi_0 = 1.0$

82

(see Fig. 12) the loss of outlet impulse in the same diffuser
($\alpha_{\text{пр}}$ = 16°) in comparison with the inlet for an isothermic mixing
comprises no longer 9.5%, but only 2%. With an increase of the
temperature drop this difference sharply decreased, and at
$\clubsuit^{*}$ = 0.88 the values of both impulses are equalized. The graph
of Fig. 12 is comprised of relative values where the horizontal
$\overline{J}_{\text{уд}}$ = 1.0 corresponds to the equality of inlet and outlet impulses,
while the curve $\overline{J}_{\text{уд}}$ = $J_{\text{уд}9}/J_{\text{уд}1}$ represents a change in the outlet
pulse relative to inlet. With a further increase in the temperature
drop the value of outlet impulse begins to prevail over its inlet
value, in which the advantages of the process mixing are
effectively realized. This increase of the output pulse,
continuously increasing, reaches at $\clubsuit^{*}$ = 0.5 values of ~4.1%.

Fig. 11. Characteristics of a
diffuser of an AMC with $\alpha_{\text{пр}}$ = 16°,
n = 3.2 according to $\clubsuit^{*}$.
KEY: (1) For separate flows.

Fig. 12. Characteristics of a
diffuser of an AMC with α_{np} = 16°,
n = 3.2 according to ϑ_o.
KEY: (1) Note: The curve of the
change in π_3 when π_o = 1.0
virtually coincides with the curve
of ϑ^* when τ_o = 1.0.

Such a change in the relationship of inlet and outlet impulses
can be explained in the following form. The investigated diffuser
mixing chamber is a two-contour system in which the energy exchange
between contours is realized with the mixing of the gas flows.
Thus the laws governing energy exchange in the model in question
are based on the theory of energy exchange in DTRD [3]. As can be
seen from Fig. 12, the speed of mixed flow is always less than the
speed of separate flows at the mixing chamber inlet. However, with
an increase of the temperature drop, this difference in the speeds
continuously grows on the strength of the fact that, with a change
of ϑ^* from one to 0.49, λ_{A1} increases by 44%, while λ_{n1} and λ_9

84

barely change. But this means that with an increase $\theta = 1/\$^*$, thrust efficiency increases and, as a result, so does the output pulse of the retarded mixed flow.

Thus, an increase in the temperature drop between the initial flows does not worsen the operation of the diffuser mixing chamber, but for the impulse, conversely, substantially improves it. Hence, it is recommended, other conditions being equal (especially with $\pi_0 = 1.0$), to select an operating mode of the diffuser mixing chamber in the region of increased temperature drops (low values $\$^*$).

§ 5. The Effect of the Geometry of A Diffuser of an AMC on the Efficiency of its Operation

It is easy to note from Figs. 13 and 14, that a drop in the total pressure in a diffuser with smoother expansion ($\alpha_{\text{пр}} = 12°$) proves to be substantially less (σ_9^* is large), than in a steeper diffuser ($\alpha_{\text{пр}} = 20°$). This advantage with respect to geometry turns out to be more essential with a smaller value of $\$^*$ and larger π_u (dot-dash lines of σ_9^* on graphs 13, 14), but, this means also during low values of y: thus, when $\pi_0 = 1.50$; $\$^* = 0.64$ and the different λ_{A1}, $\lambda_{\text{п1}}$ of the total pressure loss, upon transition to a diffuser with a lesser slope of the channel, become less than approximately on 7%, while when $\pi_0 = \$^* = 1.0$ and $\lambda_{A1} \approx \lambda_{\text{п1}}$ (solid lines of σ_9^* in Fig. 13) – it is less only by 3.4%, i.e., approximately double.

As a consequence of the lower losses p^* and λ with a decrease of the geometric parameters of the diffuser, the impulse of outward flow also increased somewhat: by 4-9%. Moreover during lesser $\pi_0(\pi_0 = 1)$ momentum grows more intensive than during larger $\pi_0(\pi_0 = 1.5)$.
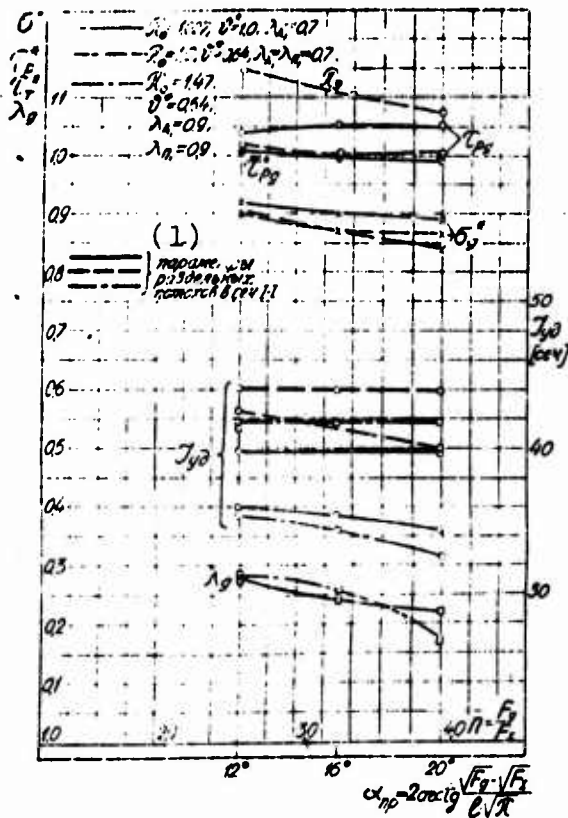
Fig. 13. The effect of the geometry of a diffuser of an AMC on its characteristics when $p_{A1}^* = 2.0$ = const and λ_{A1} = const.

KEY: (1) Parameters of separate flows into Section I-I.
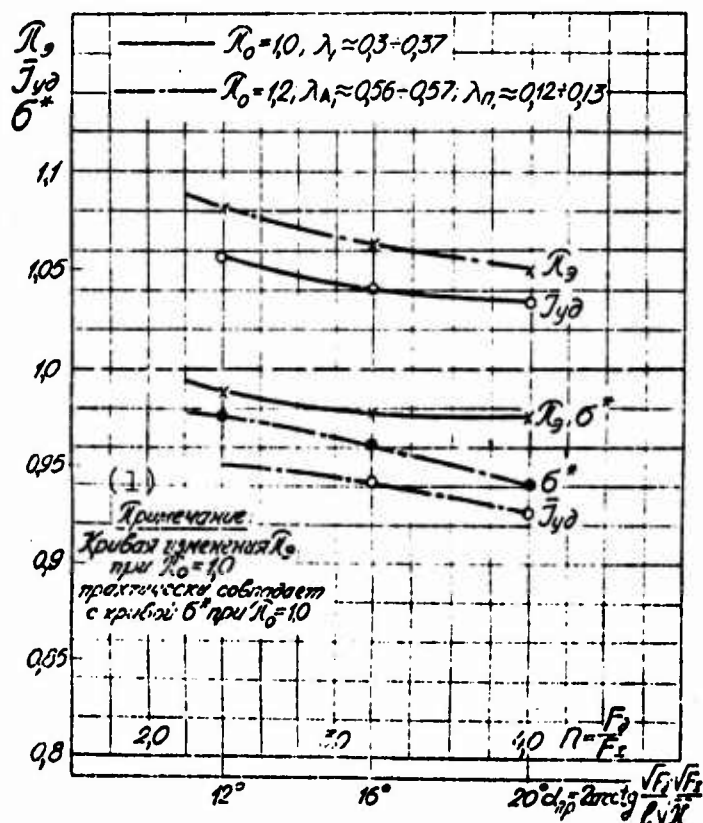
Fig. 14. The effect of the geometry of a diffuser of an AMC on its characteristics when $p_{A1}^* = 2.0$ = const, λ_{A1} = const and $\vartheta^* = 0.5$ = const.

KEY: (1) Note: The curve of the change in $\pi_{\mathfrak{z}}$ when $\pi_o = 1.0$ virtually coincides with curve of ϑ^* with $\pi_o = 1.0$.

The preferability of a diffuser with smaller values of n and α_{np} (within the limits of the investigated series of geometric parameters) also ensues from the comparison of the values of specific impulses at the inlet (heavy line) and at the outlet (fine line in Fig. 13) from a diffuser, depending on its geometry. Moreover in a diffuser of any geometry with mixing with high speeds λ_{A1} = 0.7-0.9, the losses of specific impulse were minimal when π_0 = 1.0 and $\clubsuit^*$ = 0.64 (broken lines in Fig. 13) and they composed in a diffuser, with n = 2.5 and α_{np} = 12°, altogether only 3%, i.e., the advisability is asserted for diffusers of any geometry of low pressure drops and large temperature drops.

As can be seen from Fig. 14, this advisability becomes even greater at low initial velocities which correspond to $\lambda_1 \approx 0.3$. The value of $\overline{J}_{y\text{д}}$ at such velocities and when π_0 = 1.0; $\clubsuit^*$ = 0.5, in the entire range of geometric parameters is substantially more than one, i.e., in a diffuser of an AMC of any geometry using the aforementioned gas-dynamic parameters outlet specific impulse is always greater than the inlet by a value of 3.5 to 5.5% (in proportion to a decrease in the given divergence angle). Both in the case of the greater mixing velocities ($\lambda_{A1} \geq 0.7$), and in this case when π_0 > 1.0; λ_{A1} > λ_{n1}, the relative specific impulse is considerably less than that when π_0 = 1.0 and less than one, i.e., the specific impulse at the outlet of the diffuser mixing chamber is substantially less than the specific impulse at the inlet to it. However this difference is considerably less than with large λ_1 and comprises 7.5-5%.

Thus, as the optimum combination of the geometric and gas-dynamic parameters in this study one ought to consider the organization of the mixing of heterogeneous flows with the maximum preheating of active gas jet when π_0 = 1.0 in a diffuser with n = 2.5 and α_{np} = 12°.

§ 6. Characteristics of a Diffuser of an AMC According to the Speed of Flow at the Inlet to the Model

As can be seen from Fig. 15, with an increase in the speed of the initial flows at the inlet to the diffuser mixing chamber, the total pressure recovery coefficient monotonically decreases, while when approaching the value $\lambda_{A1} = 0.8$, it falls very sharply. In the range of numbers $\lambda_1 = 0.3-0.5$ pressure recovery factor retains an approximately constant and very high value which is equal to 0.9-0.98; with a drop in total pressure, it is equal to 1.0. The further decrease of σ^{*} during an increase of λ_1 is connected with the increasing values of static-pressure gradient along the length of the diffuser, which is possible to trace on Figs. 5-8.
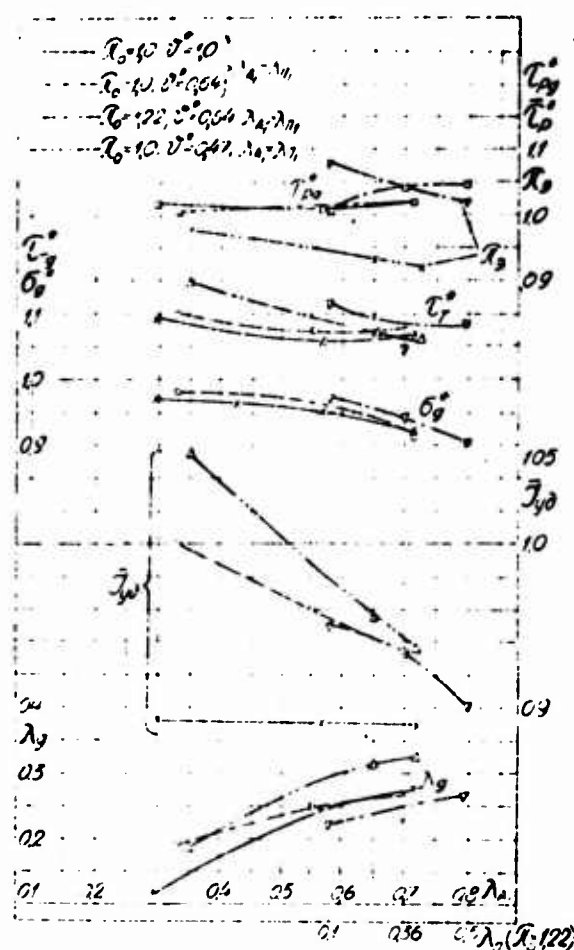
Fig. 15. Characteristics of a diffuser of an AMC with $\pi_{\text{пр}} = 12°$, $n = 2.5$ according to λ_1.

An especially noticeable drop in σ^* was observed with pressure differentials greater than one (dash-line in Fig. 15) and with larger λ_{A1}.

As has already been indicated above (§ 3), with an increase of π_0 a continuous increase of λ_{A1} and drop of λ_{n1} was noticed, so that with large $\pi_0 = 1.7-1.8$ (Fig. 9) λ_{A1} reached the transonic value $\lambda_{A1} \approx 1.0$. But even at smaller values of $\pi_0 > 1.0$ and, respectively, of $\lambda_{A1} = 0.8-0.9$ the outflow was accompanied by development in the inlet part of the active flow of the local supersonic flows (which was established by separate sensors of p_1^*) and by an increase of added losses in connection with this. Also the appearance of flow breakaway from the wall of channel with $\pi_0 > 1.0$ and large λ_{A1} (see § 2) contributed to an increase in the losses in this area.

The comparison of inlet and outlet impulses using the different parameters of mixing was of the greatest interest.

As a result of analysis, the essential effect of preheating the active jet on an increase in the outlet pulse with a decrease in the velocity coefficient at the inlet to the chamber was noticed. This effect is especially considerably pronounced with $\pi_0 = 1.0$. Thus, if, with the mixing of both "cold" flows and $\pi_0 = 1.0$ (solid line in Fig. 15), the loss of the outlet impulse in comparison with inlet in the entire range of λ_1 retained its value as a constant and equal to 11%, then, with the mixing of heterogeneous flows by temperature, its value, in the first place, became considerably less even with large $\lambda_1 = 0.7$ and the same π_0 (6.0-6.5% instead of 11%), and most important, this loss of momentum no longer remained constant with drop of λ_1, but sharply decreased, equalizing at a certain value of λ_1 of the inlet and outlet impulses (the point of intersection with the straight line

$\overline{J}_{y\text{д}}$ = 1.0). This λ_1 alignment with the increase of the degree of preheating of the active jet was displaced to the side of the greater values: up to λ_{A1} = 0.51 when $\$^* $ = 0.47.

Further decrease of λ_1 of nonisothermal flows with π_0 = 1.0 gave no further loss, but an increase of outlet impulse in comparison with the inlet, which reached 5.5% with $\$^* $ = 0.47 and λ_{A1} = 0.35. In connection with this the significant effectiveness of the preheating of active jet on the process of mixing with low λ_{A1} should be noted, which changes the relationship of the inlet and outlet impulses from 11% loss of the latter with $\$^* $ = 1.0 to 5.5% increase with $\$^* $ = 0.47 and λ_{A1} = 0.35. With an increase of λ_1, as has already been indicated above, the preheating of active jet to a lesser degree affects a change in the relationship of the inlet and outlet impulses. It is obviously possible to explain such a change $\Delta J_{y\text{д}}$ according to λ_1 by a change in the relationship of the specific gravity of the losses caused by friction, by the expansion of diffuser channel, by the mixing of flows, and, with large λ_1, also by the appearance of local supersonic zones (i.e., determined by value σ_9^*), on one hand, and losses at outlet velocity, on the other hand.

As follows from Fig. 15 during the extrapolation of all available curves $\overline{J}_{y\text{д}}$ up to λ_{A1} = 0.85-0.9 in the area of transonic speeds, variation by temperature and pressure drops gives no effect at all obviously in view of the prevailing effect of the wave losses of mixed flow. But in the area of the moderate numbers of λ_{A1} there is a noticeably larger advantage of the mixing of flows with π_0 = 1.0 and $\$^* $ < 1.0.

Conclusions

The experimental research carried out on the mixing of gas flows in diffusers of AMC made it possible to establish the following:

1. The uniformity of fields p_9^* depends not only on the value of the available pressure differential, but with π_0 = const also on the value of the available temperature drops; also exactly as the uniformity of fields T_9^* depends not only on value θ^*, but with θ^* = const also on the value of π_0. Moreover to the structure of field T_9^* change π_0 affects in larger degree, than change θ^*. In this case the geometry of a diffuser in the range α_{np} = 12-20° does not exert a substantial influence on the transformation of fields p_9^*, T_9^* with the retention of the constants of initial gas-dynamic parameters.

2. In the investigated range of gas-dynamic parameters of the given diffusers of AMC: π_0 = 1.0-1.9, θ^* = 0.4-2.5, y = 0.2-5.0, λ_1 = 0.1-0.9, completely satisfactory values of the variation factors of the pressure and temperature of the mixed flow were obtained: τ_{p9}^* = 1.00-1.08 and τ_{T9}^* = 1.03-1.14.

3. For every value of α_{np} and λ_1 of a diffuser of an AMC the limiting value of its expansion ratio, corresponding to the maximum increase in static pressure, which does not depend on the mixing parameters is established. Taking into account this distribution of pressure along the length of a diffuser of an AMC, with the purpose of a decrease in its overall sizes during the design, it follows to limit the degree of its expansion to values less than maximum, namely:

for α_{np} = 12° – to the value of n = 1.5;
for α_{np} = 16° – to the value of n = 2.0;
for α_{np} = 20° – to the value of n = 2.2.

4. The boundary of separation systems is established according to pressure differentials, which in a diffuser of an AMC with α_{np} = 12° does not occur in the entire range of the studied parameters: in a diffuser of an AMC with α_{np} = 16° passed with $\pi_0 \geq 1.5$ and $\lambda_{A1} > 0.8$, while in a diffuser of an AMC with α_{np} = 20° – at all values of available pressure differentials and $\lambda_1 \geq 0.7$.

5.   From the considerations of lesser losses and larger uniformity of the gas-dynamic parameters and retention of impulse it follows to consider the effect of the mixing of heterogeneous flows in a diffuser of an AMC when α_{np} = 12° with the small π_0 = 1.0-1.1 as the greatest and possibly the maximum preheating of the active gas jet.   Somewhat better results were obtained with values of π_0 closer to 1.1, rather than to 1.0.

6.   In a diffuser of an AMC with α_{np} = 12° and with acceptable pressure differentials for DTRD ($\pi_0 \simeq 1.0$) and with such temperatures ($\vartheta^* = 0.45$-0.5), the mixing becomes favorable for the specific impulse (but it also means for $C_{y\text{д}}$), beginning with value $\lambda_1 \leq 0.5$.   With a decrease of λ_1 using simple invariable parameters, the increasing effectiveness of the preheating of active jet for the intensification of mixing is noted.   At the different speeds of the initial flows, in relationship to inlet and outlet specific impulses, the level of the value of λ of high-pressure flow is definite, but not the difference in λ of the active and passive flows, which with λ_{A1} = const up to relationship does not affect virtually $\lambda_{A1}/\lambda_{n1}$ = 6 the relative specific momentum.

Bibliography

1. Абрамович Г. Н. Прикладная газовая динамика. Гостехтеоретиздат, М. 1969.

2. Раушенбах Б. В., Белый С. А. и др. Физические основы рабочего процесса в камерах сгорания ВРД. Машиностроение, 1964.

3. Стечкин А. Л. Теория двухконтурных ВРД (монография). Рига, 1959.

4. Фрост Т. X. Системы смешения газовых потоков в двухконтурных авиадвигателях. Э. И. «Авиастроение» № 43, 1966.

5. Pearson H., „Mixing of exhaust and by-pass flow in a by-pass engine" Journal of the R.A.S., 1962.

6. Hartmann Albrecht, „Experimentelle Untersuchungen uber die mischung bei Zweikreisturbinenluftstraltriebwerken", Jahrb. Wiss. Ges. Luft — unb Raufahrt, 1966, Braunschweig, 1957.

7. Барабанова Е. В. Экспериментальная установка для исследования смешения газовых потоков. Вып. 129, ч. 2. Труды РКИИГА, 1968.

8. Горбунов Г. М., Солохин Э. Л. Испытания авиационных воздушно-реактивных двигателей. Машиностроение, М. 1967.

BENCH CHARACTERISTICS OF THE NOISE
OF TURBOFAN ENGINES

V. G. Yenenkov

In the article the acoustic characteristics
of the basic noise sources of turbofan engine
during engine operation on a stand are examined.
Concepts about acoustic characteristics are
given and the methods of their calculational
determination are presented. Information about
the mechanisms of the excitation of noise is
given. The data of experimental studies of the
noise of DTRD with bypass ratios of y = 0-6 are
analyzed.

Introduction

The noise which accompanies takeoff, landing and flight of
contemporary aircraft, becomes the object of the fixed attention
of aviation specialists. In the countries with a highly developed
aircraft industry and civil aviation, in practice, standards, norms
and certificates are developed and introduced which determine the
permissible noise levels of aircraft during their takeoff and
landing [1]. The concept evolves that aircraft, whose noise
exceeds standardized values, are considered underfulfilled in
design and they are not allowed in operation.

The increase in the intensity of air transport, connected with the advent of heavy duty aircraft and an increase in the number of voyages, inevitably leads to the need for efficient combat with aviation noise. Many specialists consider the problem of a reduction in aircraft noise one of the most important and complex, removing it to a place immediately after flight safety control. In connection with this it is understandable, how important it is to be able to correctly estimate the acoustic characteristics of contemporary civil aviation aircraft engines, since precisely this power plant is the main noise source during takeoff and landing.

In the domestic and foreign press many works are published dedicated to the study of the individual characteristics of the gas turbine engine noise. The questions of the evaluation of the noise of turbofan engine, which have different bypass ratios and especially large $y = 4-6$, are not examined in them, as a rule. In this article primary attention is given to the acoustic characteristics of DTRD with $y = 0-6$.

§ 1. The Basic Concepts About the Acoustic
Characteristics of the Noise Sources of
DTRD

The acoustic characteristics of the noise sources of engines are described by [2]:

1) complete acoustic power;
2) sound intensity (by sound pressure or received noise levels);
3) noise spectrum;
4) directional characteristic of the noise;
5) duration of the effect of noise and by the frequency of its recurrence.

94

The acountic (sonic) power W is the complete sound energy
radiated by the noise source into the surrounding space per unit
of time. Acoustic energy is frequently expressed in the levels
of acoustic power L_W, expressed in decibels relative to the
conditional threshold value of $W_c = 10^{-12}$ W:

$$L_w = 10 \lg \frac{W}{W_\bullet} \text{ (dB)}. \tag{1}$$

The complete acoustic power is a fundamental characteristic
of a noise source as a generator of sound energy.

The *intensity* or *force of sound* I (W/m^2) is the energy content
transferred in a free field by acoustic wave for one second across
an area per 1 cm^2, normal to the direction of motion of the wave.
Sound intensity is expressed also in intensity levels

$$L = 10 \lg \frac{I}{I_\bullet} \text{ (dB)},$$

more frequently represented through sound pressure p (N/m^2) in the
form

$$L = 10 \lg \frac{I}{I_\bullet} = 20 \lg \frac{p}{p_u} \text{ (dB)} \tag{2}$$

since

$$I = \frac{p^2}{\rho_\bullet a_u}.$$

Here ρ_0 – air density; a_0 – speed of sound in air; $p_0 = 2 \cdot 10^{-5}$
N/m^2 – the conditional threshold value of sound pressure which
corresponds to threshold intensity $I_0 = 10^{-12}$ W/m^2.

Value L is called the sound pressure level and is the relation-
ship of the operating pressures or sound intensity to their
conditional threshold values.

The sound intensity determines the energy of sound vibrations
at different points of the acoustic field. For nondirectional
source I = W/F, for a directed noise source

$$I = \frac{W}{F} \Phi. \tag{3}$$

Here F - the surface through which the sound emission arises, and the value Φ characterizes the directivity of the radiation.

Noise spectrum - the totality comprising the sound pressure levels L_j (levels of acoustic power L_{wi}) obtained during the frequency response analysis of the investigated noise, which is the description of the sound pressure or power levels of the individual components of the noise signal in different frequency bands (octave, 1/2 octave, 1/3 octave). An example of the noise spectrum of a compressor is given in Fig. 1. With the noise spectrum, by means of logarithmic averaging, it is possible to determine total (overall) sound pressure level of the complex noise signal in the entire frequency range

$$L = 10 \lg \sum_{i=1}^{n} 10^{\frac{L_i}{10}} \ (\text{dB}). \tag{4}$$
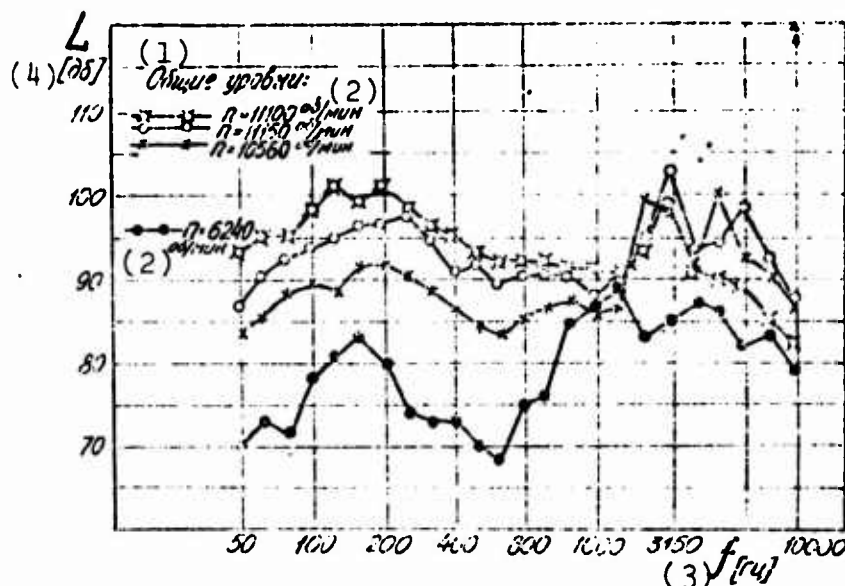
Fig. 1. The noise spectrum of the compressor of a DTRD with y = 1.0 at a distance r = 30 m, at an angle φ = 10° to the axis of the engine inlet.

KEY: (1) Total levels; (2) r/min; (3) Hz; (4) dB.

Besides the evaluation of total noise level, the spectral characteristic of the noise signal is necessary for the determination of the level of received noises - the subjective criterion which considers the noisiness of the signal depending on frequency make-up of the noise heard.

The *level of received noise* is measured in PN dB and is determined by the calculation according to noisiness in separate frequency bands expressed in "noises"[*] (Fig. 2). The total noisiness of complex sound is equal to

$$N_{o6u} = N_{\text{макс}} + F \left(\sum_{i=1}^{n} N_i - N_{\text{макс}} \right).$$

where $N_{\text{макс}}$ - the value of noisiness in the most noised frequency band; $\sum_{i=1}^{n} N_i$ - the sum of noisiness in all bands; F - the coefficient which considers the bandwidth of the filter used during measurement. For a bandwidth, equal to 1/3 octave, F = 0.15; 1/2 octave F = 0.2 and of 1 octave F = 0.3.

$$L(PN \quad dB) = 40 + 33.3 \lg N_{o6u}. \tag{5}$$

Directional characteristic - the distribution of sound pressure levels to a long acoustic field, according to different radial directions from the sound source, is constructed in polar coordinates both for the total noise (Fig. 3, [3]) and for its components in different frequency bands (Fig. 4 [4]). The long sonic field of noise source is understood to be the space, in which the sound pressure decreases inversely proportional to the distance from the

---

[*]This is a reference to an unknown/unidentifiable sound measurement unit which is obviously taken from the English word noise. Further uses will be placed in quotes to distinguish them as measurement units, rather than the term for unwanted sound.
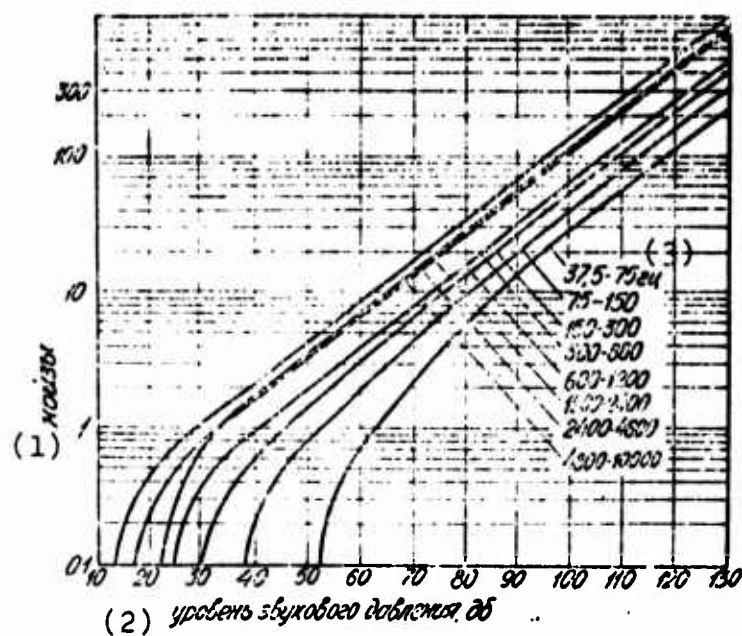
Fig. 2. The dependence of noisiness in "noise's" on sound pressure level per octave.

KEY: (1) "Noise's"; (2) The sound pressure level, dB; (3) Hz.
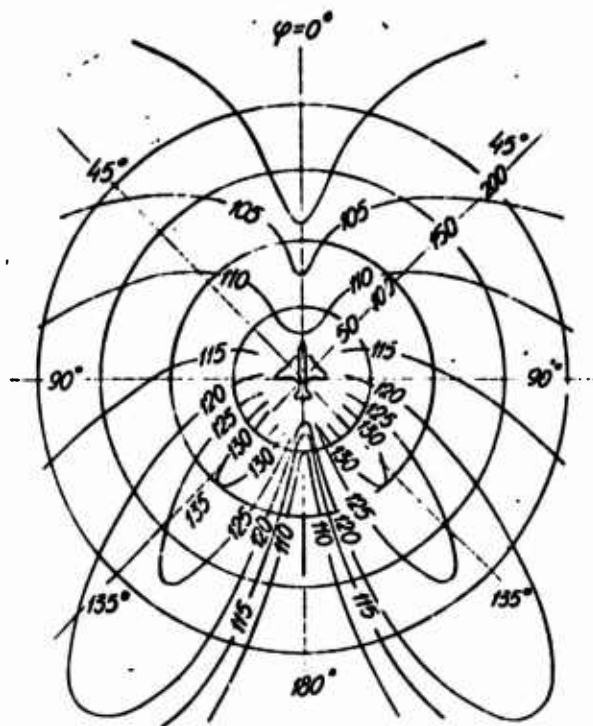
Fig. 3. The directional characteristic of the noise of an aircraft with jet engines.

center of radiation to the measuring point. From the directional
characteristic the factor of directivity of 10 lg Φ (dB) is
determined, that is, the difference between sound pressure levels
at a certain point of space from the investigated source and from
a fictitious nondirectional sound source of the same power.
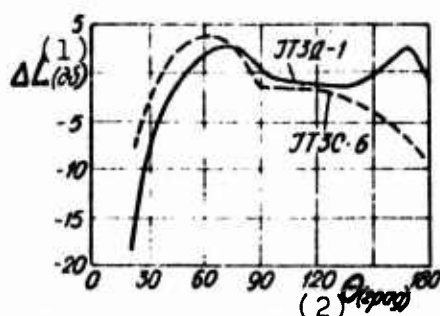
Fig. 4. The directional
characteristic of noise
of the seventh octave
(2400/4800 Hz).

KEY: (1) dB; (2) deg;
(3) The radiation pattern
of the seventh noise
octave (2400/4800 Hz).

The duration of the effect of noise is characterized by the
time of heard - by the time of effect of the upper 10 dB or noise
above the level of 90 dB. During repeated irradiations by noise
the sum of the time of sounding of upper 10 dB or of the level
90 dB is taken.

§ 2. The Basic DTRD Noise Sources

Turbofan engines have several sources of noise: the jets
of the first and secondary contours, the fan and the compressor,
the turbine, the combustion chamber and assemblies. Depending on
the bypass ratio, operating condition parameters, and engine power
rating, some of them are basic and determinate, while the noise
of others is masked by the noise of the basic ones.

Figure 5 gives the data of the experimental research on the
noise of DTRD with small bypass ratio [5]. The propagation
pattern gives a demonstrative picture of the noise source orientation
relative to the engine. Moving left to right, the observer first
encounters the noise of the compressor with maximum intensity of
radiation at about a 30° angle to the axis to the inlet which

99

prevails in the entire intake sector on the majority of systems, except those close to maximum, when the noise of the jet drowns everything. Moving to the rear sector and passing through the short section of the middle part of the engine, irradiated by the noise of the assemblies and combustion chamber, the observer enters the field of the superimposed radiation of two separate noise sources. This is the turbine noise and, as is characteristic for a bypass engine, the noise directed back from the compressor (fan), bearable through the tract of the second contour. The propagation angle of this noise changes from 60 to 80° to the axis of the jet, depending on the engine parameters, and its level is basically determined by the bypass ratio. Finally, observer enters the area of the jet noise – the most powerful source during increased engine power ratings, with the maximum intensity of propagation at a 30-60° angle to the axis of the jet. With an increase in bypass ratio from 0 to 6, the relationships between the noise intensities of different sources and directional characteristic change substantially. The fundamental picture of this change is shown in Fig. 6. Especially attention is drawn to jet noise reduction and a simultaneous increase in fan noise.
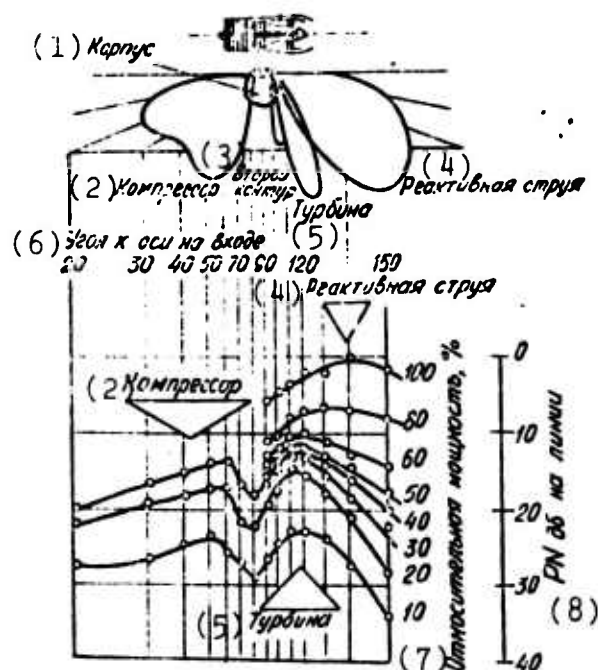
Fig. 5. The basic DTRD noise sources.

KEY: (1) Body; (2) Compressor; (3) Second contours; (4) Jets; (5) Turbine; (6) Angle to inlet axis; (7) Relative powers; (8) PN dB on line.

Fig. 6. The propogation pattern of the
DTRD noise with y = 0, 1 and 6.
KEY: (1) Compressor; (2) Engine axis;
(3) Jet; (4) Turbine; (5) Fan.

Figures 7-10 give the experimental data of the measurements of
the noise of the engine which have bypass ratios 0, 1, 2, 3 and 5.
The analysis of the directional characteristic and noise spectra
visually shows that:

a) with bypass ratio y = 0 (Fig. 7) on all engine power ratings
from the takeoff to landing, the specific noise source is the jet,
its noise exceeds the noise of the remaining sources by 10-20 dB;

b) with bypass ratio y = 1 (Fig. 8), in takeoff mode, the
noise of the jet (maximum intensity of radiation at an angle to
the axis of the jet $\Theta = 60°$) exceeds the noise of compressor by
4 PN dB, and in landing mode the noise of compressor directed
into front section prevails approximately by 5 PN dB, with the
maximum intensity of propagation at an approximately 20° angle to
the inlet axis engine;

c) with bypass ratio y = 2 (Fig. 8), at all engine power
ratings, the compressor noise directed forward exceeds the noise
of the jet: in takeoff mode by 6 PN dB, on landing - by 18 PN dB;

d) with bypass ratio y = 3 (Fig. 9), at takeoff engine power
rating the fan noise propogated from the shortened external contour,
already exceeds the noise of the jet by more than 15 PN dB with the
maximum intensity at an angle approximately 70° to the axis of the
jet. In the front sector, it is also the greatest. The noise of

101

the jet is overlapped by the noise of the turbine (almost by 10 PN dB), this is a new noise source, for which interest was not displayed at low bypass ratios and which, apparently, will have particular importance at large y [6];

e) with bypass ratio y ~ 5, the fan drowns all other sources and in the rear and front sectors, the directional characteristic of the noise of such an engine is given in Fig. 10 [7].

----- compressor noise radiated forward
− − − compressor noise radiated back
− - − jet noise
———— total noise level

y = 0
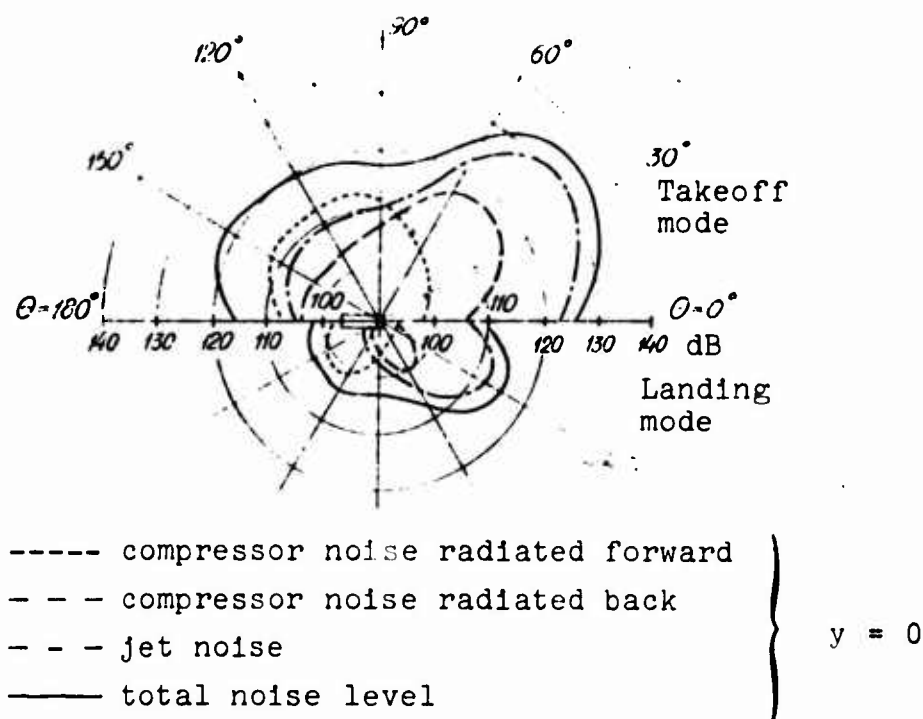
Fig. 7. The directional characteristic of the noise of turbofan engine in takeoff and landing systems.
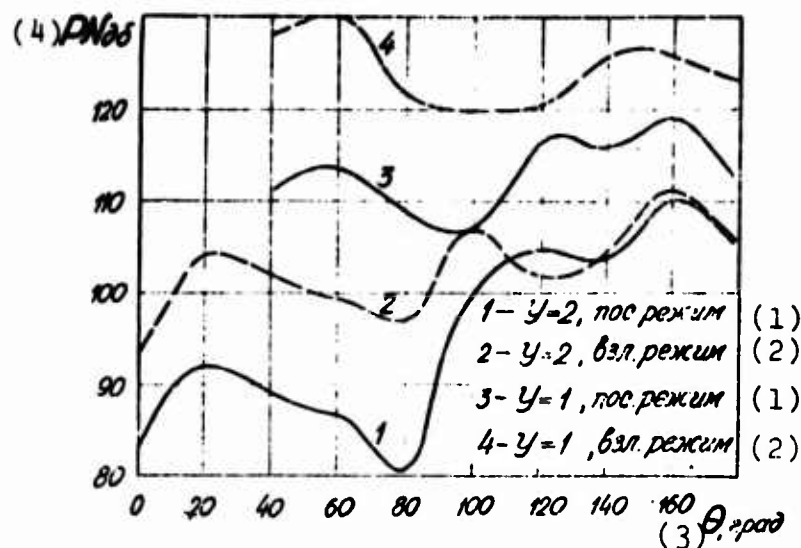
Fig. 8. The directional characteristic
of DTRD noise with y = 1 and 2 in the
takeoff and landing modes.

KEY: (1) Landing mode; (2) Takeoff mode;
(3) deg; (4) dB.
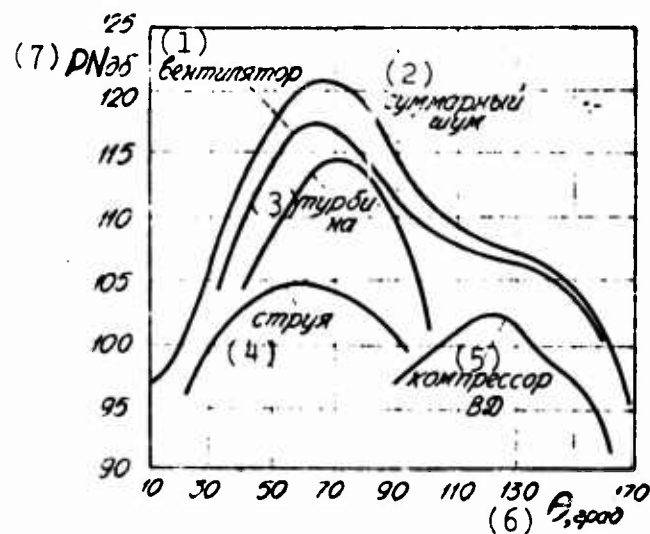
Fig. 9. The directional
characteristic of the DTRD
noise with y = 3, in takeoff
mode.

KEY: (1) Fan; (2) Total noise;
(3) Turbine; (4) Jet; (5) High
pressure compressor; (6) deg;
(7) dB.

103
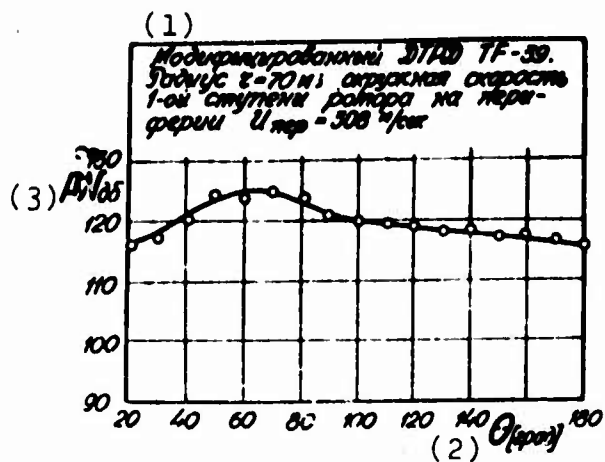
Fig. 10. The directional characteristic of the DTRD noise with y ~ 5.

KEY: (1) Modified TF-39 DTRD. Radius τ = 70 m; the peripheral speed of the 1st stage of the rotor at the periphery $U_{\text{пер}}$ = 308 m/s; (2) deg; (3) dB.

The results of the analysis made can be presented briefly in the form of a table of the determinate DTRD noise sources dependent on the bypass ratio and engine power ratings:

Table.

Bypass ratio Mode	Takeoff mode	Landing mode
0	Jet	Jet - compressor
1	Jet - compressor	Compressor - jet
2	Compressor - jet	Compressor
3 and greater	Compressor (fan)	Compressor (fan)

The comparative calculated evaluation of the noise of the fan and the jet of a DTRD with T_3^{*} = 1300°K, $\pi_{\text{ко}}^{*}$ = 17 and bench thrust R_0 = 8 T during a change in y from 0 to 9, which was carried out by the author in conjunction with B. N. Mel'nikov, also shows that at y > 2 fan noise becomes determinate.
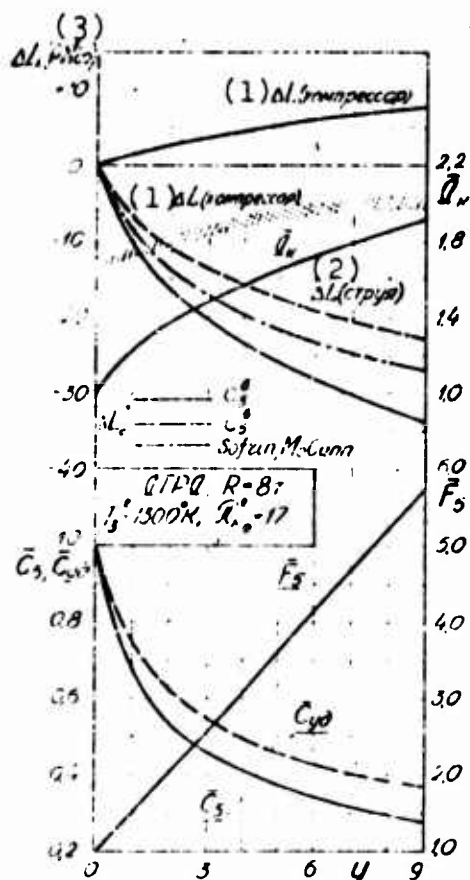
Fig. 11. The effect of bypass ratio on compressor and jet noise.

KEY: (1) Compressor; (2) Jet; (3) PN dB.

§ 3. The Nature of Noise Sources

A noise source which radiates acoustic waves in all directions, can be an oscillating sphere or monopole (Fig. 12).

Two spheres in line and which oscillate at antiphase (one is compressed, another is expanded) are a dipole sound source. Similar to this model is the radiating sphere which oscillates along a straight line. The important feature of a dipole source is the directional effect: a large part of the sound is propagated in the plane of the dipole. For dipole excitation the harmonic force w! .ch acts on the part of hard boundary is necessary.

Monopole   Dipole   Quadrupole
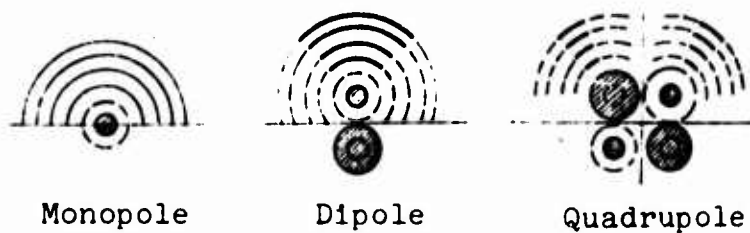
Fig. 12. An illustration of the nature of noise sources.

If we place together two dipoles, that oscillate in antiphase, a quadrupole sound source will be obtained. In this case there are two mutually perpendicular directions, every point of which obtains a compensated "null" signal. At an angle of 45° signals do not compensate for each other, since phases and amplitudes are different, and in this direction the intensity of radiation is greatest.

Of the enumerated sources, the quadrupole is the least effective noise generator.

§ 4. The Characteristics of the Noise
Created by the Jet

1. The Mechanism of the Jet Noise Generation

The noise of the jet arises as a result of the turbulent mixing of the gas flow, which escapes from the jet nozzle, with surrounding air. In the zone of turbulent mixing, which has lengths of 15-25 diameters of nozzle, fluctuations of the speeds and eddies appear, in connection with which occur the pulsations of pressures and densities. Lighthill [8] proposed to consider turbulent flow as a large quantity of centers of quadrupole radiation, driving at a certain convective speed in an ambient medium. Actually, the oscillating gas flow creates in the atmosphere those density fluctuations, which would arise in a uniform acoustic medium under the action of a system of tensions

106

applied from without to the elements of the medium. Each element of the gaseous medium, during the appearance of the tensions, experiences the effect of two equal, in magnitude, and opposed forces. But any force, acting on an element of medium, in acoustics is the equivalent of a dipole, while a pair equal in magnitude and opposed forces - to a quadrupole.

That means the jet can be broken into many volumes, equal to the dimension of an eddy, and each of them considered as a separate noise source in the form of an acoustic quadrupole.

2. The Acoustic Power of the Jet

At present, the calculation of the acoustic power of a jet, in accordance with Lighthill's theory, is conducted from the gas-dynamic and geometric parameters of the jet in the jet nozzle area. Many investigations established that the best agreement of results of calculations and experimental data for hot and cold jets is observed during the calculation of acoustic power according to formula [2][1]

$$W = K \rho_5 c_5^i F_6 a_0^{-5} \ (W).$$

(6)

By applying gas-dynamic functions for the expression of density and velocities through the parameters of stagnant flow and the given velocity λ, let us write formula (6) in the form

$$W = KB\epsilon(\lambda_5) p_5^* \lambda_5^* T_0^{-1} \left(\frac{T_5^*}{T_0}\right)^3 F_5 \ (W),$$

(7)

---

[1]These investigations are related to jets which have subsonic and small supersonic speed of outflow ($1.5 < \pi_{pc} \leq 2.2$). At a large supersonic speed of outflow the noise of the jet is proportional to the discharge velocity by the cube. At low discharge velocities ($c_5 < 300$ m/s) the acoustic thickness of the jet is proportional to c_5^6.

where

$$B = R_r' \, k_a^{-5/1} \left(\frac{2k}{k+1} \right)^4.$$

(for air B = 13.65; for gas B = 12.44).

Since, for the calculation of acoustic power, the parameters in the outlet section of a subsonic nozzle are taken, for the subcritical system of outflow of gas ($\pi_{pc} < 1.89$, $p_5 = p_0$) it is possible to write

$$W = KB \left(1 - \frac{k-1}{k+1} \lambda_5^2 \right)^{-1} p_a \lambda_5^4 T_a^{1/2} \left(\frac{T_b^*}{T_a} \right)^8 F_b. \tag{8}$$

During a supersonic system of gas outflow from a subsonic nozzle ($\pi_{pc} > 1.89$; $p_5 > p_0$; $\lambda_5 = 1.0$) formula (7) will take the form

$$W = KB \left(\frac{2}{k+1} \right)^{\frac{1}{k-1}} p_5^* T_a^{1/2} \left(\frac{T_b^*}{T_a} \right)^8 F_b. \tag{9}$$

The calculation of acoustic power for supercritical systems of outflow according to formula (9) agrees well with experiment up to values of $\pi_{pc} \leq 2.2$.

The proportionality factor K in formulas (6-9) has the following values:

a) for engines which work at nominal and maximum ratings, $K = 1.5 \cdot 10^{-4}$;

b) for engines which work under conditions less than 0.8 nominal, $K = 2.5 \cdot 10^{-4}$;

c) for gas jets which escape from a convergent nozzle, $K = 0.8 \cdot 10^{-4}$.

The calculations of the acoustic power of the jets of DTRD without the premixing of the flows of the two contours, according to presently available experimental materials, can be produced with the summation of the acoustic powers of the jets of the first and second contours

$$W_{\text{ЛТРД}} = W_{\text{I}} + W_{\text{II}}.$$

By formulas (7-9) the values of acoustic power are given in connection with the dimensionality of engine, determined by the discharge area of the jet nozzle F_5. It is possible to eliminate the effect of dimensionality, by determining the acoustic power per unit of thrust. For this F_5 is represented in the form

$$F_5 = \frac{1}{m} \frac{T_5^*}{P_5^*} \frac{1}{q(\lambda_5) R_{y1}} R_{y1}$$

while the formula of acoustic power after the transformations appear in the following manner:

$$\frac{W}{R} = \frac{KB}{m} \left(\frac{k+1}{2} \right)^{-\frac{1}{k-1}} \lambda_5^3 (T_0 T_5^*) \left(\frac{T_5^*}{T_0} \right)^3 \frac{1}{R_{y1}}. \tag{10}$$

3. The Noise Spectrum of the Jet

The noise spectrum of a jet with a subsonic pressure differential in the nozzle is continuous with a weakly marked maximum. During an increase in pressure differential and an increase in the temperature of the jet, the portion of the high-frequency component in the noise spectrum, increases with an increase in diameter, the low-frequency portion [2] increases.

The experimental research showed that the relative spectrum of acoustic power may be presented by one curve in the form of a dependence of $\Delta L_{w1} = L_{w1} - L_W$ on the Strouhal number $Sh = fd_5/c_5$ (Fig. 13). In this case, the levels comprising the spectrum, and the level of acoustic power L_w are connected by the function

109

$$l_w = 10 \lg \sum_{i=1}^{n} 10^{\frac{L_{wi}}{10}}.$$

Having calculated the total acoustic power W by one of the formulas (7-10), depending on the system of the jet outflow from the nozzle, then having determined L_w = 10 lg W + 120, it always is possible to find the level of acoustic power in 1/3 octave frequency bands with the aid of the curve given in Fig. 13.
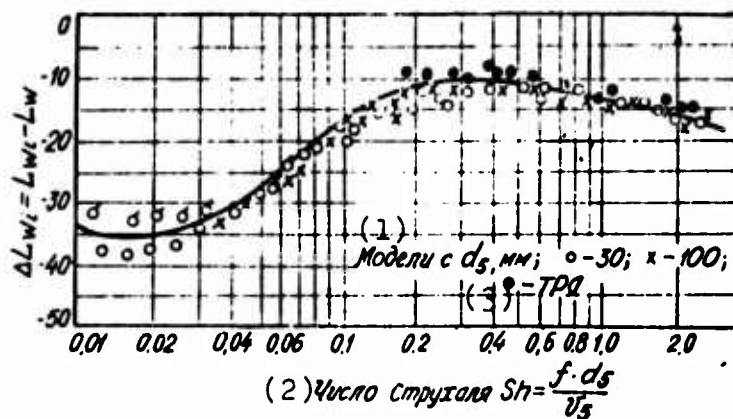

Fig. 13. The dependence of the level of acoustic power of a jet on the Strouhal number.

KEY: (1) Models with d_5, in mm;
(2) Strouhal number Sh = $f \cdot d_5/v_5$;
(3) Turbojet.
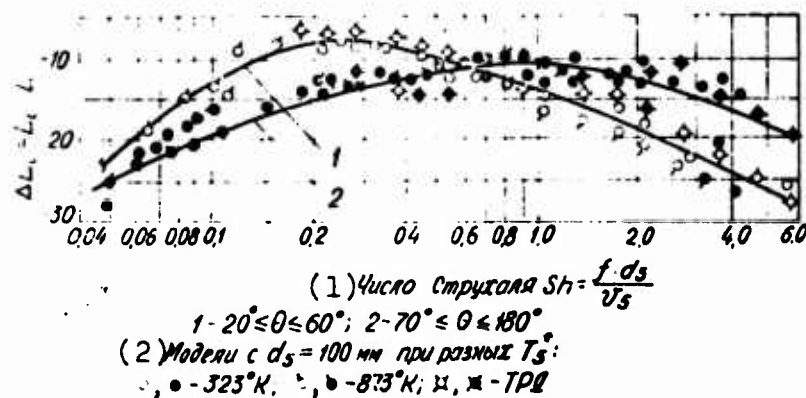
Fig. 14. The dependence of the sound pressure level of a jet on the Strouhal number.

KEY: (1) Strouhal number Sh = $f \cdot d_5/v_5$; (2) Models with d_5 = 100 mm with different T_5^*.

The dependence of the jet noise spectrum (Fig. 14) on the angular position of observation point can be reduced to the consideration of two angular areas $20° < \Theta < 60°$ (curve 1) and $70° < \Theta \leq 180°$ (curve 2).

4. Sound Pressure and Received Noise Levels

The sound pressure level, according to the determination of (2) and (3), is equal to

$$L = 10 \lg \frac{W}{I_o F} + 10 \lg \Phi \text{ (dB)}.$$

During sound propogation into hemisphere, $F = 2\pi r^2$, therefore

$$L = 10 \lg W + 10 \lg \frac{1}{I_o 2\pi} - 20 \lg r + 10 \lg \Phi \text{ (dB)}$$

or

$$L = 10 \lg W + 109 - 20 \lg r + 10 \lg \Phi \text{ (dB)}. \tag{12}$$

The factor of directivity $10 \lg \Phi$ is determined according to the results of the processing of experimental research data. Figure 15 depicts the change of this factor depending on the angle of directivity for cold and hot jets with gas temperatures up to 1000°K [2]. In the direction of the greatest intensity of radiation, the factor of directivity composes a value on the order of 8 dB.

The levels of received noise are determined from the jet noise spectrum, constructed for given d_5 and c_5 in accordance with the experimentally established distribution of the components of sound pressure levels in 1/3 octave bands (Fig. 14).

For a less strict evaluation of the levels of received noise, it is possible to recommend quite a simple method. As a result of the considerable similarity of spectra of jets, which have different gas-dynamic and geometric parameters, their levels of received noise from sound pressure levels by a certain value ΔPN dB. The adjustment of the ΔPN dB has the following expressions [2]:

111

1) for a TJE and a turbofan engine without mufflers

$$\Delta P.V \text{ dB} = 8.3 - 0.0083\, r \tag{13}$$

2) for a TJE and a turbofan engine with noise-abating nozzles of low effectiveness (3-6 dB of a reduction in the noise)
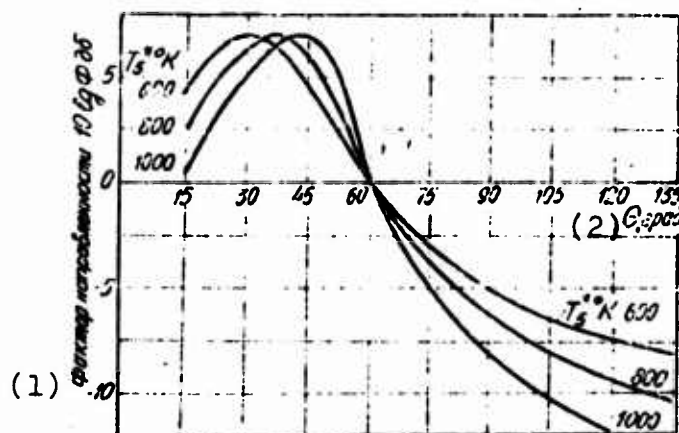
$$\Delta P.V \text{ dB} = 10.3 - 0.0083\, r \tag{14}$$

Fig. 15. The dependence of the directivity factor on the angle Θ.

KEY: (1) Factor of directivity 10 lg Φ dB; (2) deg.

Thus,

$$L(P.V \text{dB}) = l.(\text{dB}) + \Delta PN \text{ dB}.$$

5. The Order of Calculation of the Acoustic Characteristics of the Jet

The order of calculation of the jet noise can be recommended as follows:

1. The total acoustic power of the jet W is determined from one of formulas (7-10).

2. The level of the acoustic power

$$L_w = 10 \lg W + 120 \, (\text{dB}).$$

3. The components of the spectrum of acoustic power are determined in 1/3 octave frequency bands

$$L_{wi} = L_w + \Delta L_{wi}.$$

where ΔL_{wi} - components of the dimensionless spectrum of acoustic power of the jet given in Fig. 13. In this case the frequency of the spectrum

$$f = \frac{\text{Sh} \, c_i}{d_0}.$$

4. The level of the total sound pressure at the points arranged at a distance r from the nozzle edge of the engine is determined from formula (12).

5. The levels of the components of the spectrum of sound pressure in 1/3 octave bands are equal to

$$L_i = L + \Delta L_i.$$

where ΔL_i - the components of the dimensionless spectrum of sound pressure given in Fig. 14.

6. The level of received noise of the jet is determined from the spectrum of sound pressure in 1/3 octave bands or from formula (15) with the use of the approximate relationships (13) and (14).

§ 5. The Characteristics of the Noise Generated by the Compressor (Fan) of a DTRD

1. The Mechanism of Noise Excitation in the Compressor Stage and the Basic Determining Factors

The noise, generated by the compressor, is broadband noise of aerodynamic origin, against the background of which are marked several discrete components which correspond to the frequencies of blade passage (Fig. 16).

Fig. 16. The compressor noise spectrum of a DTRD with y ~ 5.

KEY: (1) Modified TF-39 DTRD. Data 1/3 octaves; R ≈ 70 m. Peripheral speed of the 1st rotor stage. $U_{пер}$ = 308 m/s Θ = 70° (maximum PN dB); (2) Frequency of blade passage of the blades; (3) 1st stage; (4) 2nd stage; (5) Hz; (6) L [dB].

The fundamental components of the noise of an axial-flow compressor are noise of rotation, eddy noise and noise from the heterogeneity of the stream which flows around the blade.

The noise of rotation is formed due to the forces of the effect of blades on the flow, has a dipole nature and are discrete in character. It is connected with the motion of the rotor wheel blades, which create a periodic disturbance of the medium in the plane of rotation.

Eddy noise is caused by the vortices which are formed as a result of air flow around the inlet components and rotor wheel blades and the stator. Eddy noise has quadrupole nature and is broadband.

Noise from the heterogeneity of flow is produced by additional forces on the blades which appear as a result of the nonuniformity of flow parameters in the plane of rotation of the wheel. The heterogeneity of flow in the stage can be caused by the features of the inlet to the compressor, and also by distortions of the field of velocities after the stator blades. Noise from the heterogeneity of flow has a dipole nature and is discrete in character.

Separate components of compressor noise are currently not studied sufficiently, and thus far, there is no strict theory. During engineering empirical and semi-rational formulas are utilized which relate the gas-dynamic, geometric and acoustic parameters.

The purpose of many very recent investigations is detailed research on the mechanisms of noise excitation in the compressor stage and isolation of its determinate factors. One of the most thorough works of this description is published by Smith and Howes [5]. The authors gave primary attention to eddy noise and noise from the heterogeneity of flow. The mechanisms of the excitation of broadband noise examined by them and the discrete comprise are visually illustrated by the diagrams A-D (Fig. 17). Diagram A gives a representation about the random process of changes of circulation, pressure, and lift, occurring on the profile. The initial flow turbulence considerably amplifies this process, therefore diagram B reflects a stronger mechanism of noise excitation. Diagram D shows routine and periodically repeated changes in the angles of attack of the rotor blades as a result of the deviation of flow lines at the exit edges preceding stator vanes, which produces the appearance of discrete currents. The

115

most intense discrete noise appears during the passage of the rotor
blades through the trailing-edge wakes of stator grid (diagram D),
when a change of the velocity in every trailing-edge wake causes
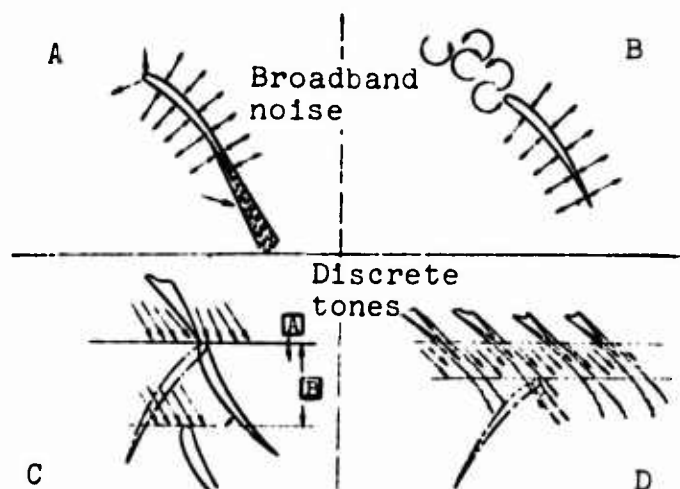a cyclic variation in the pressure on every vane of the subsequent
grid.

Fig. 17.   The diagram of the mechanisms
of the excitation of noise in compressor.

The more detailed classification of the mechanisms of noise
excitation in a compressor, described by M. Pianko [9], is given
in Fig. 18.

Thus, the basic factor which determines the noise of a
compressor is the interaction between turbulent perturbations and
the traces which are formed after preceding vanes and the
subsequent series of blades of the rotor and stator. The intensity
of this interaction, to a significant extent, depends on the axial
clearance between blades and the relative number of rotor and
stator blades in each stage. In the process of design it is
possible to control the noise of compressor by lowering the
broadband noise and determinate discrete tones by means of an
increase in the axial clearances and the selection of the optimum
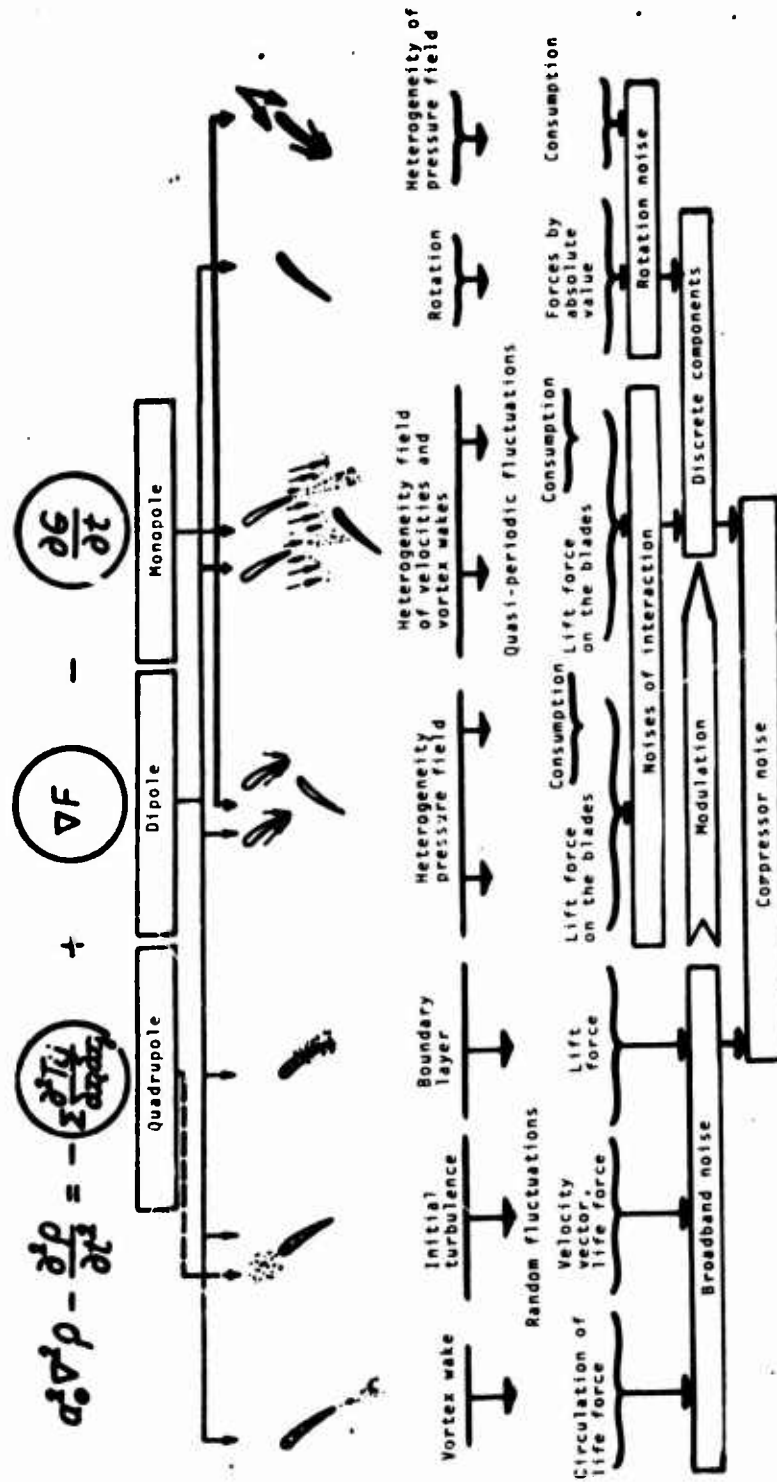relationship of numbers of blades of the stator-rotor unit.

Fig. 18. The classification of the mechanisms of noise excitation in a compressor.

2. The Basic Parameters Which Determine
Compressor Noise

Many researchers were inclined to consider the basic parameter,
determining compressor noise, to be the absolute velocity of flow
in the peripheral cross section of the rotor. The dependences of
noise level on peripheral speed established from this, evidenced
a considerable change in complete acoustic power with a change in
the engine power rating, which does not agree with experience.

The careful analysis of the results of experimental research,
made with consideration of the features of the mechanisms of the
excitation of compressor noise by Smith and Howes, showed that both
the random and regulated fluctuations of the flow velocity, pressure,
and lift on the profile depend on the magnitude of the relative
velocity vector of the flow around the blade. The specially set up
experiments confirmed the accuracy of the analysis.

In the area of the linear dependence of air consumption
through the compressor on revolutions (at invariable angles of
attack), the noise level changes according to a law, close to the
sixth power of the relative velocity.

In practice a difference in the intensity of sound emission
in front and rear sectors is observed. The transfer of larger
portions of the jet noise energy downstream than upstream serves
as the reason for this, the so-called effect of convection (if
there were no consumption of the air through the compressor, then
uniform noise distribution between front and rear hemispheres
could be expected. They propose that the portion of radiated energy
which is propagated upstream, is equal to $0.5 (1 - M)$, and downstream
$0.5 (1 + M)$, where M is equal to the Mach number of the flow in
the axial direction. Smith and Howes give corrections for noise
convection of ΔF (Figs. 19 and 20).

Noise addition in
rear sector
10 lg (1 + M)

Correction factor ΔF, dB

Experimental
broadband noise
differences
experienced in
a single-stage fan

Noise
decrease
in the
front sector
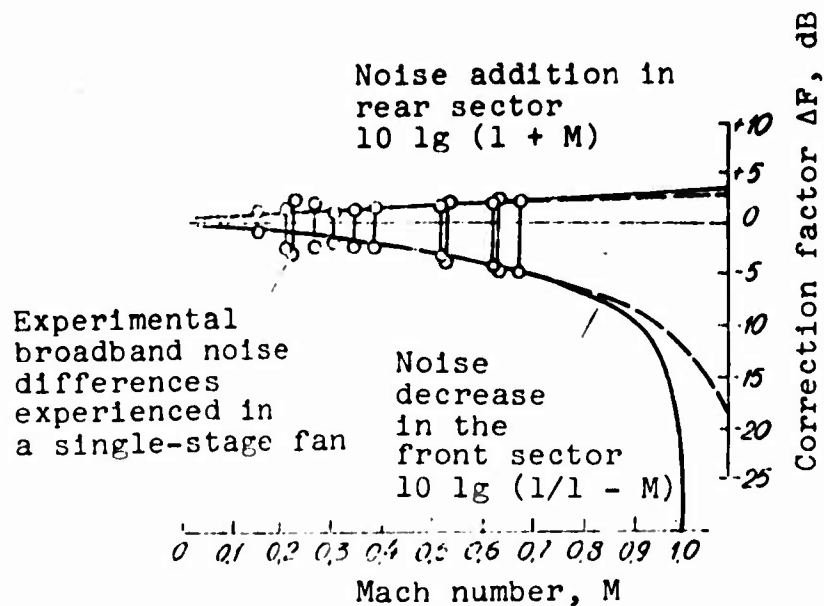10 lg (1/1 - M)

Mach number, M

Fig. 19. Correction factors for noise
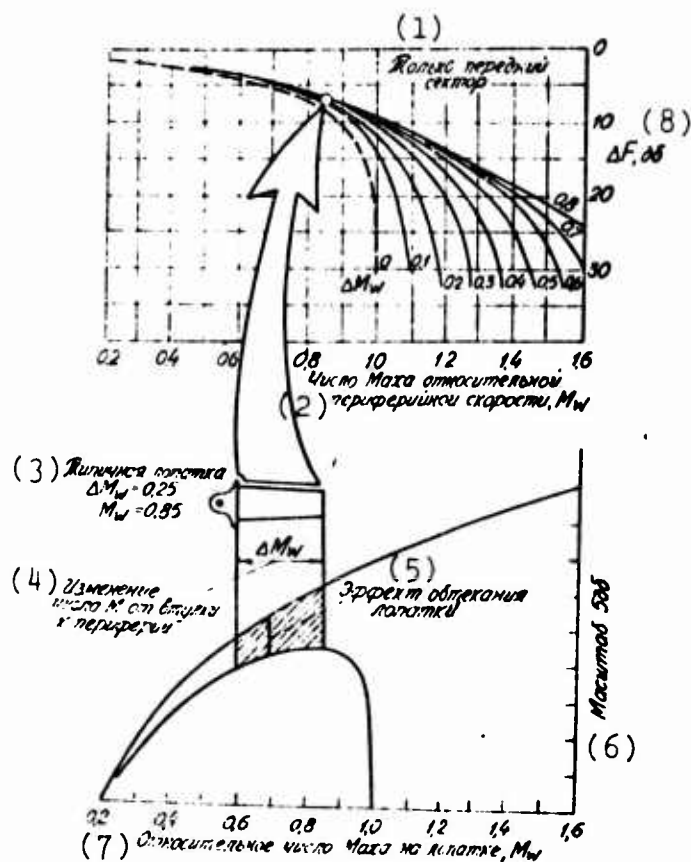convection for the front and rear sectors
of a single-stage fan.

Fig. 20. Correction
factor for noise
convection in the
front sector of a
single-stage fan.

KEY: (1) Only the
front sector; (2) Mach
number of the relative
peripheral velocity, M;
(3) Standard blade;
(4) Change in Mach
number from sleeve to
periphery; (5) Effect
of flow around blade;
(6) Scale 5 dB;
(7) Relative Mach
number for the blade,
M_w; (8) dB.

119

An important parameter which determines compressor noise is the flow turbulence in the stage. In a compound compressor the rotors of the subsequent stages are located under conditions of higher turbulence, than the first stage rotor, as a result of which the intensity of noise excitation can grow by 10 lg N/N-1 at the stage. The effect of turbulence can be combined with the effect of convection and a new correction β_N for any stage with number N obtained (Fig. 21).
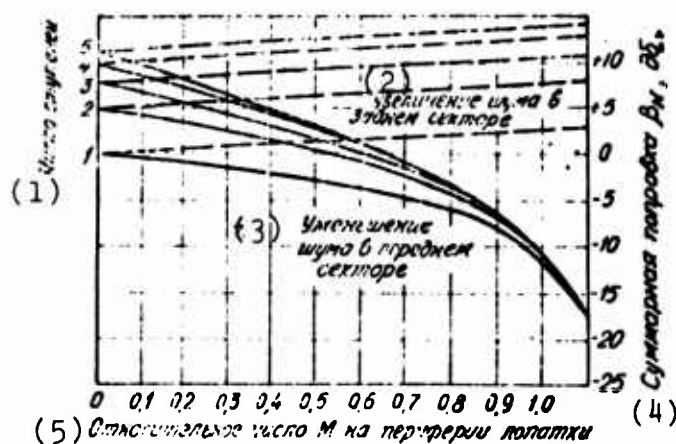

Fig. 21. Total correction for noise convection in the front and rear sectors of a compound compressor (fan).

KEY: (1) Number of stages; (2) Increase in the noise in rear sector; (3) The reduction of noise in front sector; (4) Total corrections β_N, dB; (5) Relative M number on the blade periphery.

The values of angle of attack α exert a great effect on the dependence of noise intensity on the relative velocity, however, this problem has been studied insufficiently.

The value of relative axial clearance (S/C) between stator and rotor blades substantially affects the levels of discrete and broadband noise of the compressor, however, theoretically the laws governing this effect thus far are not developed. The experimental

data in this area are quite limited, and the available information is related to models of a different dimensionality. The tendency toward a decrease in the intensity of the fundamental tone with an increase in the axial clearance is frequently emphasized, although the intensity of separate harmonics can increase in this case.

3. The Acoustic Power of a Compressor

Work [12] is dedicated to the investigation of the dependence of acoustic power of a compressor on basic determining factors, in which analytical expressions of the levels of acoustic power for the cases of the nonseparated flow and vortex flow of the blades are given. They take the form (respectively):

$$L_w = 98 + 47{,}6 \lg \frac{w}{100} + 10 \lg (1 \pm M) + 10 \lg G \ (\mathrm{dB}), \tag{15}$$

$$L_w = 118 + 34{,}4 \lg \frac{w}{100} + 10 \lg (1 \pm M) + 10 \lg G \ (\mathrm{dB}). \tag{16}$$

Here: w - relative velocity of flow around the blades in the peripheral cross section (m/s); M - Mach number at the entry to first stage; G - air consumption (kg/s).

Work [10] gives a similar expression for the level of acoustic power, in which the term which considers the factor of convection is omitted

$$L_w = 130.5 + 50 \lg \frac{w}{c_a} + 10 \lg G \ (\mathrm{dB}), \tag{17}$$

where c_a - axial velocity at the inlet to the compressor (m/s).

Formulas (15-17) give the dependence of the level of acoustic power on the relative rate of flow around the blades on the periphery, respectively in powers of 5.76, 4.44 and 6 (consumption is function of velocity to the first power). The law w^6 is characteristic for dipole noise sources.

121

4. The Compressor Noise Spectrum

In the compressor noise spectrum broadband noise and discrete component (Fig. 22) are distinctly distinguished.

Broadband noise, approximately to 1000 Hz, corresponds to the noise of the jet, and therefore can be considered as the overlapping noise from the rear end of the engine. In the range of frequencies above 1000 Hz, the broadband component of the spectrum is formed by the sonic radiation of compressor. In Fig. 23 large numbers of arbitrarily selected spectra, constructed relative to the maximum level in dB [5] are presented. Deviations at lower frequencies are caused by the difference in modes and by the effect of the introduction of the jet noise. The characteristic frequency of maximum has a value on the order of 5000 Hz, which is connected with the typical dimension of the vortices.
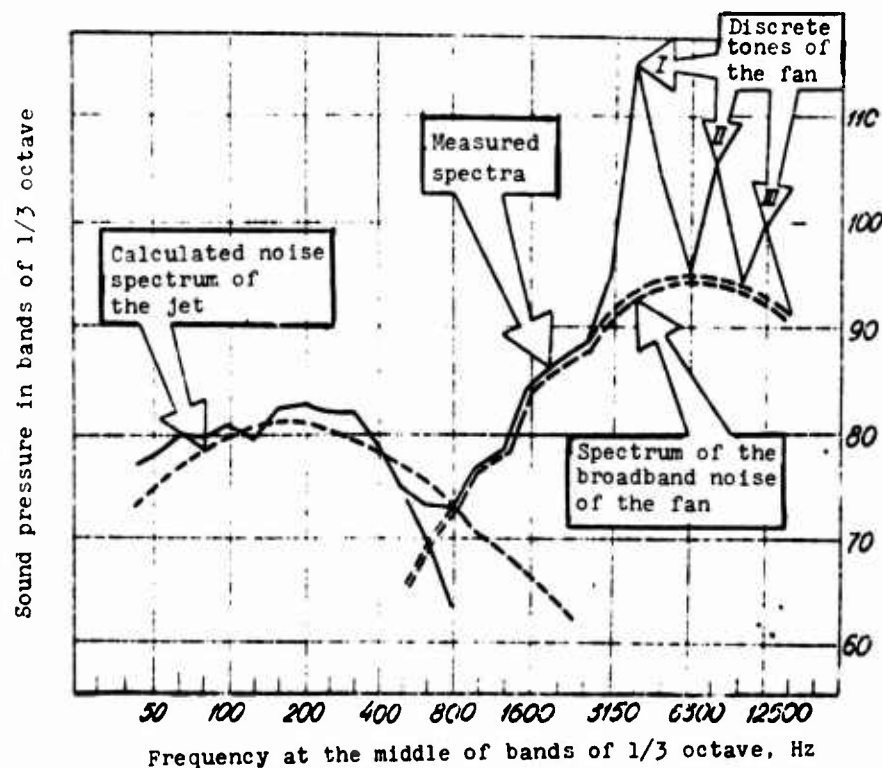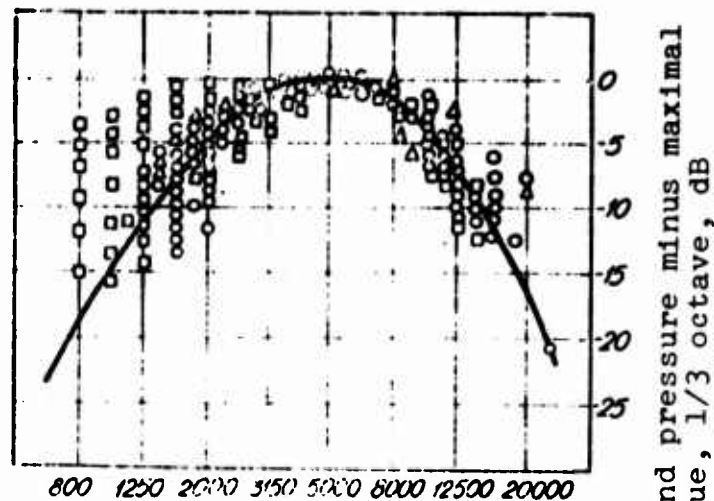

Fig. 22. A typical noise spectrum of a single-stage fan.

122

Frequency in the center of band
of 1/3 octaves, Hz

Fig. 23. Determined spectrum of broadband
noise at a distance of 30.4 m along a line.

Discrete noise tones have frequencies, multiple to the
frequencies of the passage of the blades of the rotor, and have
basic and upper harmonics of the first compressor stages. The
fundamental frequency has the value $f = nz$, where z - number of
rotor blades and n - number of revolutions per second; the second
harmonic with double frequency has a sound intensity 6 dB less
than the fundamental tone, the third on 3.5 more dB less etc.,
(in accordance with the law of reduction $10 \lg k^2$, where k - number
of harmonics).

5. The Sound Pressure Levels and Received Noise

Sound pressure levels in the zone of maximum intensity of
propagation along a line, at a distance of 30 m from the source,
can be estimated separately for broadband noise and discrete
components by the semi-empirical dependences proposed by Smith
and Howes [5].

123

A. Single-Stage Fan

The level of broadband noise at the 1/3 octave band, which has maximum intensity of propagation, is estimated with respect to the formula

$$L = 50 \lg \frac{w}{100} + 10 \lg G + \Delta F + a + 51 \; (\text{dB}), \qquad (18)$$

where a - mean deviation of attack angle from that corresponding to maximum lift (in degrees); ΔF - correction factor which considers the expenditure effect of flow on the propagation of noise (dB).

The form of the spectrum is borrowed from Fig. 23 with a frequency shift proportional to the ratio of the average width of the active and guide vanes on periphery to that accepted in investigation [5] 50 mm.

The sound pressure level of the fundamental tone of discrete component is determined from the formula:

$$L = 50 \lg \frac{w}{100} - 10 \lg \left(\frac{S}{C}\right)^2 \frac{1}{G} + \Delta F + 61 \; (\text{dB}), \qquad (19)$$

where S/C - ratio of the value of the axial clearance between the stator-rotor unit to the width of the grid on periphery.

The sound pressure levels of the second and subsequent harmonics are lower than the fundamental tone, by $20 \lg k$. The fundamental tone has frequency $f = nz$ and the harmonic frequencies are multiples of this value.

Discrete components of the fundamental tone and harmonics are included in the frequency bands corresponding to them in the spectrum of broadband noise.

124

B. Compound Compressor

The maximum level of broadband noise in the frequency band of 1/3 octaves is calculated from the formula:

$$L = 50 \lg \frac{w}{100} + 10 \lg G + x + \beta_N + 51 \text{ (dB)}, \qquad (20)$$

where β_N - correction factor which considers the expenditure effect of the flow for N similar stages (dB).

The sound pressure level of discrete components of the fundamental tone of the noise radiated forward is estimated according to the formula

$$L = 50 \lg \frac{w}{100} - 10 \lg \left(\frac{S}{C}\right)^2 \frac{1}{G} + N\Delta F + 61 \text{ (dB)}. \qquad (21)$$

It is assumed to be that every subsequent stage lowers the level of discrete components of the noise which is propagated back, by approximately 5 dB. The correction factor $N\Delta F$ in this case is replaced by $[\Delta F - 5(N' - 1)]$; ΔF is taken from Fig. 19, and N' is the number of stages counted from the end of the compressor.

The levels of received compressor noise can be determined by a noise spectrum, constructed in accordance with the given procedure.

M. Pianko, in work [9], gives semi-rational formulas for the calculation of the maximum level of the received noise in PN dB, determined at a distance 300 m from the source.

$$L(PN \text{ dB}) - 10 \lg R = 46 \lg w - 10 \lg \frac{G}{\pi r_H^2} - 10 \lg R_{y\text{д}} - 15.$$

Here r_H - outside radius of the compressor (m); R - thrust (given); $R_{y\text{д}}$ - specific thrust (kg/kg·s).

6. Order of Calculation of the Compressor Noise

The following can be recommended for the order of calculation of the noise of compressor:

1. The maximum level of broadband noise in a 1/3-octave frequency band is determined from formulas (15) or (17).

2. The spectrum of broadband noise is constructed in accordance with the results of the processing of a large number of experimental data which is presented in Fig. 23.

3. The sound pressure levels of the discrete components are determined from formulas (16) and (18) and will pertain to the spectrum of broadband noise in the appropriate frequency bands.

4. The level of received noise is determined from the compressor noise spectrum in 1/3-octave bands, or from the semi-rational formula (22).

Conclusions

1. The basic noise sources which determine the acoustic characteristics of turbofan engines are the jet and the compressor (fan). Depending on the bypass ratio, operating conditions parameters, dimensionality, and engine power rating, either the noise of the jet or the compressor turns out to be prevalent. Thus, in takeoff mode with $y < 2$ the jet noise predominates, with $y > 2$ - the compressor noise. In landing mode, the compressor noise exceeds the jet noise already at $y > 1$.

2. The acoustic responses of the jet (in the range of the gas expansion ratios $1.5 < \pi_{pc} < 2.2$) have been investigated at present with sufficient completeness. A strict theoretical base has been created, on the basis of which engineering methods of

calculation have been developed. Results of vast experimental
research will confirm the reliability of the calculation methods.

3.   Compressor (fan) noise has been little studied, these
experimental studies are insufficiently clear, and the obtained
results do not always agree with each other. A strict acoustic
theory of the compressor thus far does not exist, therefore during
the engineering calculations semi-empirical dependences are
utilized.   The primary attention of the researcher during research
is now concentrated on the physical processes of noise generation
and on their analytical description, which itself agrees with
experiment.

Bibliography

1. Власов Е. В., Квитка В. Е., Мельников Б. Н., Мунин А. Г. Ограничение шума самолетов (проект советского стандарта). «Гражданская авиация» № 2, 1970.

2. Расчеты и измерения характеристик шума, создаваемого в дальнем звуковом поле реактивными самолетами. Под редакцией Л. Н. Соркина. М., Машиностроение, 1968.

3. Ribner H. S. Jets and Noise. CAS Journal vol. 14, 1969, № 10.

4. Marsh A. H., Mc Pike A. L. Noise Level of Turbojet — and Turbofan — Powered Aircraft. Sound. 1963, 2, № 5.

5. Смит, Хаус Внутренние источники шума в газотурбинных двигателях. Измерения и теория. Труды Американского общества инженеров-механиков. Серия A «Энергетические машины и установки». Русский перевод. М., «Мир», № 2, 1967.

6. Hay J. A. The Estimation of Jet Engine Noise. Presented of Aeron. Acoust. Symp., Toulouse, 6÷8, Mar., 1968.

7. Progress of NASA Research Relating to Noise Alleviation of Large Subsonic Jet Aircraft. (NASA SP—189). Presented of Conference Held at Langley Research Center. 1968.

8. Лайтхилл М. Шум струи. Ракетная техника и космонавтика. № 7, 1963.

9. Pianko M. Etude theorique et experimentale du bruit de compresseur Serv Techn. Aeron., Paris, avr. 1969.

10. Kobrynski M. Recentes mesures de bruit de jets et de compresseurs. ONERA, T. p. № 602, 1968.

11. Prediction of Turbine Engine Compressor or Fan Noise. SAE Proposed air 973.

12. Bragg S. L., Bridge R. Noise from Turbojet Compressors. JRAS, 1964, 68, № 637.

13. Францев В. К. Определение уровня шума и параметров шумоглушителя авиационных газотурбинных двигателей. Рига, 1964.

SOME PROBLEMS OF THE CREATION OF AN OPEN
STAND FOR ACOUSTIC STUDIES OF DTRD

A. I. Balmakov, V. G. Yenenkov

In the article the contemporary methods of
the experimental research on the acoustic
characteristics of DTRD are examined. Primary
attention is given to the full-scale experiment
on an open stand. The purposes of the acoustic
studies of DTRD, and the basic requirements for
test conditions, facilities and equipment of
the open stand are set forth. Two versions of
the structural solution of the stand are
described: stationary and mobile. Basic
information about necessary facilities and
equipment of the open stand is given.

Introduction

Recently in civil aviation, jet aircraft with the turbofan
engines with high bypass ratios y have been accepted. With the
use of such DTRD the jet noise of the exhaust gases decreased,
but the noise generated by the fan simultaneously increased.

To solve the problems of turbofan engine noise reduction,
it is first necessary to conduct detailed experimental studies,
both model and full-scale.

In the course of the model experiment it is also possible to test a large quantity of diverse variants of the investigated object with insignificant expenditures, to study the mechanism of the noise generation by different sources in detail, and to develop methods of its reduction.

Model tests are carried out, as a rule, in muffled (anechoic) chambers (Fig. 1). The internal surface of the chambers is covered with the sound-absorbing wedges, which makes it possible to produce acoustic measurements at frequencies above 250 Hz without distortions caused by reflections from the walls.

Fig. 1. The preparation of the model experiment in an anechoic chamber.

The studies of noise problems of individual and coaxial jets, in connection with the diagrams of the nozzles of the first and second contours of DTRD the power jets of supersonic transport planes, and also DTRD compressors (fans) (Fig. 2), are carried out in anechoic sound chambers.

Full-scale experimentation on an open stand is necessary for the purpose of final proof of these studies of models, and for the generalization of them in connection with turbofan engines.

Fig. 2. The interior of an anechoic chamber with a model of a muffler.

Fig. 3. An overall view of an engine installation on the open stand.

The open stand for full-scale DTRD (Fig. 3) makes it possible to carry out studies not only of acoustic characteristics, but also to test the operational reliability of the engine.

In the open stand it is possible to make a study of the intake and exhaust devices (air intakes, engine nacelles, nozzles), a highly reliable final adjustment of the elements and systems of the engine by applying methods of the early flaw detection, etc.

A study program can also include testing of thrust reverse and research on the effect of the rate of the growth of load and its cyclic recurrence on the engine lifetime. The open stand makes it possible to study the questions of the icing of air intakes and engine nacelles and prevention of the incidence foreign objects into the engine, and other problems.

From the aforesaid, it is evident that the multipurpose open stand which has concrete purpose (investigation of the acoustic characteristics of DTRD) makes it possible to study a wider circle of problems of theoretical and operational nature. Thus, at present the creation of open stands is extremely necessary and real. Requirements for such a stand very high, and the stand itself should be universal.

In this article the problems of the creation of the multipurpose open stand for the study of the acoustic characteristics of turbofan engine are brought to light.

§ 1.   Purposes of Experimental Acoustic
Studies on an Open Stand

1.   The Study of the Characteristics of the
Ambient Engine Noise in a Distant Acoustic
Field

On the open stand it is possible to produce a study of the characteristics of the ambient noise, both of production and experimental engines, in distant and near acoustic field.

In a distant acoustic field the sound-pressure decreases inversely proportional to distance from the center of radiation to measuring point. During stand tests it is desirable to produce measurements at a distance of 50-300 m.

These problems enter into the study of the characteristics of the ambient engine noise in a distant acoustic field:

a) the determination of directional characteristics in the levels of the received noise and in sound pressure levels during engine operation under basic conditions;

b) obtaining spectral characteristics in octave (or 1/3 octave) frequency bands at all measuring points;

c) establishment of the maximum level of the received noise created by the engine;

d) the plotting of curves of noise reduction in the direction of the maximum propagation at a distance of 50-300 m and characteristic noise spectra in octave frequency bands.

On the basis of the findings it is possible to give a comparative evaluation of engines with regard to ambient noise.

2. The Study of the Characteristics
of Ambient Noise in a Near Acoustic
Field

In the immediate proximity of the engine there is a field of hydrodynamic pressure which is called the near acoustic field. During the study of the characteristics of DTRD noise the need for producing measurement in the near field frequently arises.

The following enters into the study of the characteristics of near field noise:

a) determination of sound pressure levels under basic conditions of engine operations;

b) determination of directional characteristics;

c) obtaining spectral characteristics in octave bands at the measuring points of the near field;

d) establishment of the maximum noise level.

The numerous experimental studies of the near field show, that the greater the signal frequency, the less the distance of the sound pressure maximum from the source.

3. The Study of Methods of Noise Reduction

The basic purpose of the open stand for acoustic studies of DTRD should be considered the development, testing, and evaluation of the effectiveness of the different methods of noise reduction.

The basic principle of aviation noise reduction is the principle of the suppression of its sources. For DTRD, this principle is realized, for example, by following solutions:

a) an increase in the bypass ratio for the purpose of a reduction in the jet noise;

b) removal of the inlet guide ring;

c) an increase in the clearance between vane rings, etc. for the purpose of reduction in compressor noise.

This principle is most labor-consuming, requires prolonged experimental research and change of engine design. But this principle is also the most effective.

Another principle obtained wide dissemination - the principle of the energy absorption of noise on the path of its propagation. The sound-absorbing facing of the channels at the inlet and exit from the compressor (fan) works according to this principle. A change in the form of the channels of the inlet and exit gives the same result. For the facing of the intake and outlet ducts of the fan contour, a porous sound-absorbing material is used. For example, for the RB211 engine installed in the Lockheed L-1011 airbus, 18.5 m^2 of facing material (Fig. 4) is required for the indicated purposes.
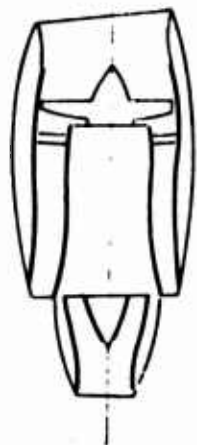

Fig. 4. Treatment of exhaust ducts of a turbofan engine with the sound-absorbing facing.

§ 2. Requirements for Acoustic Tests

1. Assurance of Conditions of a Distant Acoustic Field

This requirement should be fulfilled maximally strictly, since the accuracy of measurement of all acoustic characteristics depends on it.

Near the noise sources, the points of the arrangement of microphones, and between them, there should not be any obstructions (Fig. 5). Since the noisy object (DTRD) has a determinate length from air intake to a certain, not completely clearly limited, but distant from the nozzle edge, cross section, during the study of the directional characteristic and sound pressure levels in the distant field, it is necessary to make noise measurements at a sufficient distance from the engine.

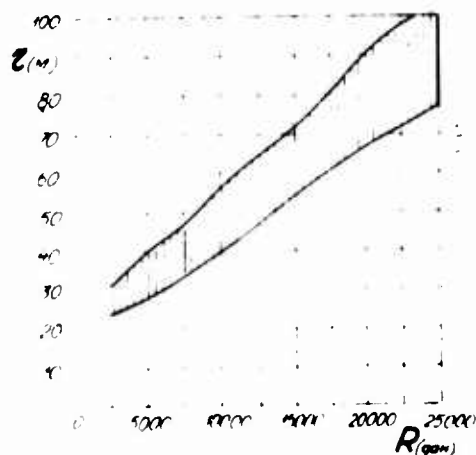Fig. 5.   Overall view of the open stand.

Fig. 6.   The effect of engine dimensionality on the value of the necessary distance between the engine and microphones, with which the conditions of distant field are provided.

135

The value of the necessary distance from the studied object
to the points of the microphones arrangement depends on the engine
model and its dimensionality (Fig. 6). Then the observer can
consider the engine as a point source of noise.

It is necessary also to eliminate the effect of the ground
in order to avoid the interaction of the jet with soil.

Extraneous noise sources should be at a sufficient distance
in order to not introduce distortion into the acoustic measurements.

2. Requirements for Stand Equipment

The test bench should be equipped with devices for measuring
thrust, fuel consumption, temperature, and gas pressure in basic
sections of the DTRD. The requirements for the accuracy of
measurement of the parameters are just as rigid as during the study
of the characteristics of the effectiveness and cost-effectiveness
of the engine, since the latter are directly connected with the
characteristics of noise.

Test floor should be equipped with equipment for continuous
recording of the rate and wind direction, of the barometric
pressure and air humidity. These data substantially affect the
distribution of sound. At wind velocities 7.5-8 km/h, measurements
in a distant acoustic field are not stable.

It is necessary to have a sufficient quantity of microphones
for simultaneous recording of data measurements in many points in
order to eliminate errors from a change in wind velocity,
refraction, conditions of engine operation, etc. The use of a
large number of microphones will make it possible to decrease the
combustion duration and to lower consumption for experiment.

136

During the study of intake and outlet devices of unsymmetric form, it is necessary to produce measurements in both the horizontal and vertical planes passing through the engine.

3. Requirements for Audio Equipment

When selecting metering equipment for acoustic studies it is advantageous to use the recommendations of International Electrotechnical Commission (1961).

The frequency band of the measuring circuit should be within the limits of 20 to 12,500 Hz. Measuring circuit in this case should conform to the following requirements:

1) nonuniformity of the frequency characteristic of measuring circuit in every octave band should be not more than ±3 dB;

2) error for measuring circuit, taking calibration into account, should be not more than ±2 dB;

3) level of internally-produced noise should be 5 dB lower than maximum level of measuring noise;

4) microphone should be weakly directed in the entire range of operating frequencies;

5) measuring circuit should be calibrated, and before beginning and after measurements - recalibrated.

The obtained acoustic characteristics should be supplemented by the following information fixed into the protocol of the tests:

- date;
- engine model, its series and operating mode;
- atmospheric conditions near the earth (relative air humidity, temperature, barometric pressure, the velocity and wind direction);

137

- the layout of the measuring points (radius measurement, number of points, etc.).

§ 3. The Types of Open Stands for Full-Scale
Acoustic Investigations

A. The Stationary Open Stand

For the creation of the stationary open stand the presence of free areas of sufficient large dimensions is necessary. The design of such a stand can be analogous to the design of a stand for usual engine tests outside the cell. The stand is the experimental station which has the engine and its maintenance systems. The tool for the measurement of thrust is fastened to a general mounting which is immobilely connected to the load-bearing elements of the foundation. The stand is established on an open site distant from projecting buildings and constructions and also from noise sources.

In order to eliminate the effect of the ground, it is necessary to raise the engine by a height of 1.7-2.0 m and higher, depending on the overall dimensions of the engine and its arrangement on the aircraft. It is most advisable to completely or partially bury the control room and the fuel tank in the ground, 10-15 m from the engine. In this case, all power-supply and engine control systems will pass in bunkers and have comparatively low length. It is convenient to locate the entire control panel to the side of the engine, armoured with slits for the survey of the engine during operation (Fig. 7).

The application of a ground-level, mobile, control panel is possible. It must be removed to a considerable distance (20-30 m), which makes survey worse, complicates throttle circuits, and maintenance.

138
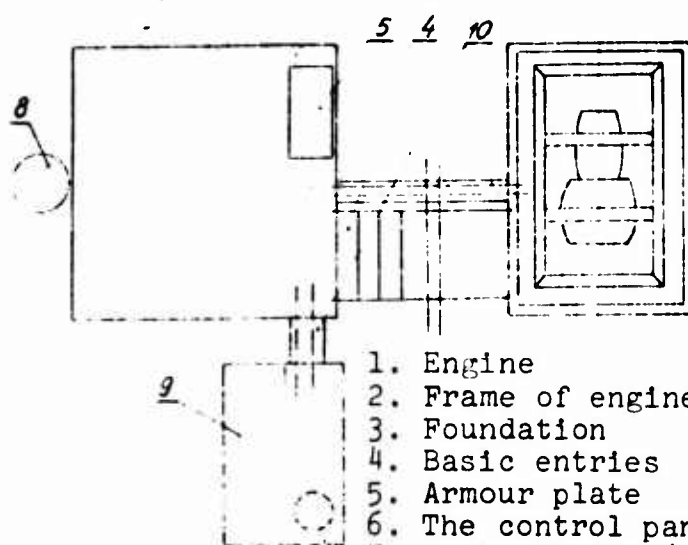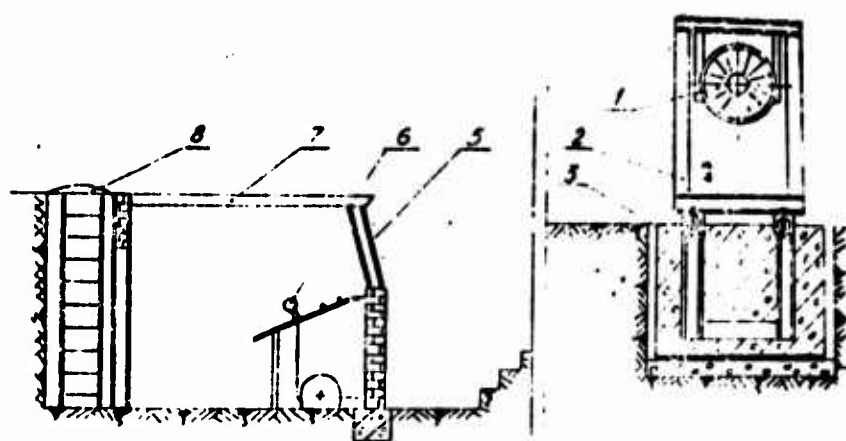
1. Engine
2. Frame of engine attachment
3. Foundation
4. Basic entries
5. Armour plate
6. The control panel
7. Control room (shack)
8. Emergency exit
9. Fuel tank
10. Bunkers for the power-supply and control systems

Fig. 7. The layout of engine and systems on the open stand.

During the rational selection of all parameters a stationary stand possesses the advantages, the basic of which are: simplicity of the design, maintenance and organization of the measurements of noise at different points (site can be equipped with stationary all-weather microphones).

B. The Mobile Open Stand

Frequently the scientific research organizations are not furnished with large free areas for a stationary open stand. Then it is necessary to create mobile open stand (Fig. 8). It can be mounted on the base of a chassis (trailers, etc.). The condition of free field is satisfied in this case sufficiently simply, since there is the possibility of producing the selection of a testing place (field, wood clearing, etc.) by the transportation of movable stand.

For the delivery of the stand into the area of tests, the tow car or a special airport mobile power unit [AMPU] (АПА) is utilized. In the latter case the problem of starting the engine is considerably simplified.

It is desirable to transport the mobile open stand, and the equipment available in the airport weather service makes it possible to obtain the necessary atmospheric characteristics. In this case, the maintenance of the engine and its systems, fuel loading, fuel and lubricants, and special fluids are simpler.

For test work, the mobile stand is established on a level site, the supports which impart lateral stability to the stand are extended, and the chassis wheels are chocked. All systems of the fueling and control of the engine are furnished on an isolated frame, which can be moved in height with the aid of rigid adapters, or on self-raising frame with a hydraulic cylinder.

For a change of the slope angle of the engine, in the vertical plane, the truss-adapters between frames should have different heights. When using hydraulic hoists in such cases, the rigid, mechanical locking of its legs is necessary.

Fig. 8. Engine installation
of a mobile platform.

During the arrangement of new position, the upper frame with
engine, panel, etc., is raised by a crane or hoists, fixed in
a determined position, and then both frames are rigidly fastened.
The use of other methods of a change in the height of the engine
installation is possible also.

Also, the control panel, fuel tank, the system of thrust
measurement, and part of the measuring apparatus are installed
on the mobile frame.

The control panel in this case can be utilized for the
limitation of conditions regarding noise in the cabin of the
aircraft (during the use of similar sound-absorbing material,
engine power rating, etc.).

At the location of conducting the research, it is necessary
to make the arrangement of microphones and to lay cable to them.
It must be considered that stand variations will occur, and
therefore it is necessary to provide the protective measures for
especially precise and sensitive equipment on the control panel.

The mobile open stand is considerably more complex in design than the stationary, but is also more universal.

§ 4. The Basic Equipment of the Open Stand

1. For equipping the stand with a thrust measurement system, a non-rigid test stand design on connecting rods or flexible strips may be used (Fig. 9).

Fig. 9. A closeup of the engine, prepared for noise measurements on a open stand.

2. In turbofan engine the temperature of gases and pressure in different cross sections should be measured.

3. For the measurement of pressures (complete and static) on a test stand, different adapters, manometers, vacuum gages and differential manometers can be applied.

4. For flow velocity measurements (in Mach numbers of λ), they use a combined adapter of complete and static pressures, and also measure complete or static temperature. Directivity of the velocity vector can be determined with the aid of multichannel adapters.

5. For the measurements of fuel consumption, tachometer sensors, flowmeter, and also volumetric and mass flowmeters can be applied. Flow meters are usually used for more precision determination of the consumption with regard to engine operating mode. For the measurement of instantaneous fuel consumption they use tachometer sensors.

6. For the measurement of r/min electrical, strobotacs and the total revolution counters are applied. All measured values enumerated above are available on control instruments, the panel (in the cabin) according to which operation of the engine and its systems is evaluated: the engine-control lever, stopcock, the starting switches, the thrust indicators, tachometer, the thermometer of exhaust gases, the oil thermometer, the fuel and oil pressure gauges, fuel-metering device, the signaling of the position of the organs of nozzle control, compressor, etc.

7. The test stand is supplied with the following of systems:

a) by the electric power wiring;
b) 6 or 12 V electric wiring for operation of the portable illumination sources and power tools;
c) 27 V direct current electric wiring, that provides operation of meters and starting the engine and turbine starters from electric starters;
d) wiring, carrying the load of the engine's generators;
e) compressed air feed system;
f) oil system;
g) hydraulic circuit (in the presence of hydroaggregates);
h) propellant feed system.

§ 5. The Measurement of Engine Acoustic Characteristics

The study of engine acoustic characteristics has the purpose of measuring and registering sound pressure levels at a certain radius from the engine. In connection with the fact that the domestic industry does not produce standardized audio equipment which makes it possible to produce complete acoustic measurements under varied conditions, the measurements of sound pressures can be made with the aid of the following assemblies of equipment:

a) for the registration of levels to 135 dB use of the equipment manufactured by Danish firm Brüel and Kjaer A/S is more expedient, including the chart recorder (Type 2304), analyzer (Type 2110) and capacitor microphones (Type 4111, 4112, 4113). It is possible to also apply domestic capacitor microphones of the MK-5A and MK-6 type, as well as electrodynamic microphones of the type: MD-45, MD-59, MD-62, etc.;

b) for registration of levels greater than 140 dB it is possible to use the domestic MIK-5 microphone with the UPU-2 amplifier, the vacuum tube MIK-5 voltmeter with the UPU-2 amplifier, or the vacuum tube voltmeter and analyzer and the chart recorder of the firm of Brüel and Kjaer A/S;

c) for the magnetic recording of noise on the ground and in flight, a modified magnetic tape recorder (for example M-30, MEZ-28S, MEZ-41, MEZ-63, Kometa, Yauza-10, Reporter-3, etc.). For a magnetic recording, tape type 6 is recommended.

The magnetic recording of noise is reproduced on tracing paper in the form of the total noise level and frequency components (with the aid of the Brüel and Kjaer analyzer and chart recorder). The modification of the magnetic tape recorder consists of the conforming of its input and output with the equipment connected to it;

144

d) for a selective control, in terms of total noise levels, in the experiment there should be a reliable and thoroughly calibrated objective audio-noise meter (of Type Sh-60, Sh-63 and Sh-52, Sh-2, General Radio's 759A or similar), and also domestic octave filters OF-1, 1/2-octave PF-1, 1/3-octave AW-2M, etc.

For frequency response analysis, the octave filters of the firm of Brüel and Kjaer of Type 1612, 1613, 1/3-octave - 2111, 2112, domestic narrow-band analyzers S5-3 and S4-7 and an analyzer of Type 2107 from the firm of Brüel and Kjaer are applied.

For the registration of level - monitors N-110, Type 2305 from Brüel and Kjaer; for calibration a pistonphone of Type 4220, a ball bearing calibrator of Type 4240 and an instrument of Type 4142 from Brüel and Kjaer. Also applied are the audiofrequency oscillators, Type ZG-4, ZG-12, GAII-1 and GNII-2, voltmeters V-3-13, VK2-6, oscillograph S-1-19, etc.

During the investigation of acoustic characteristics it is necessary to maintain certain conditions.

1. Before beginning, and during the period of measurements, the entire equipment should routinely undergo calibration. These adjustments are dated and are introduced into these equipment. Equipment from the firm Brüel and Kjaer may be calibrated only once - before beginning the experiments (if in the process of measurements sharp jolts and impacts are not undergone).

Besides standardization, and independently of it, the equipment before every measurement and after it should be calibrated.

2. When using Brüel and Kjaer equipment in field conditions, one ought to transport to the place of experiment in a warm vehicle and on a spring suspension. During measurements the equipment remains in the vehicle, and only lengtheded cables to the microphones are installed. The microphone cannot be shielded.

145

3. If the tape recording of noise is not immediately reproduced, then the magnetic tape is placed in iron cover (for protection from stray fields). Between finish of the recording and at the start of its reproduction there is a period no more than days.

4. At wind velocity more than 7 m/s one should not make measurement of ambient noise.

5. A change in the temperature of air with height leads, just as the presence of wind, to refraction. If temperature decreases with height, then sonic rays are bent upwards and the distance of signal reception decreases and vice versa. With a drop in the temperature of more than 3.5-4°C at heights from 0 to 500 m one should not make the measurement of noise.

6. One must take into account that audio equipment (including the firm of Brüel and Kjaer) has only one channel of the recording of noise; it records either the total noise level or the level in any determined frequency band (octave, 1/3-octave, 1/4-octave).

In the absence of a large number of microphones, measurement can be produced as shown in Fig. 10 with the aid of one microphone which is moved on a circular arc, in the center of which the noise source is located - the engine. With a change in radius, the process of measurement is repeated.

Fig. 10. Overall view of the cell for acoustic tests.

Conclusions

1. At the contemporary stage of studies of the acoustic characteristics of turbofan engine with high bypass ratios, where the determinate noise source is the compressor (fan), experiments on model and full-scale objects have great significance. Model experiment is carried out, as a rule, in anechoic chambers. To conduct a full-scale experiment, the creation of an open stand is necessary.

2. The open stand for the acoustic tests of DTRD can be executed in stationary and mobile versions. It should be equipped with all systems necessary for the measurement of the parameters of the effectiveness and cost-effectiveness of the engine and its acoustic characteristics.

3. The open stand which has as a basic purpose acoustic investigations, may obtain multipurpose application – for tests of the characteristic of engine operational reliability.

4. Clearly formulated requirements for an open stand for acoustic tests of DTRD thus far do not exist, and available separate recommendations do not reflect a complete picture of the specific character of the studies. Thus it is necessary to develop commercial norms and standards which determine the conditions of assuring distant acoustic field, stand equipment and audio equipment.

Bibliography

1. Расчеты и измерение характеристик шума, создаваемого в дальнем звуковом поле реактивными самолетами. Под редакцией Л. Н. Соркина. М, Машиностроение, 1968.

2. Гортон   Установки и аппаратура для исследований шума авиационных двигателей. Труды Американского общества инж.-мех. Серии А

«Энергетические машины и установки». Русский перевод. М., «Мир», № 1, 1967.

3 Борьба с шумом. Под ред. Е. Я. Юдина. М., Стройиздат, 1964.

4. Горбунов Г. М., Солохин Э. Л. Испытания авиационных воздушно-реактивных двигателей. М., Машиностроение, 1967.

5. Халс, Ларж. Механизмы образования шума в модели компрессора. Труды Американского общества инж.-мех. Серия А Энергетические машины и установки. Русский перевод. М., «Мир», № 2, 1967.

6. Вопросы испытания воздушно-реактивных двигателей. Труды Куйбышевского авиационного института. Выпуск VIII, 1959.